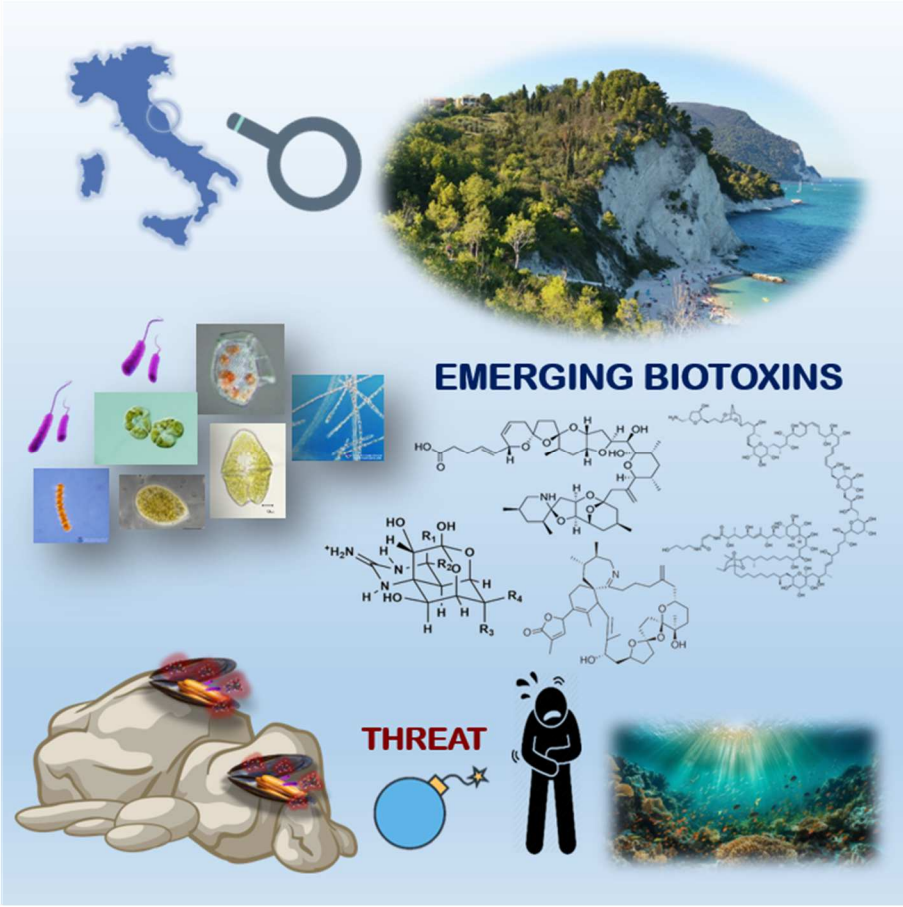

Emerging Biotoxins in marine organisms: chemical methods of analysis, bioaccumulation and eco-toxicological studies.

Melania Siracusa

Life and Environmental Sciences PhD Course
Università Politecnica delle Marche

UNIVERSITA' POLITECNICA DELLE MARCHE
DEPARTMENT OF LIFE AND ENVIRONMENTAL SCIENCES
DOCTORAL PROGRAMME IN LIFE AND ENVIRONMENTAL SCIENCES

Emerging Biotoxins in marine organisms: chemical methods of analysis, bioaccumulation and eco-toxicological studies.

Doctoral Dissertation of

Melania Siracusa

Tutor:

Prof. Stefania Gorbi

Co- Tutor:

Dott.ssa Arianna Piersanti

Co- Tutor:

Dott. Simone Bacchiocchi

The Chair of the Doctoral Program:

Prof. Paolo Mariani

2022/2023 – XXXVI Cycle

Final Examination

Date: 06 March 2024
Università Politecnica delle Marche, Dipartimento di Scienze della Vita e dell'Ambiente, Ancona, Italy

Cover illustration. *A look at Emerging Biotoxins: may be a threat in the future?*

Contents

Abstract 1

Introduction 4

Marine Biotoxins: a focus on Emerging Marine Biotoxins 4

EMBs presence in the North Adriatic Sea (Italy) 9

Methods of detection and quantification for CIs, AZAs, TTXs and PLTX 10

Study of EMBs biological effects 11

Aim and specific objectives of the project 13

1.1 Introduction 16

1.1.1 CIs 16

1.1.2 AZAs 20

1.2 Materials and Methods 21

1.2.1 Sampling 21

1.2.2 Algal cultures 23

1.2.3 Chemical analysis 23

1.3 Results and Discussion 32

1.3.1 Method Performances 32

1.3.2 LC-MS/MS analysis of phytoplankton 33

1.3.3 CIs in mussels 34

1.3.4 AZAs in mussels 36

2 Study of TTX presence and its origin in the North-Central Adriatic Sea

2.1 Introduction **39**

2.2 Materials and Methods **42**

2.2.1 Sampling **42**
2.2.2 Chemical analysis **43**
2.2.3 Microbiological and molecular analysis **49**

2.3 Results and Discussion **54**

2.3.1 Method Performances **54**
2.3.2 TTX in mussels from Marche coast **54**
2.3.3 TTX distribution in mussel tissue **56**
2.3.4 TTX in biota from *Molo Portonovo* **57**
2.3.5 *Vibrio alginolyticus* in biotic and abiotic samples **60**

3 PLTXs: study of their presence in in wild mussels from the Conero Riviera and of trophic transfer in seabreams *Sparus aurata*

3.1 Introduction **64**

3.2 Materials and Methods **68**

3.2.1 Sampling **68**
3.2.2 Exposure experiment **69**
3.2.3 Chemical analysis **70**
3.2.4 Biological analyses **75**

3.3 Results and Discussion **79**

3.3.1 Method Performances **79**
3.3.2 OVTXs in wild mussels from the Conero Riviera **79**

3.3.3 Chemical characterization of *O.* cf. *ovata* strain and exposed mussels **83**

3.3.4 Toxin levels in *Sparus aurata* fed with OVTX-contaminated mussels **85**

3.3.5 Transcriptomic responses in livers of fish fed with OVTX-contaminated diet **86**

3.3.6 Lipid content in liver of fish fed with OVTX-contaminated diet **98**

Conclusions **102**

Bibliography **105**

Abbreviations **122**

List of publications/conferences/courses/schools **127**

Acknowledgements **130**

Abstract

Emerging Marine Biotoxins (EMBs) are defined as those toxins of microalgal and/or bacterial origin for which incidence and geographical distribution are increasing but toxicity data are still limited. They include, among others, Palytoxins (PLTXs), Cyclic Imines (CIs), Azaspiracids (AZAs) and Tetrodotoxins (TTXs). Information on EMBs is until now restricted which is why EFSA (European Food Safety Authority) stressed on the need to investigate on this topic. In the last years, they are often detected in the Mediterranean Sea causing great concerns for the environmental status, human health and fishing industry.

The first aim of this PhD project was to investigate the presence of EMBs in coastal waters of Marche Region evaluating their levels in mussels and other biotic and abiotic matrices. Further aspects such as origin, ecological distribution and trophic transfer of these toxins were also addressed through a multidisciplinary approach.

Different sampling points, in the frame of marine biotoxins regional monitoring plan along the Marche coast, and collection time, on the basis of contamination type, were identified for the investigated EMBs. For TTXs, being its presence linked to particular features of habitat, a supplementary sampling point named *Molo Portonovo* (not included in official control) was identified along the Conero Riviera.

For Ovatoxins (OVTXs), exposure experiments were conducted in laboratory conditions, to investigate toxin trophic transfer. Mussels, exposed to the OVTX-producer *Ostreopsis* cf. *ovata,* accumulated OVTXs and were used as feeding fish in the exposure of seabreams (*Sparus aurata*). Transcriptomic

analysis based on RNA sequencing, FTIRI measurements and histological analysis were carried out in fish liver samples, to investigate possible alteration in macromolecules profile in exposed fish. LC-MS/MS methods for the analysis of EMBs in different matrices were set-up and implemented with good performances.

CIs were found at low levels with Spirolides (SPXs) as main components with maximum contaminations of 12-14 µg Kg^{-1} recorded in the first part of the year. Gymnodimine A (GYM A) was found, even if just above the LOQ level. Also AZAs were found in mussels of Marche Region at low levels (10-13 µg AZA eq. Kg^{-1}), especially in the last month of the year and with the predominance of AZA2 in the toxin profile. The LC-MS/MS analysis of phytoplankton samples, previously identified as potentially toxic, didn't show detectable levels of CIs and AZAs. Mussels from Pesaro and Ancona natural beds resulted contaminated by Tetrodotoxin (TTX), with some samples (5%), from Ancona wild sites that exceeded the EFSA guidance level. The highest TTX levels (about 300 µg kg^{-1}) were reported in early June in mussels from *Molo Portonovo* sampling site where other biotic matrices (mesozooplankton, phytoplankton) resulted contaminated. Compartmentalization studies in mussel's tissues showed a preferential accumulation of TTX in the digestive gland. Microbiological analysis to characterize potential TTX-producer bacteria was performed: *V. alginolyticus* was isolated and identified by PCR in the vast majority of mussel samples tested but also in phytoplankton, seawater and sediment, with the highest concentration in July 2021. *V. alginolyticus* bearing NRPS and/or PKS genes (suspected TTX biosynthesis genes) were isolated from about 50% of samples.

PLTXs were measured at low levels (about 30 µg Kg^{-1}) in mussels collected in September 2021 from the natural beds of Ancona area.

Mussels exposed to *O.* cf. *ovata* in laboratory conditions accumulated OVTXs up to 188 µg Kg^{-1}. Seabreams fed with contaminated mussels didn't accumulate OVTXs at detectable levels in their tissues however analysis in

livers indicated that an OVTX-enriched diet induced alterations of genes involved in the lipid metabolism. FTIRI and histological analysis showed a decrease of lipid content in exposed seabreams, suggesting biological effects in exposed organisms.

This research findings confirmed the presence of EMBs in mussels of Marche coast and in other biotic and abiotic investigated matrices. This suggests the need to include them in mussels monitoring plans taking into account that, even if they do not yet represent a risk for human health and environment, the ongoing climate changes could favour their development in the future

Introduction

Marine Biotoxins: a focus on Emerging Marine Biotoxins

Marine Biotoxins (MBs) are natural compounds produced by certain types of toxic algae and/or bacteria. Exposure to marine biotoxins can occur through direct contact by swimming, inhaling seawater droplets containing aerosolized toxins or eating contaminated seafood [1]. The food chain is surely the most important threat for human health. It is well known that MBs can accumulate in the tissues of some marine organisms, particularly filter feeding bivalves. During Harmful algal blooms (HAB), some phytoplankton species produce toxins that can store through the marine food web, since seawater may contain several million algal cells per liter and mussels filter approximately 20 L water h^{-1} [2].

MBs are thermostable toxins and can be distinguished in hydrophilic and lipophilic ones according to their solubility. On the basis of their poisoning symptoms, they are also classified as toxins causing Paralytic Shellfish Poisoning (PSP), Amnesic Shellfish Poisoning (ASP), Diarrhetic Shellfish Poisoning (DSP), Neurotoxic Shellfish Poisoning (NSP), and Ciguatera Fish Poisoning (CFP) [3].

Saxitoxin and its analogues (STX-group toxins) cause PSP intoxication in humans with symptoms ranging from a slight tingling sensation or numbness around the lips to fatal respiratory paralysis. STX-group toxins are closely related tetrahydropurines that interfere with voltage-gated sodium channels functionality blocking the Na^+ ions flux.

They are mainly produced by dinoflagellates belonging to the genus *Alexandrium* [4].

Domoic acid (DA) and its isomers are responsible of amnesic shellfish poisoning in humans with gastrointestinal effects (nausea, vomiting, diarrhoea or abdominal cramps) within 24 hours of consuming contaminated shellfish and/or neurological symptoms, confusion, loss of memory, or other serious signs such as seizure or coma, occurring within 48 hours. DA is a water-soluble cyclic amino acid that binds with glutamate receptors in central nervous system causing over-stimulation of these receptors [5]. DA is mainly produced by diatoms of the genus *Pseudo-nitzschia* [6].

Okadaic acid (OA) and its analogues, the Dinophysistoxins (DTXs) cause DSP syndrome characterised by symptoms such as diarrhoea, nausea, vomiting and abdominal pain. They are lipophilic and heat stable toxins, responsible of serine/threonine phosphoprotein phosphatases inhibition and produced by dinoflagellates of *Dinophysis* and *Prorocentrum* genera [7].

Azaspiracids (AZAs) are marine compounds similar to DSP toxins, in fact, human consumption of AZA-contaminated shellfish can result in severe acute gastrointestinal symptoms, even if the mechanism of action is still not clarified [8]. Yessotoxins (YTXs) and its analogues are polycyclic ether compounds produced by the dinoflagellates *Protoceratium reticulatum*, *Lingulodinium polyedrum* and *Gonyaulux spinifera*, initially included in the DSP group because they were detected simultaneously with OA and DTXs. Nowadays, due to the absence of phosphatase inhibition activity and gastrointestinal toxicity, they are classified separately [9].

Brevetoxins (BTXs) are the marine toxin group that cause NSP intoxication, with different symptoms such as nausea, vomiting, diarrhoea, paraesthesia, cramp bronchoconstriction, paralysis, seizures and coma. Typically occur within 30 minutes to 3 hours of consuming contaminated shellfish and last for a few days. BTXs are lipid-soluble cyclic polyether compounds, primarily produced by a dinoflagellate *Karenia brevis* [10].

Ciguatoxins (CTXs) are marine toxins obtained from the biotransformation of precursor gambiertoxins produced by the dinoflagellate of genus

Gambierdiscus. CTXs are lipid-soluble polyether compounds typical of tropical and subtropical coral reef areas and found in large predatory fishes. CTXs are responsible of Ciguatera (CFP) syndrome characterised by a wide variety of symptoms such as gastrointestinal (nausea, vomiting, abdominal pain, and diarrhoea), neurological (tingling, itching) and cardiovascular (hypotension, bradycardia). In the severe cases effects may appear within 30 minutes after ingestion of contaminated fish, while in the milder cases they may be delayed for 24 to 48 hours. Although the vast majority of CFP is observed after ingestion of carnivorous fish, other marine species are suspect in human ciguatera intoxication [11].

As regards the mechanism of action, both BTXs that CTXs act on excitable membranes, in particular on voltage sensitive sodium channels, keeping they in an open state [12].

Maximum permitted limits (MPLs) in bivalve molluscs for biotoxins associated with PSP, ASP and DSP syndromes are established by Regulation (EC) 853/2004. MPLs are set equal to 160 µg OA eq. kg^{-1} for OA and DTXs, 3.75 mg YTX eq. kg^{-1} for YTXs, 160 µg AZA eq. kg^{-1} for AZAs, 20 mg of domoic acid kg^{-1} for DA, 800 µg STX·2HCl eq. kg^{-1} for PSP [13]. Official controls through regional monitoring plan are regularly conducted by the Competent Authority in the production areas, as requested by Regulation (EU) 627/2019 [14]. Thus, the production sites are periodically checked for the presence of toxic phytoplankton-producing toxin and the occurrence of MBs in molluscs. Controls are highly effective in terms of consumer protection but entails important economic losses for the producer because of the regulatory closures. The Regulation (EU) 627/2019 describes official methods, internationally recognized, for the determination of the regulated marine biotoxins [14].

The definition of “Emerging Marine Biotoxins” (EMBs) is quite versatile.

It has been applied to focus on: i) recently discovered marine toxins; ii) known marine toxins that only recently appear in waters and seafood where they were previously absent; iii) non-regulated known marine toxins, which are considered as a possible threat but for which toxicity data are yet limited [15]. Probably the global warming and the anthropologic activities favoured the migration and establishment of these toxins in temperate waters, representing a new threat to human public health [16]. In particular, climate changes cause an increase of water temperature and sea level, impacting on the physicochemical characteristics of the marine environment and aquatic organisms at all trophic levels, then potentially promoting the spread and growth of toxic microalgae [17-18].

EMBs include different classes of toxins such as Cyclic Imines (CIs), AZAs, Tetrodotoxins (TTXs), Palytoxins (PLTXs), CTXs and BTXs.

CIs are marine lipophilic toxins that include different molecular subgroups, the most important are Spirolides (SPXs), Gymnodimines (GYMs), Pinnatoxins (PnTXs) and Pteriatoxins (PtTXs). They are mainly produced by dinoflagellates *Alexandrium ostenfeldii* and *A. peruvianum* (SPXs), *Karenia selliformis* (GYMs) and *Vulcanodinium rugosum* (PnTXs).

Structurally they are macrocyclic compounds characterized by imine and spiro-linked ether moieties, with an acute neurotoxicity in mice upon intraperitoneal injection, which is why they are also called “fast acting“ toxins. Based on the toxicological available information, CIs exhibit the ability to bind and block acetylcholine receptors in the central and peripheral nervous systems. Until now CIs are not regulated but EU Reference Laboratory for Monitoring of Marine Biotoxins (EURLMB) proposed a guidance level of 400 µg sum of SPXs kg^{-1} shellfish meat [19].

TTXs are potent neurotoxins produced by marine bacteria most commonly of genus *Vibrio*, famous to be responsible of the pufferfish poisoning in humans. After eating contaminated seafood, symptoms occur rapidly ranging from mild, as numbness on mouth, to extremely severe as paralysis or even death. Chemically TTXs are alkaloids with a guanidium moiety, responsible of their toxicity, because it binds to the voltage-gated sodium channels blocking them. A MPL is not established for TTXs but a guidance level of 44 µg TTX eq. kg^{-1} shellfish meat was proposed by the European Food Safety Authority (EFSA) [20].

PLTXs include toxins such as Ovatoxins (OVTXs), produced by benthic dinoflagellates of *Ostreopsis* genus, with structure similar to the parent compound Palytoxin (PLTX), a very potent natural toxin. Palytoxin blocks the active transport of Na^+ and K^+ ions, converting the pump in a non-selective cation channel. TTXs are complex polyhydroxylated compounds with both lipophilic and hydrophilic properties. Currently there are no regulations on this toxin group but, in 2005 the EURLMB proposed a provisional limit of 250 µg kg^{-1} shellfish and EFSA set a safe level of 30 µg kg^{-1} of the sum of PLTX and ostreocine-D in shellfish meat [21]. To date acute toxicity studies are limited on a few PLTX congeners, but toxic blooms of *Ostreopsis* cf. *ovata* have been associated with respiratory difficulties, dermatitis and eye irritation, upon direct contact with cells and/or via inhalation of aerosolized toxins [22].

In the recent years EMBs were found in seafood from European waters affecting human health [23], but monitoring plans in the production areas are still absent or insufficient. Moreover the lack of reference materials, analytical methodology and regulatory limits makes the question of urgent interest. Also EFSA stressed on the need to investigate on this topic, being information about EMBs still restricted both from a scientific and legislative point of view.

EMBs presence in the North Adriatic Sea (Italy)

Until now among EMBs only CIs, AZAs, TTXs and PLTXs were reported in North Adriatic Sea (Italy). These evidences may represent a potential hazard of concern for Italian mussels, then it is necessary and urgent to explore this issue.

CIs and AZAs

High levels of SPXs were found in mussels harvested along the Emilia Romagna coast in the North Adriatic Sea, at the end of November 2003, as a consequence of a relevant *A. ostenfeldii* bloom [24-25].

Mussels from the Marche coast (North-Central Adriatic Sea) resulted contaminated by SPXs during 2014-2015. Traces of gymnodimine A (GYMA) were also found, representing the first report of GYMs in the Italian coastal waters [26]. As regards AZAs, traces were found in mussels from Marche coast in 2012-2013, with the predominance of AZA2 in the toxin profile. This was the first report of AZAs in Mediterranean seafood [27].

TTXs

TTXs were detected for the first time in Italy (2015-2017) in shellfish from Syracuse Bay [28]. The detection of significant amount of Tetrodotoxin (TTX), the highest found in bivalve molluscs in Europe, was reported in *Mytilus galloprovincialis* samples collected in the Northern Adriatic Sea (Marano Lagoon, Friuli Venezia Giulia) in 2017 and 2018 [29].

PLTXs

Intense blooms of *O.* cf. *ovata* periodically occurred in the North-Central Adriatic Sea since 2006 [30-31]. Shellfish (*M. galloprovincialis*) collected in late summer-early autumn 2016 along the Conero Riviera (Marche coast) showed PLTXs contaminations above the EFSA guidance level and in some case also above the EURLMB one [32].

Methods of detection and quantification for CIs, AZAs, TTXs and PLTXs

CIs and AZAs

Various receptor-based methods were developed to detect CIs in shellfish [23]. Recently they were included in multitoxin methods in Liquid Chromatography coupled to tandem Mass Spectrometry (LC-MS/MS), as an implementation of the official method for the determination of regulated lipophilic marine toxins [26, 33].

As regards AZAs, different methods, based on the production of monoclonal and polyclonal antibodies against AZAs such as competitive enzyme-linked immunosorbent assay (ELISA), were developed [23]. Moreover, the analytical methodology based on LC-MS proved to be the best approach. To detect regulated AZAs in molluscs (AZA1, 2 and 3), the official LC-MS/MS method for the determination of regulated lipophilic marine toxins is used [27, 34]. To investigate on emerging AZAs congeners for which standards are not available, both in shellfish that in algae samples, different targeted and untargeted LC-MS approaches were set [35-38].

The advantages of LC-MS methods for CIs and AZAs are many, the use of fragmentation pathways allow to identify and quantify in unique and accurate mode the different analogues eventual present in the sample, then to describe the contamination profile.

TTXs

Regarding methods of TTXs detection and quantification, there are three main types of methodologies used: cell-based assays, antibody-based methods, and chemical methods based on Hydrophilic Interaction Chromatography coupled to tandem Mass Spectrometry (HILIC-MS/MS). Cell-based assays are able to assess the toxicity of TTX analogues, antibody-based methods are used as rapid qualitative screening approaches [23]. Also

in this case, however, chemical methods in LC-MS/MS are surely the most suitable to separate, identify, and quantify TTXs. In the frame of a collaborative study, a multitoxin method including PSP toxins and only the parent TTX was implemented and validated [39]. In 2021 the EURLMB published a standard operating procedure “Determination of Tetrodotoxin by HILIC-MS/MS” to evaluate the incidence of TTX and its analogues in bivalves and gastropods [40].

PLTXs

Currently, there is no reference method for the analysis of PLTXs. Mouse bioassays have been traditionally utilized for PLTXs monitoring in seafood, however these methodologies are currently being replaced by methods based on functional assays and chemical methods [23]. Several LC-MS/MS methods for the detection and characterization of PLTXs in shellfish and algal species were implemented with good performances [31, 41-42].

Study of EMBs biological effects

Biomarkers represent a wide variety of cellular and biochemical responses, useful to study the effects of toxins on aquatic ecosystems. There are several types of biomarkers such as biochemical (enzyme activity measurement), chemical (detection and quantification of compounds), genotoxicity (DNA damage measurement and DNA mutations), neurotoxicity (behavioural changes and neurotransmitters quantification), morphological (histopathology), molecular (gene transcriptional changes and specific genomic and epigenetic markers), metabolomic (metabolites measurement) and physiological (ion regulation) [43]. Biomarkers of exposure can be used as early-warning systems of toxins presence in aquatic environments [44]. Behavioural and physiological parameters can be used in this context, especially using non-vertebrate species that raise less ethical concerns.

For EMBs (AZAs, PLTXs, BTXs, CTXs) the majority of studies focuses on cell

viability, oxidative damage and DNA damage effect, quantification of neurotransmitters and their metabolites, evaluation of expression patterns of candidate genes [43]. Few studies to investigate the biological effects of AZAs in marine animal models were conducted *in vivo*, although they are the main targets and sources of AZA contamination [45-46]. Recently the biological responses to AZAs produced by the dinoflagellate *Azadinium dexteroporum*, were investigated in *M. galloprovincialis* after a laboratory exposure experiment. The results showed a clear biological impact of AZAs, and suggested their use as early indicators of contamination both for seafood and marine organisms [37].

As regards PLTXs, in particular OVTXs, immunological, histological, lysosomal and neurotoxic alterations were observed in mussels exposed to *O.* cf. *ovata* blooms, both in field and laboratory conditions [47-49]. *In vitro* cell models such as neuro-2a assay were also implemented for the evaluation of cytotoxicity of palytoxin and tetrodotoxin [50].

An *ex vivo* approach with the precision-cut tissue slices (PCTS) has been recently validated in mussel *M. galloprovincialis* as promising tool to investigate molecular and cellular responses in ecotoxicological research [51].

Critical gaps are still present regarding the EMBs toxic effects following acute exposure, therefore it is necessary to develop and implement effective alternative ecotoxicological biomarkers for these compounds, e.g. mechanism of action of each toxin [43].

Aim and specific objectives of the project

GENERAL AIM: *investigation on the presence and ecotoxicological impact of Emerging Marine Biotoxins through a multidisciplinary approach including chemical, microbiological and ecotoxicological methods.*

Information about EMBs are still scarce but recently they appeared in our sea. Then it is important to investigate on this topic, evaluating the threat that they actually represent for seafood and marine ecosystems.
The PhD project focused on four EMBs groups: CIs, AZAs, TTXs and PLTXs based on their previous findings in the Mediterranean Sea and in particular in the North Adriatic Sea, being Marche coast the study area**.**
The project was conducted in collaboration with Polytechnic University of Marche and the "Istituto Zooprofilattico Sperimentale dell'Umbria e delle Marche Togo Rosati".

The *specific objectives* of the project were:

- Implementation and validation of LC-MS/MS methods for the determination of EMBs and of their complex toxin profiles in different biotic matrices (marine algae, invertebrates and fish organisms).

- Studies on field samples to investigate bioaccumulation of toxins in different marine species.

- Investigation on toxins primary producers by chemical and microbiological approaches.

• Study of the trophic transfer of algae and/or toxins and ecotoxicological effects (biomarkers) in marine organisms exposed in laboratory conditions**.**

The PhD project will be illustrate in the chapters briefly described below:

CHAPTER 1

Study of seasonal and geographical trends for CIs and AZAs from mussels of Marche coast: investigation on their primary producers

The implementation and validation of LC-MS/MS methods for the analysis of CIs and AZAs in mussels and phytoplankton were reported. Mussels collected in the frame of Marine Biotoxins regional monitoring plan along the Marche coast in 2021, were analysed to study their toxin profiles and the annual and geographical trends of contaminations. Potential phytoplanktonic producer organisms were isolated and analysed.

CHAPTER 2

Study of TTX presence and its origin in the North-Central Adriatic Sea

The implementation and validation of LC-MS/MS method for the analysis of TTXs in mussels and other biotic matrices (mesozooplankton, flatworms and phytoplankton) were described. Contamination level and spatio-temporal trends of TTX in mussels from the natural beds of Marche Region were evaluated. Microbiological and molecular methods for isolation, identification and characterization of *Vibrio* spp., as potential TTX-producer bacteria, from various matrices were optimized. Compartmentalization studies were performed to evaluate TTX distribution in different mussel tissues. As regards the specific sampling point *Molo Portonovo*, LC-MS/MS analysis of different

biotic matrices such as mussels, mezooplankton and phytoplankton-net was performed to evaluate TTX contamination.

Microbiological, molecular analyses and enumeration of *Vibrio* spp. were done on biotic and abiotic matrices from Conero Riviera (Ancona) area to identify biological producer.

CHAPTER 3

PLTXs: study of their presence in wild mussels from the Conero Riviera and of trophic transfer in seabreams Sparus aurata

A LC-MS/MS method for the analysis of PLTXs in mussels, algal pellet and fish tissues was implemented and in-house validated. Samples collected from natural beds of Conero Riviera in late summer-early autumn 2021 were checked for PLTXs contaminations. Accumulation and toxin profile of field samples and their eventual relationships with *Ostreopsis* cf. *ovata* blooms were investigated.

For OVTX trophic transfer, exposure experiment was conducted. In a first step mussels were fed with *Ostreopsis* cf. *ovata*. In a second step mussels contaminated by OVTXs, were used as feeding fish in the exposure of the seabreams (*S. aurata*). At the end of the experiment, seabreams were dissected and the different tissues collected.

LC-MS/MS method was used to evaluate OVTX accumulation in mussels and seabream tissues, during the various steps of exposure experiment. Transcriptomic analysis based on RNA sequencing, Focal Plane Array (FPA)-Fourier Transform Infrared Spectroscopy Imaging (FTIRI) measurements and histological analysis were carried out in liver samples of control and exposed fish to study eventual alterations induced by the OVTX-enriched diet.

Chapter 1

Study of seasonal and geographical trends for CIs and AZAs from mussels of Marche coast: investigation on their primary producers

1.1 Introduction

CIs and AZAs are emerging lipophilic marine toxins of interest in last years, because they are found with increasing frequency as contaminants of fish and shellfish, important nutrients of a healthy human diet.

1.1.1 CIs

CIs are toxins soluble in organic solvents such as methanol, acetone, chloroform and ethyl acetate [19]. The different subgroups belonging to CI class, chemically show a similar structure, characterized by a spiroimine, or cyclic imine subunit, that gives the name to this class of marine toxins. The spiroimine subunit is embedded within a large carbocyclic polyether framework that ranges in size from 14 or 16 to 27 members.

PnTXs and PtTXs are one of the largest subgroups of CIs. They also represent the highest risk for human health due to their potent oral toxicity, unlike other subgroups that lose their potency if administered orally.

GYMs are among the smallest molecular weight members of CIs. The unsubstituted 6-membered cyclic imine is a unique feature of these toxins. The SPXs exhibit the union between the spiroimine subunit of PnTXs and the substituted cyclohexene of GYMs [52]. The analogues SPX E and F are shellfish metabolites of SPX A and SPX B respectively, biologically inactive because the cyclic imine is hydrolysed [19].

The major molecular subgroups belonging to CIs with their analogues detected in mussels and algae, reported in the literature so far, were showed in Figure 1.1 [26, 53].

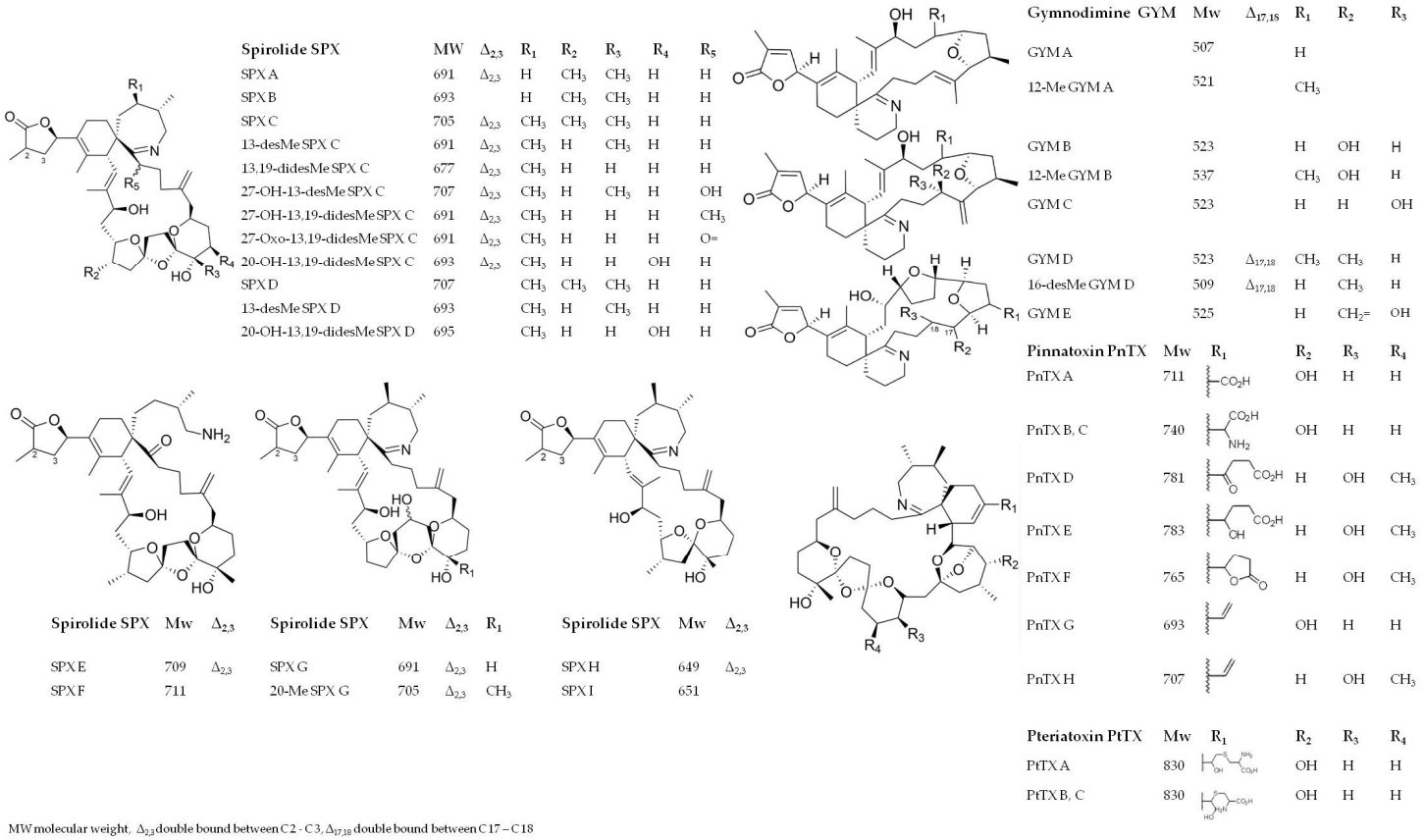

Spirolide SPX	MW	$\Delta_{2,3}$	R_1	R_2	R_3	R_4	R_5
SPX A	691	$\Delta_{2,3}$	H	CH_3	CH_3	H	H
SPX B	693		H	CH_3	CH_3	H	H
SPX C	705	$\Delta_{2,3}$	CH_3	CH_3	CH_3	H	H
13-desMe SPX C	691	$\Delta_{2,3}$	CH_3	H	CH_3	H	H
13,19-didesMe SPX C	677	$\Delta_{2,3}$	CH_3	H	H	H	H
27-OH-13-desMe SPX C	707	$\Delta_{2,3}$	CH_3	H	CH_3	H	OH
27-OH-13,19-didesMe SPX C	691	$\Delta_{2,3}$	CH_3	H	H	H	CH_3
27-Oxo-13,19-didesMe SPX C	691	$\Delta_{2,3}$	CH_3	H	H	H	O=
20-OH-13,19-didesMe SPX C	693	$\Delta_{2,3}$	CH_3	H	H	OH	H
SPX D	707		CH_3	CH_3	CH_3	H	H
13-desMe SPX D	693		CH_3	H	CH_3	H	H
20-OH-13,19-didesMe SPX D	695		CH_3	H	H	OH	H

Gymnodimine GYM	Mw	$\Delta_{17,18}$	R_1	R_2	R_3
GYM A	507		H		
12-Me GYM A	521		CH_3		
GYM B	523		H	OH	H
12-Me GYM B	537		CH_3	OH	H
GYM C	523		H	H	OH
GYM D	523	$\Delta_{17,18}$	CH_3	CH_3	H
16-desMe GYM D	509	$\Delta_{17,18}$	H	CH_3	H
GYM E	525		H	CH_2=	OH

Pinnatoxin PnTX	Mw	R_1	R_2	R_3	R_4
PnTX A	711	CO_2H	OH	H	H
PnTX B, C	740	CO_2H, NH_2	OH	H	H
PnTX D	781	CO_2H	H	OH	CH_3
PnTX E	783	CO_2H, OH	H	OH	CH_3
PnTX F	765		H	OH	CH_3
PnTX G	693		OH	H	H
PnTX H	707		H	OH	CH_3

Pteriatoxin PtTX	Mw	R_1	R_2	R_3	R_4
PtTX A	830		OH	H	H
PtTX B, C	830		OH	H	H

Spirolide SPX	Mw	$\Delta_{2,3}$
SPX E	709	$\Delta_{2,3}$
SPX F	711	

Spirolide SPX	Mw	$\Delta_{2,3}$	R_1
SPX G	691	$\Delta_{2,3}$	H
20-Me SPX G	705	$\Delta_{2,3}$	CH_3

Spirolide SPX	Mw	$\Delta_{2,3}$
SPX H	649	$\Delta_{2,3}$
SPX I	651	

MW molecular weight, $\Delta_{2,3}$ double bound between C2 - C3, $\Delta_{17,18}$ double bound between C17 – C18

Figure 1.1: CI analogues identified in mussels and algae, reported in the literature so far (from Bacchiocchi et al. [26]

CIs were discovered during the last 25 years because of their interference with the mouse biological assay, the only official method recognized by the European Community until July 2011 for regulated lipophilic toxins in bivalve molluscs [54]. Until now, the dinoflagellates *Alexandrium ostenfeldii* and *Alexandrium peruvianum*, globally distributed species, are the only SPX-producer organisms [55-57].

At the end of November 2003, an intense *A. ostenfeldii* was reported along the Emilia-Romagna coast in the North Adriatic Sea (Italy). On that occasion, mussels harvested during the algal bloom accumulated high levels of SPXs. The toxin profile of both *A. ostenfeldii* and mussels was characterized by 13-desmethyl spirolide C (13-desMe SPX C) and 13,19-didesmethyl spirolide C (13,19-didesMe SPX C) as the major components, with several minor spirolides like 27-hydroxy-13,19-didesmethyl spirolide C, 27-hydroxy-13-desmethyl spirolide C and 27-oxo-13,19-didesmethyl spirolide C [24-25]. Mussels from the Marche coast (North-Central Adriatic Sea) resulted contaminated by SPXs during 2014-2015 and only the analogues 13-desMe SPX C and 13,19-didesMe SPX C analogues were found [26].

In early 1990s, the dinoflagellate *Karenia selliformis* was identified as a GYM-producer organism [58]. Recently (2014-2015) traces of GYMA were found in a few mussel samples from the Marche coast, representing the first report of GYMs in the Italian coastal waters [26]. The only PnTX-producer organism described so far is the dinoflagellate *Vulcanodinium rugosum*. PnTXs in Europe were found in France [59] Spain [60], and also in Italy [61], but never in the North Adriatic Sea. It was hypothesized that PtTXs may be shellfish metabolites, but they are scarcely studied as other CIs subgroups [62].

Although CIs are known to occur in microalgae and/or shellfish worldwide, they have never been related to human illness until today. However, EFSA requested more data to properly assess the CI risk for shellfish consumers,

in fact currently no regulation but only a guidance level was established [19].

1.1.2 AZAs

AZAs are characterized by polyether rings with cyclic amine (aza group), a trispiro-group and a carboxylic acid group. In Figure 1.2 the structure of the toxin parent AZA1 was reported. At physiological pH (7.4), AZAs are present as zwitterions, neutral molecules with both positive and negative charges [8].

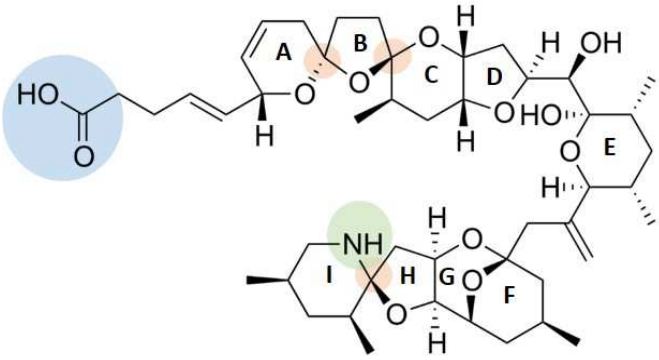

Figure 1.2: AZA1 chemical structure: a cyclic imine (aza group in green), a trispiro-group (orange) and a carboxylic acid group (blue) (from Giuliani et., [37]).

The AZA group consist of more than 60 compounds mainly produced by dinoflagellates from *Azadinium* and *Amphidoma* genera [23]. The first identified primary AZA-producer was *Azadinium spinosum*, followed by *Azadinium poporum*, *Amphidoma languida* and *Azadinium dexteroporum* [63-65]. Some other AZAs are metabolites and products from oxidation, hydroxylation, decarboxylation, and dehydration occurring in shellfish. AZA17 and AZA19 were found to be the main mussel metabolites of AZA1 and AZA2, respectively [35]. AZAs have been detected in several marine mollusc and crustacean species from different areas of Europe (i.e., Ireland, Norway, England, Spain, France, Denmark, Portugal and Sweden) [66].

Recently, traces of AZAs were detected in *M. galloprovincialis* samples from the Italian coasts of North-Central Adriatic Sea (Marche Region) [27]. The first intoxication in humans, due to the consumption of mussels contaminated by AZAs occurred in 1995. Symptoms such as vomiting, severe diarrhoea, and stomach cramps were similar of those of DSP, but being the illness causative toxins different from OA and DTXs and the action mechanism questionable, a new toxic syndrome called Azaspiracid Poisoning (AZP) was identified [12]. Only 3 analogues AZA1, AZA2, AZA3, the most relevant with regards to abundance and toxicity [8], are regulated as sum of their content in bivalve molluscs, with a MPL of 160 µg AZA eq. kg^{-1} [13]. These analogues are constantly monitored in the production areas using the LC-MS/MS official method [34], as imposed by Regulation (EU) 627/2019 [14].

The aim of this chapter was to study by LC-MS/MS analysis, the toxin profiles and the annual and geographical trends of contaminations for CIs and AZAs. Moreover potential phytoplanktonic producer organisms were investigated through isolation and chemical analysis.

1.2 Materials and Methods

1.2.1 Sampling

In the frame of Marine Biotoxins regional monitoring plan, samples of *Mytilus galloprovincialis* were collected from 22 breeding sites and 7 wild sites (3 of Pesaro area Mississipi, Vallugola, Sotto la Croce, and 4 of Conero Riviera Ancona nord, Ancona sud, Sirolo nord, Sirolo sud) located along the Marche coast (North-Central Adriatic Sea), in 2021 with a biweekly frequency.
Phytoplankton samples were obtained from monthly monitoring activity of Dipartimento di Scienze della Vita e dell'Ambiente (DISVA— Polytechnic University of Marche) in the Senigallia station (SG01 located at 1.2 nM from

the coast, 43° 45.86′ N, 13° 13.00′ E) and Portonovo station (PN located at about 3 nM from the coast, 43°36.201’ N, 13°36.705’ E) in the period February 2019 - August 2021, but analyzed in the frame of this PhD project. The sampling points studied in this project are reported in the Figure 1.3.

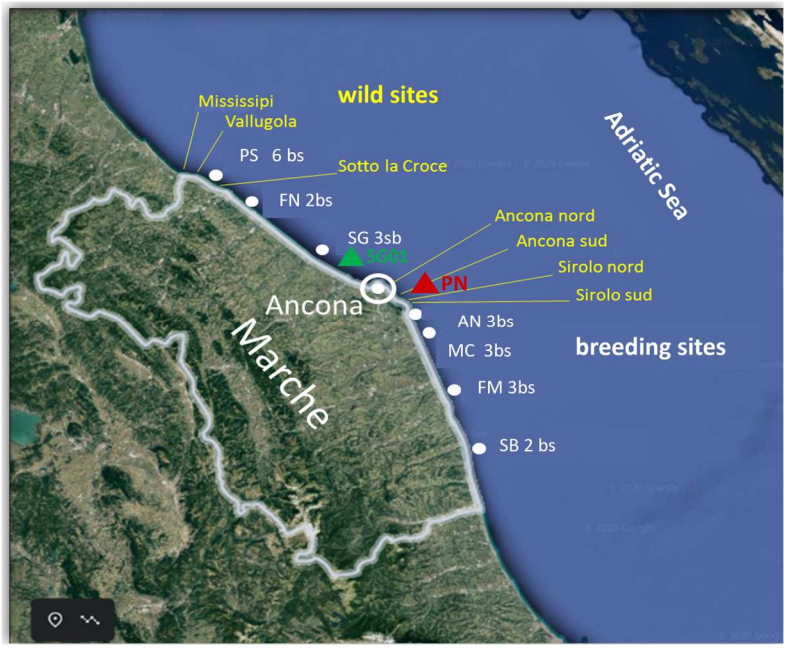

Figure 1.3: bs:breeding sites (white), wild sites (yellow) and phytoplankton stations (SG01 Senigallia, PN Portonovo) along the Marche coast: PS (Pesaro), FN (Fano), SG (Senigallia), AN (Ancona), MC (Macerata), FM (Fermo) and SB (San Benedetto del Tronto). Image (data SIO, NOAA, U.S. Navy, NGA, GEBCO; image Landsat/Copernicus) from Google Earth.

Overall, 602 samples of mussels and 38 samples of phytoplankton were collected and analysed by LC-MS/MS for the presence of CIs and AZAs.

1.2.2 Algal cultures

Monoclonal cultures of species potentially toxic, isolated by phytoplankton samples collected, were prepared by the marine botany group of DISVA.

1.2.3 Chemical analysis

Chemicals and Standards

All chemicals were of analytical reagent grade: acetonitrile and 25% ammonia (LC-MS grade), methanol (HPLC grade), sodium hydroxide, 37% hydrochloric acid, acetone (analysis grade). Ultrapure water (18.2 MΩ cm) was produced by a MilliQ water purification system (Millipore Ltd., Bedford, MA, USA).

Certified reference solutions of 13-desMe SPX C (NRC CRM 13-desMe SPX C), PnTX G (NRC CRM PnTXG) and GYM A (NRC CRM GYM) were purchased from the National Research Council Certified Reference Materials Program (Institute for Marine Biosciences, Halifax, NS, Canada) and used for identification and quantification purposes. A non-certified standard solution of 13,19-didesMe SPX C (QCS 13,19- didesMeC) was purchased from CIFGA (Lugo, Spain) and used only for identification.

Certified reference solutions for azaspiracid 1 (CRM-AZA1), azaspiracid 2 (CRM-AZA2) and azaspiracid 3 (CRM-AZA3) were purchased also from CIFGA.

Moreover a matrix certified reference material (FDMT1) containing many analogues of CIs and AZAs was obtained from the National Research Council Certified Reference Materials Program (Institute for Marine Biosciences, Halifax, NS, Canada), to test the performances of the implemented methods.

The certified reference solutions were diluted in solvent to obtain stock solutions, from which were prepared matrix-matched calibrants.

Sample treatment

Mussels after harvest were transported to the laboratory in refrigerated conditions (4 °C). Molluscs were opened immediately, sand and solid residues removed under running water. Then were taken out of the shells and drained on a net. For each sample, about 150 g of whole flesh, was pooled and finely homogenized by an Osterizer blender [34].

Monoclonal cultures (aliquot of 2L with a concentration of 1×10^6 cell L^{-1}), upon arrived in laboratory were centrifuged at 2000 x g for 15 min and the pellets collected.

Mussel homogenates and algal pellets were stored at –20 °C until chemical analysis.

CIs and AZAs extraction from mussels

The extraction was performed following the official EU-Harmonized Standard Operating Procedure for lipophilic marine biotoxins in molluscs by LC–MS/MS [34] which enabled the extraction of CIs and AZAs together with the other regulated marine lipophilic toxins.

Briefly shellfish homogenate (2.00 ± 0.05 g) was extracted twice with 9 mL of methanol. After the first methanol addition, the sample was vortex-mixed for 3 min at 2000 rpm with a Multi Reax, the extract centrifuged for 10 min at 2000 x g and the supernatant transferred to a 20 mL volumetric flask. During the second methanol addition, the mixture was homogenized with an Ultra Turrax T25 mixer for 1 min at 10000 rpm, the extract centrifuged (10 min at 2000 x g) and the supernatant combined with the first extract. The whole extraction volume was brought to final volume of 20 mL with methanol. An aliquot of the methanolic extract was filtered through a syringe filter (0.2 µm in nylon) and submitted to LC-MS/MS analysis.

CIs and AZAs extraction from algal pellet

AZAs and CIs were extracted from algal cultures using modified procedure described by Jauffrais el al. [67] and optimizing that described by Giuliani et al. [37]. Briefly algal pellet was re-suspended in 5 mL of acetone, vortex-mixed for 1 min and bath-sonicated for 10 min. After sonication, the sample was centrifuged for 10 min at 2000 x g (20 °C) and the supernatant transferred to 100 mL evaporation flask. Pellet extraction was repeated twice, the supernatant combined and evaporated under nitrogen stream at 35 °C. The residue was dissolved in 1 mL of methanol and filtered through a syringe filter (0.2 µm in nylon) before LC-MS/MS analysis.

LC-MS/MS conditions

LC-MS/MS analyses were performed using a hybrid triple–quadrupole/linear ion trap 3200 QTRAP mass spectrometer (AB Sciex, Darmstadt, Germany) equipped with a Turbo V source and an electrospray ionization (ESI) probe. The mass spectrometer was coupled to an Agilent 1200 HPLC (Palo Alto, CA, USA), equipped with solvent reservoir, in-line degasser, quaternary pump, refrigerated autosampler and column oven.

The chromatographic separation was achieved according to Gerssen et al. [33] and optimizing the conditions implemented in the previous publications [26-27, 37].

The chromatographic conditions adopted for both CIs and AZAs are reported in Table 1.1. Mobile phase A was water and B acetonitrile/water (90:10, v/v), both containing ammonium hydroxide (0.05% v/v) (pH 11).

Table 1.1: LC conditions for CIs and AZAs analysis.

Column	Gemini® NX-C18 3 µm, 2.1 mm x 100 mm		
Flow	0.4 mL min^{-1}		
Injection volume	5 µl		
Column temperature	40°C		
Gradient	Time (min)	Mobile phase A (%)	Mobile phase B (%)
	0	90	10
	2	90	10
	9	10	90
	14	10	90
	15	90	10
	25	90	10

Mass conditions were optimized following the approaches implemented in the previous publications [26, 37]. Moreover an integration of new analogues was done based on literature, for a total of 34 CIs and 90 AZAs monitored.
Infusion experiments were performed using certified reference materials available, listed in the section "Chemicals and Standards" to set turbo IonSpray source parameters (Table 1.2).

Table 1.2: MS source parameters.

Source type	ESI
Curtain gas (CUR)	20 psi
Collision gas (CAD)	medium
IonSpray voltage (IS)	4500 v
Source temperature (TEM)	650 °C
Ion source Gas 1 (GS1)	40 psi
Ion source Gas 2 (GS2)	60 psi

The mass spectrometer was operated in multiple reaction monitoring (MRM) mode and in positive polarity (ESI^+), selecting two transitions for each toxin to allow for quantification and identification (Table 1.3, 1.4). The identification of 13-desMe SPX C, 13,19-didesMe SPX C, GYM A, PnTX G, AZA1, AZA2 and AZA3 in the analyzed samples was based on: retention times and ion ratios. For all the other analytes, the identification was based only on the characteristic transitions reported in literature.

Table 1.3: MS/MS transitions for CIs.

Toxin	Prec. ion (m/z)	Prod. ion 1 (m/z)	Prod. ion 2 (m/z)	Dwell time (msec)	DP	EP	CEP	CE	CXP
SPIROLIDES (SPXs)									
SPX H	650,4	**402,3**	164,1	35	55	10,0	30	39	6
SPX I	652,5	**402,3**	164,1	35	55	10,0	30	35	8
13,19-didesMeSPX C	678,4	**430,2**	164,1	35	55	10,5	30	50	8
SPX A	692,4	**444,3**	150,1	35	55	10,5	30	45	6
27-Oxo-13,19-didesMeSPX C			178,1	35	55	10,5	30	50	6
13-desMeSPX C			164,1	35	55	10,5	30	50	6
SPX G	692,5	**378,2**	164,1	35	55	10,5	30	50	6
27-OH-13,19-didesMeSPX C	694,4	**464,3**	180,1	35	55	10,5	30	50	6
20-OH-13,19-didesMe SPX D	694,4	**446,3**	292,1	35	55	10,5	30	50	8
SPX B	694,5	**444,3**	150,1	35	55	10,5	30	50	8
13-desMe SPX D			164,1	35	55	10,5	30	50	6
20-OH-13,19-didesMe SPX C	696,4	**446,3**	292,5	35	55	10,5	30	50	6
SPX C	706,5	**458,3**	164,1	35	55	10,5	30	50	6
27-OH-13-desMeSPX C	708,4	**478,3**	180,1	35	55	10,5	30	50	6
SPX D	708,5	**458,3**	164,1	35	55	10,5	30	50	6
SPX E	710,5	**444,3**	164.1	35	55	10,5	30	50	8
SPX F	712,5	**444,3**	164.1	35	55	10,5	30	50	8
20-Me SPX G	706,5	**392,3**	164,1	35	55	10,5	30	50	6
GYMNODIMINES (GYMs)									
GYM A	508,3	490,3	162,1	35	55	10,5	30	45	6
16-desMeGYM D	510,3	492,3	160,1	35	55	10,5	30	45	6
12-Me GYM A	522,3	504,3	162,1	35	55	10,5	30	45	6
GYM B/C	524,3	506,3	162,1	35	55	10,5	30	45	8
GYM D				35	55	10,5	30	45	8
GYM E	526,3	508,3	160,1	35	55	10,5	30	45	6
PINNATOXINS (PnTXs)									
PnTX G	694,5	**458,3**	164,1	35	55	10,5	30	50	6
PnTX H	708,5	**440,3**	164,1	35	55	10,5	30	50	6
PnTX A	712,5	**458,3**	164,1	35	55	10,5	30	50	6
PnTX B,C	741,5	**458,3**	164,1	35	55	10,5	30	50	8
PnTX F	766,5	**446,3**	164,1	35	55	10,5	30	50	8
PnTX D	782,5	**446,3**	164,1	35	55	10,5	30	50	6
PnTX E	784,5	**446,3**	164,1	35	55	10,5	30	50	6
PTERIATOXINS (PtTXs)									
PtTX A, B, C	831,4	**458,3**	164,1	35	55	10,5	30	50	6

DP = Declustering Potential (V); EP = Entrance Potential (V); CEP= Cell Entrance Potential(V); CE = Collision Energy (eV); CXP = Cell Exit Potential (V).

Table 1.4: MS/MS transitions for AZAs.

Toxin	Prec. Ion (m/z)	Prod. ion 1 (m/z)	Dwell time (msec)	DP	EP	CEP	CE	CXP
AZA33	716,5	698,5	35	81	4.5	64	55	6
AZA33 P	796,5	778,5	35	81	4.5	64	55	6
AZA25	810,5	792,5	35	81	4.5	76	55	8
AZA34, 39	816,5	798,5	35	81	4.5	76	55	8
AZA26, 27	824,5	806,5	35	81	4.5	68	55	6
AZA48	826,5	808,5	35	81	4.5	68	55	6
AZA3, epi, 43, 58, 60	828,5	810,5	35	81	4.5	68	55	6
AZA35, 38, 52, 53	830,5	812,5	35	81	4.5	64	55	6
AZA28	838,5	820,5	35	81	4.5	64	55	6
AZA49	840,5	822,5	35	81	4.5	76	55	8
AZA1, epi, 6, 29, 40, 50	842,5	824,5	35	81	4.5	76	55	8
AZA4	844,5	826,5	35	81	4.5	68	55	6
AZA5	844,5	826,5	35	81	4.5	68	55	6
AZA56 o 57	844,5	826,5	35	81	4.5	68	55	6
AZA37	846,5	828,5	35	81	4.5	64	55	6
AZA41	854,5	836,5	35	81	4.5	64	55	6
AZA2, Me-AZA1,epi,30	856,5	838,5	35	81	4.5	76	55	8
AZA7,epi,8,9,10,36,51	858,5	840,5	35	81	4.5	76	55	8
AZA13,59	860,5	842,5	35	81	4.5	68	55	6
AZA55	868,5	850,5	35	81	4.5	68	55	6
Me-AZA2,32,42,54,62	870,5	852,5	35	81	4.5	68	55	6
AZA11,12,17	872,5	854,5	35	81	4.5	64	55	6
AZA14,15	874,5	856,5	35	81	4.5	64	55	6
AZA57 o 56	884,5	866,5	35	81	4.5	76	55	8
AZA18,19	886,5	868,5	35	81	4.5	76	55	8
AZA16,21,44	888,5	870,5	35	81	4.5	68	55	6
AZA34 P,39 P	896,5	878,5	35	81	4.5	68	55	6
AZA20,31	900,5	882,5	35	81	4.5	68	55	6
AZA22,23,45,46	902,5	884,5	35	81	4.5	64	55	6
AZA52 P,35 P,38 P,53 P	910,5	892,5	35	81	4.5	64	55	6
AZA24	916,5	898,5	35	81	4.5	76	55	8
AZA47	918,5	900,5	35	81	4.5	76	55	8
AZA1 P,7 P,40 P,50 P	922,5	904,5	35	81	4.5	68	55	6
AZA37 P	926,5	908,5	35	81	4.5	68	55	6
AZA41 P	934,5	916,5	35	81	4.5	68	55	6
AZA2 P	936,5	918,5	35	81	4.5	64	55	6
AZA36 P	936,5	920,5	35	81	4.5	64	55	6
AZA51 P	938,5	920,5	35	81	4.5	76	55	8
AZA59 P	940,5	842,5	35	81	4.5	76	55	8
AZA42 P,54 P,62 P	950,5	932,5	35	81	4.5	68	55	6
AZA11-phosphate	952,5	934,5	35	81	4.5	68	55	6

Toxin	Prec. Ion (m/z)	Prod. Ion 2 (m/z)	Dwell time (msec)	DP	EP	CEP	CE	CXP
AZA33	716,5	462,5	35	81	4.5	64	55	6
AZA33 P	796,5	760,5	35	81	4.5	64	55	6
AZA25	810,5	658,5	35	81	4.5	76	55	8
AZA34	816,5	462,5	35	81	4.5	76	55	8
AZA39	816,5	448,5	35	81	4.5	68	55	6
AZA26	824,5	672,5	35	81	4.5	68	55	6
AZA27	824,5	788,5	35	81	4.5	68	55	6
AZA48	826,5	362,5	35	81	4.5	64	55	6
AZA3, epi AZA3, AZA58	828,5	658,5	35	81	4.5	64	55	6
AZA43	828,5	360,5	35	81	4.5	76	55	8
AZA60	828,5	348,5	35	81	4.5	76	55	8
AZA35	830,5	462,5	35	81	4.5	68	55	6
AZA38	830,5	448,5	35	81	4.5	68	55	6
AZA52, AZA53	830,5	348,5	35	81	4.5	68	55	6
AZA28	838,5	362,5	35	81	4.5	64	55	6
AZA49	840,5	362,5	35	81	4.5	64	55	6
AZA1, epi AZA3	842,5	672,5	35	81	4.5	76	55	8
AZA6	842,5	658,5	35	81	4.5	76	55	8
AZA29, AZA50	842,5	362,5	35	81	4.5	68	55	6
AZA40	842,5	348,5	35	81	4.5	68	55	6
AZA4	844,5	448,5	35	81	4.5	68	55	6
AZA5	844,5	464,5	35	81	4.5	64	55	6
AZA56 o 57	844,5	362,5	35	81	4.5	64	55	6
AZA37	846,5	448,5	35	81	4.5	76	55	8
AZA41	854,5	670,5	35	81	4.5	76	55	8
Me-AZA1, AZA2, epi AZA2	856,5	672,5	35	81	4.5	68	55	6
AZA30	856,5	820,5	35	81	4.5	68	55	6
AZA7, epi AZA7	858,5	672,5	35	81	4.5	68	55	6
AZA8	858,5	688,5	35	81	4.5	64	55	6
AZA9	858,5	658,5	35	81	4.5	64	55	6
AZA10	858,5	674,5	35	81	4.5	76	55	8
AZA36	858,5	448,5	35	81	4.5	76	55	8
AZA51	858,5	348,5	35	81	4.5	68	55	6
AZA13	860,5	674,5	35	81	4.5	68	55	6
AZA59	860,5	362,5	35	81	4.5	68	55	6
AZA55	868,5	362,5	35	81	4.5	64	55	6
Me-AZA2, AZA42, AZA54, AZA62	870,5	834,5	35	81	4.5	64	55	6
AZA32	870,5	362,5	35	81	4.5	76	55	8
AZA11	872,5	672,5	35	81	4.5	76	55	8
AZA12	872,5	688,5	35	81	4.5	68	55	6
AZA17	872,5	658,5	35	81	4.5	68	55	6
AZA14	874,5	688,5	35	81	4.5	68	55	6
AZA15	874,5	674,5	35	81	4.5	64	55	6
AZA57 o 56	884,5	848,5	35	81	4.5	64	55	6
AZA18	886,5	850,5	35	81	4.5	76	55	8

Toxin	Prec. Ion (m/z)	Prod. Ion 2 (m/z)	Dwell time (msec)	DP	EP	CEP	CE	CXP
AZA19	886,5	658,5	35	81	4.5	76	55	8
AZA16	888,5	688,5	35	81	4.5	68	55	6
AZA21	888,5	658,5	35	81	4.5	68	55	6
AZA44	888,5	362,5	35	81	4.5	68	55	6
AZA34 P, AZA39 P	896,5	860,5	35	81	4.5	64	55	6
AZA20, AZA31	900,5	864,5	35	81	4.5	64	55	6
AZA22, AZA45	902,5	866,5	35	81	4.5	76	55	8
AZA23	902,5	658,5	35	81	4.5	76	55	8
AZA46	904,5	868,5	35	81	4.5	68	55	6
AZA52 P, AZA35 P, AZA38 P, AZA53 P	910,5	874,5	35	81	4.5	68	55	6
AZA24	916,5	880,5	35	81	4.5	68	55	6
AZA47	918,5	882,5	35	81	4.5	64	55	6
AZA1 P, AZA7 P	922,5	802,5	35	81	4.5	64	55	6
AZA40 P, AZA50 P	922,5	886,5	35	81	4.5	76	55	8
AZA37 P	926,5	890,5	35	81	4.5	76	55	8
AZA41 P	934,5	898,5	35	81	4.5	68	55	6
AZA2 P	936,5	802,5	35	81	4.5	68	55	6
AZA36 P	936,5	902,5	35	81	4.5	68	55	6
AZA51 P	938,5	902,5	35	81	4.5	64	55	6
AZA59 P	940,5	824,5	35	81	4.5	64	55	6
AZA42 P, AZA54 P, AZA62 P	950,5	914,5	35	81	4.5	76	55	8
AZA11-phosphate	952,5	818,5	35	81	4.5	76	55	8

DP = Declustering Potential (V); EP = Entrance Potential (V); CEP= Cell Entrance Potential(V); CE = Collision Energy (eV); CXP = Cell Exit Potential (V).

Analytical performances evaluation

The performances of the quantitative procedure for CIs and AZAs were studied only for the toxins with certified reference standards. Instrumental linearity was investigated by the matrix-matched calibration curves on 5 concentration levels (0.2, 0.3, 0.6, 1.0, 2.0 ng mL^{-1}) for 13-desMe SPX C and GYM A, on 7 concentration levels (1, 3, 6, 10, 20, 30, 40 ng mL^{-1}) for AZA1, AZA2 and AZA3. All the calibration points were injected in triplicate in different days and the curves (y = bx + a) were obtained plotting the toxins chromatographic peak areas (y) against their concentrations (x). The best-fit curves were obtained using the least squares regression model. Linearity was evaluated from the correlation coefficients. The quantification limit (LOQ) was

calculated based on a signal/noise (S/N) ratio. The limit of detection (LOD) was derived from the LOQ by dividing by 3.3. Subsequently, the estimated LOQ was experimentally confirmed by spiking blank mussel samples with the available standards.

Accuracy in terms of recovery (R%) and precision in terms of intra-day repeatability (intra-day relative standard deviation RSDr%) for CIs and of within-laboratory reproducibility (inter-day relative standard deviation RSD_R%) for AZAs were calculated, performing replicated analyses (N = 6 in 1 day) on blank mussel samples spiked at 1.0 µg kg^{-1} with 13-desMe SPX C and 1.0 µg kg^{-1} with GYM A, and replicate analyses (N = 12 in 6 days) on blank mussel samples spiked at 10 µg kg^{-1} with AZA1, AZA2 and AZA3 respectively. These levels were chosen because showed the suitable standard deviations in the experiments carried out. The drift in the retention times was considered acceptable if below 1%.

A double stage analytical approach was implemented to make the investigation of CIs and AZAs easier and reliable. A qualitative screening was performed monitoring only one characteristic fragment. If the transition was detected, the toxins were confirmed monitoring a second fragment more diagnostic and quantified.

Matrix-matched calibration curves were used because of the non-negligible matrix effect. Assuming an equimolar response, analogues belonging to the SPX group were quantified with the analogue 13-desMe SPX C, GYMs with GYM A, PnTXs and PtTXs with PnTX G. As regards AZAs, AZA1 was used to quantify all the AZA analogues except AZA2 and AZA3 that were quantified with own certified standards respectively.

1.3 Results and Discussion

1.3.1 Method performances

The developed method was able to reveal the CIs and AZAs presence in mussels from the North-Central Adriatic Sea with good analytical performances. The results obtained in terms of linearity, accuracy (R%), precision (RSDr% for CIs and RSD_R% fro AZAs) are reported in the Table 1.5.

Table 1.5: Validation parameters of LC-MS/MS method for CIs and AZAs.

Toxins	Linearity (R^2)	Accuracy (R%)	LOQ (µg kg^{-1})	LOD (µg kg^{-1})	Precision (RSDr % for CIs RSD_R% for AZAs)
GYM A 13-desMe SPX C	> 0.99	94 (GYM A) 92 (13-desMe SPX C)	0.45	0.14	5 (GYM A) 9 (13des-Me SPX C)
AZA1, AZA2, AZA3	> 0.99	101 (AZA1) 99 (AZA2) 97 (AZA3)	0.6	0.18	11 (AZA1, AZA2, AZA3)

The drift in the retention times was widely below 1%. Moreover, the method was tested using the matrix reference material FDMT1 obtaining successful results in terms of identification and quantification with an accuracy (R%) ranging from 89 to 116 %.

For phytoplankton, the method was tested on the SZN-B848 strain of *Azadinium dexteroporum* isolated in the Gulf of Naples [65] and used to perform exposure experiment in previous research [37]. The toxic profile obtained was similar to that described by Rossi et al. [38], where the principal analogues were AZA54, 3-epi-AZA7 and AZA55.

1.3.2 LC-MS/MS analysis of phytoplankton

The LC-MS/MS analysis of the monoclonal cultures, previously identified as potentially toxic, did not show detectable levels of toxins (Table 1.6).

Table 1.6: Phytoplankton samples analyzed by LC-MS/MS.

Number	*Taxon*	Identification code	Toxins potentially produced	station	Isolation time
1	*Alexandrium* sp.	6192	PSP + spirolides	SG01	06/2019
2	*Alexandrium* sp.	219	PSP + spirolides	SG01	18/02/2019
3	*Alexandrium* sp.	DINSEN06193	PSP + spirolides	SG01	06/2019
4	*Alexandrium* sp.	DINSEN06192	PSP + spirolides	SG01	06/2019
5	*Alexandrium* sp.	Alex06191	PSP + spirolides	SG01	09/2019
6	Amphidomataceae	A	Azaspiracids	PN	26/04/2021
7	Amphidomataceae	B	Azaspiracids	PN	26/04/2021
8	Amphidomataceae	C	Azaspiracids	PN	26/04/2021
9	Amphidomataceae	D	Azaspiracids	PN	08/2021
10	Amphidomataceae	E	Azaspiracids	PN	08/2021
11	Amphidomataceae	F	Azaspiracids	PN	08/2021
12	Amphidomataceae	H	Azaspiracids	PN	08/2021
13	Amphidomataceae	I	Azaspiracids	PN	08/2021
14	Amphidomataceae	M	Azaspiracids	PN	08/2021
15	Amphidomataceae	N	Azaspiracids	PN	08/2021
16	Amphidomataceae	O	Azaspiracids	PN	08/2021
17	Amphidomataceae	Q	Azaspiracids	PN	08/2021
18	Amphidomataceae	05 4	Azaspiracids	SG01	05/2019
19	Amphidomataceae	06 3	Azaspiracids	SG01	06/2019
20	Amphidomataceae	06 4	Azaspiracids	SG01	06/2019
21	Amphidomataceae	05 6	Azaspiracids	SG01	05/2019
22	Amphidomataceae	06 2	Azaspiracids	SG01	06/2019
23	Amphidomataceae	05 5	Azaspiracids	SG01	05/2019
24	Amphidomataceae	05 3	Azaspiracids	SG01	05/2019
25	Amphidomataceae	06 1	Azaspiracids	SG01	06/2019
26	Amphidomataceae	AZA1	Azaspiracids	SG01	04/2021
27	Amphidomataceae	AZA2	Azaspiracids	SG01	04/2021
28	Amphidomataceae	AZA3	Azaspiracids	SG01	04/2021
29	Amphidomataceae	AZA4	Azaspiracids	SG01	04/2021
30	Amphidomataceae	AZA5	Azaspiracids	SG01	04/2021
31	Amphidomataceae	Aza6	Azaspiracids	SG01	04/2021
32	Amphidomataceae	Aza7	Azaspiracids	SG01	04/2021
33	Amphidomataceae	Aza8	Azaspiracids	SG01	04/2021
34	Amphidomataceae	6192	Azaspiracids	SG01	06/2019
35	Amphidomataceae	DINSEN06194	Azaspiracids	SG01	06/2019
36	Amphidomataceae	DINO060821 (AZA-like)	Azaspiracids	PN	06/08/2021
37	Amphidomataceae	170621 1	Azaspiracids	PN	17/06/2021
38	Amphidomataceae	AZALIKE260421	Azaspiracids	PN	26/04/2021

1.3.3 CIs in mussels

Only SPXs and GYMs were found at low levels in 497 (85%) of 602 samples analyzed. SPXs were the most abundant toxins, detected in the 72% of samples analyzed, with a maximum contamination of 13 µg Kg^{-1} recorded in in the first part of the year (January-April). The 13-desMe SPX C and the 13,19-didesMe SPX C were the only two SPX analogues found, their seasonal trends are reported in Figure 1.4.

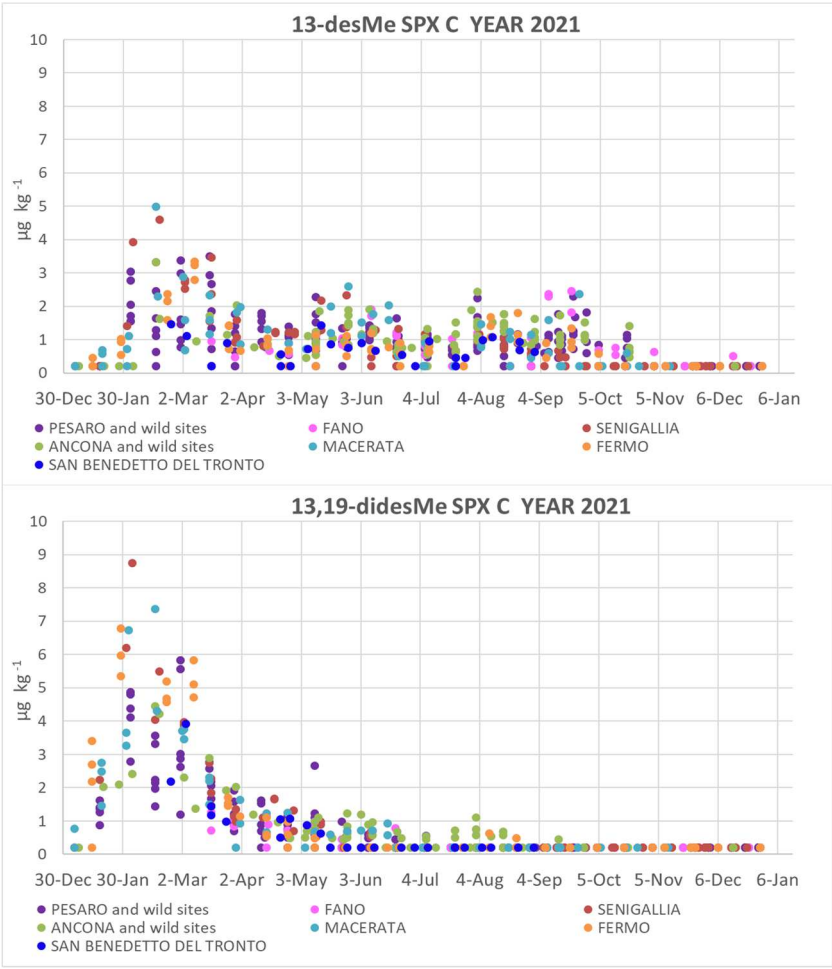

Figure 1.4: Seasonal trends of 13-desMe SPX C and the 13,19-didesMe SPX C in mussels from Marche coast in 2021.
*Non quantifiable data were reported as 0.2 µg kg^{-1} (½ LOQ, medium bound approach).

The two toxins showed the highest concentrations between January and March, but the 13-desMe SPX C was present all over the year, although at low levels, instead the 13,19-didesMe SPX C showed a maximum of contamination in the first part of the year but became undetectable at the end of 2021. The mussel toxic profile matched with that described by Bacchiocchi et al. in mussels from Marche coast between 2014 and 2015 [26] and Ciminiello et al. in mussels from Emilia Romagna in 2003 [25]. The SPX levels found in 2021 were however lower than those detected in 2014-2015 in mussels from the Marche coast while the seasonal trend fitted perfectly with that already described [26]. As previously observed, the seasonal trend seems to be different from the known one for the other lipophilic toxins (okadaic acid and yessotoxins) which accumulate in shellfish during and or just after summer and reach the highest levels in autumn [27], in agreement with the well described phytoplankton dynamic in the Adriatic Sea [68-69]. SPX primary producer's probably exhibit different ecophysiological characteristics, since SPX contamination in mussels reached its maximum in winter [26, 70]. The 13-desMe SPX C is generally reported as the major analogue of the SPX contamination in European shellfish [19], but the different SPX profile found in this study can be explained by the variable toxin production of phytoplankton. Various SPX profiles in *A. ostenfeldii* strains have been described in the literature [71-73]. Some studies demonstrated that SPX proportions can vary considerably depending on factors such as salinity, temperature and light intensity [73]. However, although 13-desMe SPX C was the most frequently observed analogue in the *A. ostenfeldii* toxin profile [74], the 13,19-didesMe SPX C, if present, resulted often predominant [73, 75-76]. Another possible explanation for the SPX profile variation in mussels could be the different detoxification kinetics towards the individual

SPX compounds, as a result of the different molecular structures and therefore, different tissue affinity [26].

Due to low detected levels, it was not possible to describe a geographical trend, unlike of samples contaminated by SPXs in 2014-2015, where higher concentrations generally reached in the southern Marche coast [26].

The low contamination levels found in mussels caused by a likely low number of microalgal cells in seawater could justify the difficulty in isolating and identifying the SPX primary producer.

Only traces of GYM A were found in 10% of samples analyzed with a maximum level of 4 µg Kg^{-1}. Its presence was reported in Italian coastal waters, for the first time, in mussels during 2014-2015 at higher levels (12 µg Kg^{-1}) [26]. GYM A contaminations in mussels were detected in in August and December, as already occurred in 2014-2015. Unlike SPXs, the presence of this toxin is linked to seasonal biomass growth dynamics as for other marine lipophilic toxins [27]. This findings suggests that the GYM A primary producer may be different from that of SPXs. Because of low contamination levels, it was difficult to carry out a seasonal and geographical trend.

1.3.4 AZAs in mussels

AZAs were detected in mussels from Marche coast in the majority of analysed samples (92%), even if at low levels. The maximum concentration recorded was of 13 µg AZA eq. Kg^{-1}. AZA2 was the predominant analogue (65-100%) in the mussel toxin profile but in the higher contaminated samples traces of AZA1 were also found (0-30%).

The mussel toxic profile matched with that described by Bacchiocchi et al. in mussels from Marche coast between 2012 and 2013, that represented the first evidence of the presence of AZAs in Mediterranean seafood [27].

This toxin profile differs from that generally reported for shellfish of the North Sea [64] but resembles that described for shellfish from the Atlantic coasts of Morocco and Portugal, perhaps as a consequence of the presence of AZA producers other than *Azadinium spinosum* such as *Azadinium poporum* [77]. In 2021 the AZAs levels detected were approximately double those previously found [27]; moreover AZA2 is the regulated toxin with the highest toxicity.

The seasonal trend of AZA contamination expressed as sum of AZA1 and AZA2, in terms of Toxicity Equivalency (TEQ) is reported in Figure 1.5. In 2021 two periods of AZA maximum accumulation were identified, during April-July in the South of the region and October-December in the North area. The seasonal trend fitted well with that already reported by Bacchiocchi et al. [27], but in 2021 the maximum concentrations were recorded in autumn-winter, instead in 2012-2013 in the summer.

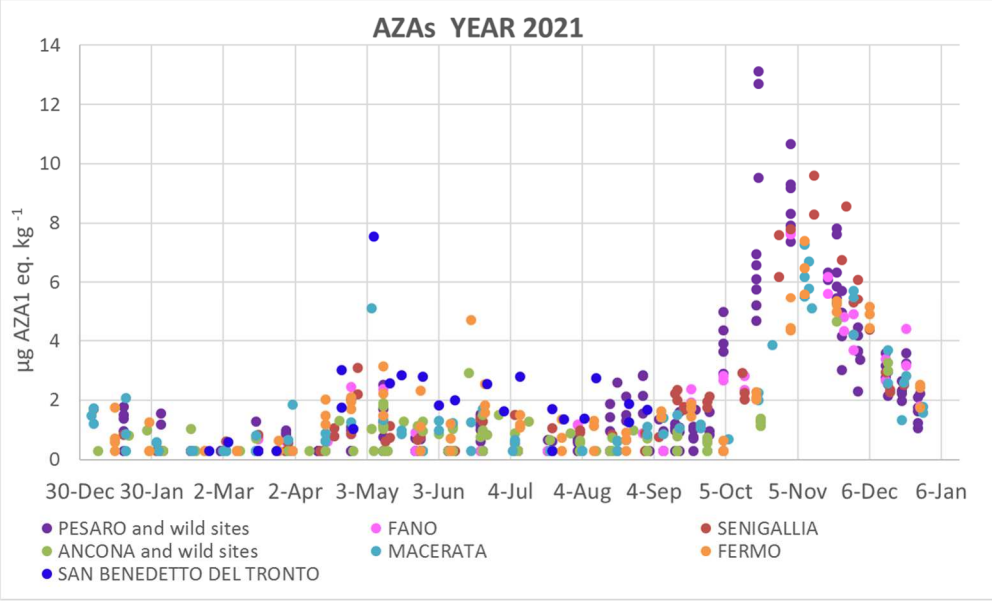

Figure 1.5: Seasonal trends of AZAs in mussels from Marche coast in 2021.
*Non quantifiable data were reported as 0.3 µg kg^{-1} (½ LOQ, medium bound approach).

Considering these results, the critical periods identified for two AZA episodes are in agreement with the phytoplankton dynamic in the Adriatic Sea. Two major annual biomass increases are identified: the first in spring/early summer, corresponding to the general increased irradiance, water thermal stratification and nutrient availability in seawater, and the second in autumn, mainly caused by new nutrient input due to the increased inflow of freshwater from the Po River [68-69].

Moreover in 2021, in concomitance with AZA traces, high levels of okadaic acid often above the MPL were found, then this confirms that the phytoplankton dynamic for these toxins is similar to other marine lipophilic toxins [27]. For the same reasons of CIs, the low contamination levels found in mussels might suggest a likely low number of toxic microalgal cells in seawater, justifying the lack of AZA primary producer isolation.

Chapter 2

Study of TTX presence and its origin in the North-Central Adriatic Sea

The contents described in this chapter have been reported in the following papers:

- Bacchiocchi, S.; Campacci, D.; **Siracusa, M**.; Dubbini, A.; Leoni, F.; Tavoloni, T.; Accoroni, S.; Gorbi, S.; Giuliani, M.E.; Stramenga, A.; Piersanti, A. Tetrodotoxins (TTXs) and *Vibrio alginolyticus* in Mussels from Central Adriatic Sea (Italy): Are They Closely Related? *Marine Drugs* **2021**, 19, 304.

- Bacchiocchi, S.; Campacci, D.; **Siracusa, M**.; Dubbini, A.; Accoroni, S., Romagnoli, T.; Campanelli, A.; Griffoni, F.; Tavoloni, T.; Gorbi, S., Totti, C.; Piersanti, A. A Hotspot of TTX Contamination in the Adriatic Sea: Study on the Origin and Causative Factors *Marine Drugs* **2023**, 21, 8.

2.1 Introduction

Tetrodotoxins (TTXs) are surely the most famous compounds, among EMBs, for the lethal pufferfish poisoning they cause in humans. TTX is the best-known member of the group, but it co-exists with some other natural occurring congeners. There have been 30 structural analogues reported to date, with different degrees of toxicity depending on their chemical structure [78-79].

In Figure 2.1 the most investigated TTX analogues are illustrated.

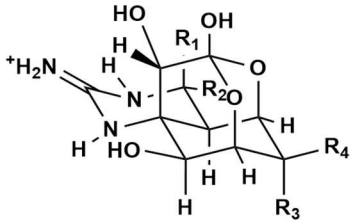

Toxin	R_1	R_2	R_3	R_4
TTX	H	OH	OH	CH_2OH
4-epi-TTX	OH	H	OH	CH_2OH
11-deoxy TTX	H	OH	OH	CH_3
6,11-dideoxy TTX	H	OH	H	CH_3
11-norTTX-6(S)-ol	H	OH	OH	H
11-norTTX-6(R)-ol	H	OH	H	OH

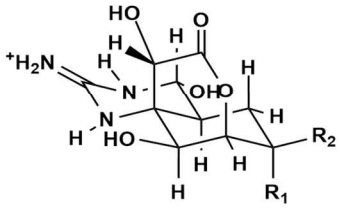

Toxin	R_1	R_2
5-deoxy TTX	OH	CH_2OH
5,6,11-trideoxy TTX	H	CH_3

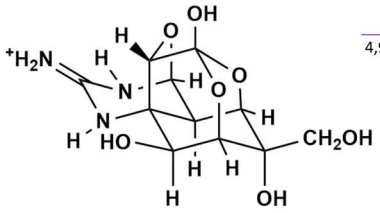

Toxin
4,9-anhydro TTX

Figure 2.1: Molecular structure of the most investigated TTX analogues.

Despite the TTXs' chemical structures and the toxicity mechanism are already well known, this toxin group is still deeply studied because its origin, biosynthetic pathway, and the mechanism of its accumulation in organisms are still uncertain. TTX, as a result of symbiotic bacterial synthesis by different species of genus *Vibrio*, *Bacillus*, *Pseudomonas*, *Actinomyces*, and *Micrococcus* has been widely documented [80-83], in particular *V. alginolyticus* and *V. parahaemolyticus* are the most frequently reported [84-86]. However, some authors suggested the possible involvement of microalgal dinoflagellates [87-89]. The hypotheses on biosynthetic pathway of TTX in bacteria are based on the involvement of enzymes such as the non-ribosomal peptide synthetase (NRPS) and the polyketide synthase (PKS) [90-91]. Therefore, NRPS and PKS encoding genes have been targeted in protocols for detection of potential TTX-producing bacteria [86].

Assuming as the most likely the bacterial origin of TTX, it is difficult to explain the high toxin levels found in some organisms taking into account the very low level of *in vitro* bacteria toxin production [92]. Then two hypotheses have been proposed: an enhanced TTX synthesis by TTX producer bacteria inside their endosymbiotic hosts (endogenous hypothesis) or an accumulation of toxins throughout the food web (exogenous hypothesis) [93].

Historically associated only to pufferfish, TTXs have been thought for a long time a risk limited to the Indo-Pacific area (Japan, Thailand, Bangladesh and the Philippines), where the consumption of this type of fish causes several deaths every year [79]. The Japanese regulations for food safety specify a limit of 2 mg TTX eq. kg^{-1} [20]. Recently TTXs were found in bivalves and gastropods from diverse geographical areas within European waters (Greece, the UK, the Netherlands, Spain, Portugal [85-86, 88, 94-95]. Specific environmental features such as low salinity, shallow water seemed to play a role as causative factors in TTX findings [86, 95-96]. TTXs were detected also in Italy, in shellfish from Syracuse Bay (Sicily) [28], and Marano Lagoon (Friuli Venezia Giulia) [29].

TTXs are not yet regulated and only a guidance level is established in shellfish meat [20]. Moreover, the European legislation imposes the ban on the sale of poisonous Tetraodontidae and derived products [13].

The aim of this chapter was to investigate by LC-MS/MS analysis, contamination level and spatio-temporal trends of TTX in mussels from the natural beds of Marche Region. Moreover microbiological and molecular analyses were performed to characterize *Vibrio* spp. as potential TTX-producer bacteria from various matrices. To better evaluate the TTX risk biotic and abiotic matrices from the specific sampling point *Molo Portonovo* were analysed.

2.2 Materials and Methods

2.2.1 Sampling

Mussel samples (*Mytilus galloprovincialis*) were collected from May to September 2021 with biweekly frequency from 7 natural beds and a mussel breeding site located along the Marche coast (North-Central Adriatic Sea, Italy, Figure 2.2). In natural beds, mussels live clinging to rocks generally in shallow water (<5 m) near the cliffy coast. Three natural beds are located in the Pesaro area (named Sotto la Croce, Vallugola and Mississipi) and 4 in the Ancona's along the Conero Riviera (named Ancona Nord, Ancona Sud, Sirolo Nord and Sirolo Sud). In the mussel farm (Coop PN), located in the Portonovo Bay (Conero Riviera), mussels grow attached to a submerged concrete structure in shallow water (<5 m) exhibiting very similar environmental features to natural beds. Moreover, a further specific sampling point named *Molo Portonovo* (MP, 43° 33′ 55″ N, 3° 35′ 26″ E, Figure 2.2) was sampled with a weekly frequency from June to August 2021. In each sampling day, the meteorological parameters were recorded. A CTD Model 30 Handheld Salinity, Conductivity and Temperature System, YSI (Yellow Spring, OH USA) was used to measure surface temperature and salinity.

To better investigate the TTX distribution and circulation in the ecosystem not only mussels but additional biotic and abiotic matrices were collected in MP site. Mussels were harvested from natural beds, sediment samples (50 g) were collected using sterile Falcon tubes directly on the sediment surface by SCUBA divers, as well as surface sea water (50 mL) was collected with sterile Falcon. Phytoplankton was sampled through a net (mesh diameter 20 µm). Overall, 64 samples of mussels from the 7 natural beds and the mussel breeding site along Marche coast and 11 samples of mussels (and other biotic and abiotic matrices) were collected from the specific MP site and subjected to chemical and microbiological analyses.

Figure 2.2: Sampling sites along the Marche coast. Seven officially monitored natural beds: Mississipi, Vallugola, Sotto la Croce (Pesaro area), Ancona nord, Ancona sud, Sirolo nord, Sirolo sud, the breeding site Coop PN and the not routinely monitored natural bed Molo Portonovo (MP) (Ancona area). Images (data SIO, NOAA, U.S. Navy, NGA, GEBCO; image Landsat/Copernicus) are from Google Earth.

After collection, samples were transported to the laboratory in refrigerated conditions (4 °C) and immediately processed for microbiological analysis. Further aliquots were frozen until the chemical analysis.

2.2.2 Chemical analysis

Chemicals and Standards

All the reagents were of analytical grade: acetonitrile (LC-MS grade), methanol (HPLC grade), ammonium hydroxide (≥25% in water, LC-MS grade) formic acid (LC-MS grade) and glacial acetic acid (reagent grade). Ultrapure water (18.2 MΩ cm) was produced by a MilliQ water purification system (Millipore Ltd., Bedford, MA, USA).

Tetrodotoxin Certified Reference Material (CRM-003-TTXs) was obtained from Cifga Laboratory (Lugo, Spain). The CRM was a mixture of tetrodotoxin (25.9 ± 1.2 μg g^{-1}) and 4,9-anhydro tetrodotoxin (2.99 ± 0.16 μg g^{-1}).

A stock solution in water was prepared from the CRM. Matrix-matched calibration standards were obtained for dilution of the stock solution using and extract of a blank sample. Moreover, the stock solution was used to prepare quality control for testing method performances.

Sample treatment

Once arrived in the laboratory, mussel were immediately opened, and organisms colonizing the mussel bed were harvested directly from the valves or from the water collected with mussels picking them up with tweezers or with a pipette. Flatworms, identified as *Stylochus mediterraneus* (1–3 specimens), and/or small crustaceans (5–10 specimens of 0.1–1.0 cm size, mesozooplankton) were sampled and finely homogenized by Ultra Turrax.

As regards the mussels, sand and solid residues were removed under running water, then were taken out of the shells and drained on a net. For each sample, about 150 g of whole flesh, was pooled and finely homogenized by an Osterizer blender. Ten specimens of the ten contaminated mussel samples harvested on 9 and 22 June from the Conero Riviera natural beds were dissected, and the digestive gland (DG), gills (G), mantle (M) and the remaining tissues (RT) were pooled for each sample and weighted to calculate their contribution to the whole body. The pools were then finely homogenized by Ultra Turrax mixer and analyzed separately in order to investigate the tissues distribution of TTXs.

Phytoplankton-net samples were centrifuged at 3000 x g for 10 min and pellets collected.

All the homogenates prepared as described above, were stored at –20 °C until chemical analysis.

TTX extraction from mussels, flatworms and mesozooplankton

The extraction was performed following the EU-SOP "Determination of Tetrodotoxin by HILIC-MS/MS" [40], with some modifications. The clean-up step was removed, and only the final dilution was applied to reduce matrix effect. Moreover, the applicability of the method was extended to other matrices such as flatworms and mesozooplankton. The details are described below. Homogenates (5.0 ± 0.1 g for mussels or mussel tissues, 2.0 ± 0.1 g for flatworms and 0.5 ± 0.01 g for mesozooplankton) were extracted with 5 mL (or 2 mL for flatworms and mesozooplankton) of acetic acid (1% v/v), vortex-mixed for 3 min and placed in a boiling water bath (100 ˚C) for 5 min. The extract was cooled to room temperature, vortex-mixed for 3 min and centrifuged at 3000 x g for 10 min. Supernatant (1 mL) was transferred to a microcentrifuge tube, to which 5 µL ammonium hydroxide was added, and the sample was vortex-mixed for 3 min and centrifuged at 10000 x g per 1 min. The final extract was diluted (1:2) with a solution of acetonitrile (80% v/v) containing acetic acid (0.25% v/v), filtered through a syringe filter (0.2 µm in nylon), and analyzed by HILIC-MS/MS.

TTX extraction from phytoplankton-net

Phytoplankton-net pellets (0.1 ± 0.01 g) were extracted with 2 mL of acetic acid (1% v/v), vortex-mixed for 3 min and bath-sonicated for 10 min. After sonication, the aliquots were centrifuged for 10 min at 2500 x g (4 °C), and the supernatants were transferred to a 100 mL evaporation flask. Pellets extraction was repeated three times, and the supernatants were combined and evaporated to dryness by a rotavapor. The residue was reconstituted in 1 mL of acetonitrile (80% v/v) containing acetic acid (0.25% v/v) and filtered through a syringe filter (0.2 µm in nylon) and analyzed by HILIC-MS/MS.

LC-MS/MS conditions

Instrumental analysis was performed on the ACQUITY I-Class-Xevo TQ-S micro IVD system (Waters, Milford, MA, USA) equipped with electrospray ionization (ESI) source. The chromatographic separation was achieved according to the EU-SOP "Determination of Tetrodotoxin by HILIC-MS/MS" [40], the details are reported in Table 2.1.

Table 2.1: HILIC conditions for TTX analysis.

LC PARAMETERS			
Column	Glycan BEH Amide 130 Å 1.7µm, 2.1x150 mm (Waters)		
Injection Volume	2 µL		
T° Column manager	60 °C		
T° Sample manager	6 °C		
Mobile phase A	500 mL H_2O + 300 µL NH_4OH + 75 µL CH_2O_2		
Mobile phase B	700 mL CH_3CN + 300 mL H_2O + 100 µL CH_2O_2		
Time(min)	**Flow (mL/min)**	**A (%)**	**B (%)**
0.00	0.4	2	98
7.00	0.4	2	98
9.50	0.4	50	50
11.00	0.5	50	50
11.50	0.5	2	98
12.00	0.6	2	98
12.50	0.6	2	98
13.00	0.4	2	98
14.00	0.4	2	98

Infusion experiments were performed on TTX CRM to optimize the mass parameters.

Nine analogues were monitored via Multiple Reaction Monitoring (MRM), with two transitions selected for each toxin to allow correct identification and quantification. The MS acquisition method is described in Table 2.2.

Table 2.2: MS parameters and MRM transitions for TTX analysis.

MS/MS PARAMETERS					
Source type	ESI				
Capillary	3,5 kV				
Desolvatation temperature	600 °C				
Desolvatation	1000 L/Hr				
Cone	150 L/Hr				
Source temperature	150 °C				
Ionization mode	ESI^+				
MRM TRANSITIONS					
Compound	**Prec. ion (m/z)**	**Prod. ion (m/z)**	**Dwell (sec)**	**Cone (V)**	**CE (V)**
TTX/4-epi TTX	320.1	302.1	0.026	40	30
		162.1	0.026	40	40
11-nor TTX-6-ol/ 6,11-dideoxyTTX	290.1	272.1	0.026	40	30
		162.1	0.026	40	30
5-DeoxyTTX/ 11-Deoxy TTX	304.1	286.1	0.026	40	30
		162.1	0.026	40	30
11-oxo-TTX	336.1	318.1	0.026	40	30
		300.1	0.026	40	30
5,6,11 TrideoxyTTX	272.1	254.1	0.026	40	30
		162.1	0.026	40	30
4,9-anhydroTTX	302.1	256.1	0.026	40	30
		162.1	0.026	40	30

The unequivocal identification of the TTX chromatographic peak was obtained by retention time comparison and ion ratio verification for the two characteristic transitions in the samples and in a matrix-matched standard. All the other analytes, for which no reference materials were available, were identified by selecting specific transitions from the literature.

Analytical method performance assessment

Method performances were evaluated through in-house validation in mussels, focusing on TTX, which was the only CRM available. The instrument used was a hybrid triple–quadrupole/linear ion trap 3200 QTRAP mass spectrometer (AB Sciex, Darmstadt, Germany) equipped with a Turbo V source, an electrospray ionization (ESI) probe and coupled to an Agilent 1200 HPLC (Palo Alto, CA, USA).

Linearity was investigated via matrix-matched calibration curves on 6 concentrations, (6.5, 13, 19, 26, 65, 130 ng mL^{-1}), prepared in triplicate and run for intra-laboratory reproducibility. The mussels used for matrix-matched calibration curve preparation showed TTX levels <LOD. The calibration curves ($y = bx + a$) were obtained by plotting the toxin's chromatographic peak areas (y) against concentrations (x). The best-fit curves were obtained by using the least-squares regression model. Linearity was evaluated from the correlation coefficients and response factor variation.

LOQ was estimated as the concentration giving S/N ratio of 10, for the least intense (qualifier) transition monitored. The LOD used was derived from the LOQ by dividing by 3.3. Subsequently, the estimated LOQ was experimentally confirmed by spiking blank mussel samples with the TTX CRM. Accuracy in terms of R% and precision in terms of intra-day repeatability (intra-day relative standard deviation RSDr%) were assessed by replicated analyses (N = 6) on blank mussel samples spiked at 75 µg kg^{-1} and 251 µg kg^{-1} (TTX levels often found in European shellfish).

Subsequently the method was transferred to a new generation instrument ACQUITY I-Class-Xevo TQ-S micro IVD system (Waters, Milford, MA, USA) described above, by which the sample analyses reported in this PhD project were carried out.

The performances in terms of linearity, accuracy and precision were only checked. Instead, the LOQ and LOD were recalculated being the new instrument more sensible.

All analogs included in the method, were quantified with TTX matrix-matched calibration curve, assuming an equimolar response.

In suspicious cases or in matrices different from bivalves, such as flatworms, mesozooplankton and phytoplankton-net, the samples were subjected to co-chromatography, in which they were spiked with a comparable amount of TTX to indubitably confirm the analyte identification.

2.2.3 Microbiological and molecular analysis

Sample treatment

Mussel samples were externally cleaned with potable water and prepared for analysis in accordance with ISO 6887-3 [97]. In aseptic working conditions, about 10 individuals were opened and the flesh meat and intervalvular fluids were pooled together.

Vibrio spp. isolation from mussel samples

Vibrio spp. was isolated according to ISO 21872-1:2017 [98-99]. Briefly, 25 g of bivalve sample was weighed, 225 mL of alkaline saline peptone water (ASPW) was added, and the sample was homogenized in a blender and incubated at 37 °C for 6 ± 1h. After the first enrichment, 1 mL of the culture was tenfold diluted with ASPW and incubated again at 37 °C for 18 ± 3h. After the second enrichment broths were subcultured onto selective media,

Thiosulfate citrate bile sucrose agar (TCBS) and CHROM™ agar *Vibrio* (CHROMagar, France). These subcultures were further incubated at 37 °C for 24 ± 3 h. After incubation, colonies were selected on the basis of distinctive morphology and color. At least five yellow and/or green colonies from each TCBS plate, and mauve, blue, and white colonies from each CHROM™ agar *Vibrio* plate were isolated; colonies were subcultured on Tryptic soy agar (TSA) with 3% NaCl (TSAs, Oxoid) at 37 °C for 18 ± 3h and identified via molecular assay.

Vibrio alginolyticus isolation and enumeration (mussels, water, sediment, phytoplankton-net)

Bivalve samples (25g) were homogenized in a blender and tenfold diluted with ASPW (10^{-1} dilution). Sediment samples (10 g) were tenfold diluted with ASPW and vortex-mixed for 15 min at 2000 x g with a Multi Reax (10^{-1} dilution). Water and phytoplankton-net samples were vortex-mixed for 15 min at 2000 x g with the Multi Reax.

From seawater and phytoplankton-net raw samples and the 10^{-1} dilution of mussel and sediment samples further serial dilutions (10^{-1} to 10^{-4}) were prepared in ASPW (1 + 9 mL), then 1 mL of each dilution was surface-spread plated on TCBS agar (Difco Laboratories, Detroit, MI, United States) and incubated at 37± 1 °C for 18 ± 3h. After incubation, yellow colonies growing on TCBS agar plates were counted (only plates with 3 to 150 colonies were considered) for *V. alginolyticus* enumeration [100-101]. The results were reported as UFC per gram of mussels/sediment or UFC per milliliter of water/ phytoplankton-net sample.

DNA Extraction—Operative Method

Bacterial colonies were suspended in 500 µL sterile distilled water, heated to 99 °C for 10 min, and centrifuged at 13200 x g for 1 min [102]. The supernatant was either tested by Polymerase Chain Reaction (PCR) immediately or stored at −20 °C. Possible *V. alginolyticus* colonies were submitted to PCR analysis for the species-specific gyrB gene [103].

PCR analysis

All the PCR amplifications were performed with a Mastercycler pro Thermal Cycler (Eppendorf).

- **gyrB species-specific gene**

Yellow colonies suspected of belonging to *V. alginolyticus* strains were submitted to PCR analysis for detection of the species-specific gyrB gene [103]. AlgF1 and AlgR1 primers (Invitrogen, Thermo Fisher) were employed for the amplification of the gyrB gene fragment (568 bp) [103]. *V. alginolyticus* ATCC 33787 strain (American Type Culture Collection, Manassas, VA, USA) was used as positive control of amplification ($CTRL^+$) while ultrapure distilled nuclease-free water was used as a negative amplification control ($CTRL^-$), in all analytical batches. After the amplification reaction, the products were displayed by electrophoresis run in 1.5% agarose gel under UV light. The bacterial isolates were identified as *V. alginolyticus* when PCR amplification generated products of the expected size (568 bp) by comparison to a 100 bp DNA ladder molecular weight marker and the positive control strain.

- **NRPS and PKS biosynthesis genes**

The bacterial isolates identified as *V. alginolyticus* were subjected to PCR analysis for the presence of PKS and NRPS genes. A2gamF and A3gamR primers were employed for the amplification of the NRPS gene fragment (300bp) [104] and DKF and DKR degenerate primers were used for the amplification of PKS gene fragment (300 bp) [86, 105]. *V. parahaemolyticus* ATCC 17802 strain was used as a positive control of amplification ($CTRL^+$) for both target genes while ultrapure distilled nuclease-free water was used as a negative amplification control ($CTRL^-$), in all analytical batches. The *V. alginolyticus* and *V. parahaemolyticus* isolates were considered to be NRPS and/or PKS positive when PCR amplification generated products of the expected size (300 bp for both genes) by comparison to the molecular weight marker and the positive control strain, after visualization by electrophoresis in 1.5% agarose gel under UV light. PCR amplification protocols optimized are described in Table 2.3.

Table 2.3: Reagents, reaction mix and protocols for PCR on *Vibrio* spp.

Fragments	***Primers***				***Target***
gyrB (560bp)	AlgF1 AlgR1	5'-TCA GAG AAA GTT GAG CTA ACG ATT-3' 5'-CAT CGT CGC CTG AAG TCG CTG T -3'			*V. alginolyticus*
NRPS (300bp)	A2gamF A3gamR	5'-AAG GCN GGC GSB GCS TAY STG CC-3' 5'-TTG GGB IKB CCG GTS GIN CCS GAG GTG - 3'			*V. alginolyticus*
PKS (300bp)	DKF DKR	5'-GTG CCG GTN CCR TGN GYY TC-3' 5'-GCG ATG GAY CCN CAR CAR MG -3'			*V. alginolyticus*
Amplification Protocols					***Reaction Mix***
Denaturation	94 °C x 4 min	94 °C x 3min	94 °C x 2 min		Ultrapure water 12.45 µL
Denaturation	94 °C x 30 s	94 °C x 1 min	94 °C x 1 min		Buffer Go Taq DNA Flexi polimerase 5x (promega) 5.0 µL
Annealing	58 °C x 30 s **32 cycles**	60 °C x 1 min **35 cycles**	60 °C x 1 min **30 cycles**		$MgCl_2$ (25mM) 2.0 µL
Extension	72 °C x 1 min	72 °C x 2 min	72 °C x 1 min		$dNTP_s$ (2,5 mM) 2.0 µL
Extension	72 °C x 8 min	72 °C x 7 min	72 °C x1 min		Primer (20µm) 0.5 µL
Target	***gyrB*** Luo et al. [103]	**NRPS** Tambadou et al. [104]	**PKS** Moffit et al. [105]		Primer (20µm) 0.5 µL GO Taq Flexi DNA polymerase (5u/µl) (promega) 0.05 µL
Positive CTRL+	*V. alginolyticus* ATCC 33787	*V. parahaemolyticus* ATCC 17802			Volume mix 22.5 µL DNA 2.5 µL
Negative CRL-	Ultrapure water	Ultrapure water			Final volume 25.0 µL

2.3 Results and Discussion

2.3.1 Method performances

The developed HILIC-MS/MS method showed good analytical performances. Matrix-matched calibration curves exhibited good linearity with correlation coefficients greater than 0.99 and response factor drift < 10%. The LOD 3 µg kg^{-1} and LOQ 8 µg kg^{-1} were adopted for all the matrices included in the study. The sensitive obtained was good, considering the significant matrix effect of the analysis (signal suppression of 50–60%) and the instrument features: the system can be classified as a medium-sensitivity system, as described by Turner et al. [39]. Then, the method was excellently suited to identify TTX contamination at the EFSA guidance level of 44 µg eq. kg^{-1} for TTX.

Good recoveries (R%) of 99% and 97% and acceptable intra-day repeatability (RSDr%) of 7% and 8% were obtained in mussels spiked at 75 µg kg^{-1} and 251 µg kg^{-1} respectively.

2.3.2 TTX in mussels from Marche coast

During 2021, 16 (25%) mussel samples from Marche coast showed TTX levels > LOQ (11–65 µg kg^{-1}) with 4 of them (6%) belonging to the Ancona area, at levels above the EFSA warning limit (47–64 µg kg^{-1}). The Pesaro contaminated samples showed lower levels (11–23 µg kg^{-1}). Additionally, the contaminated samples were collected between June and early July, and only the parent toxin TTX was detected.

In Figure 2.3 the TTX levels found in mussels from Mache coast in the sampling points studied, are reported.

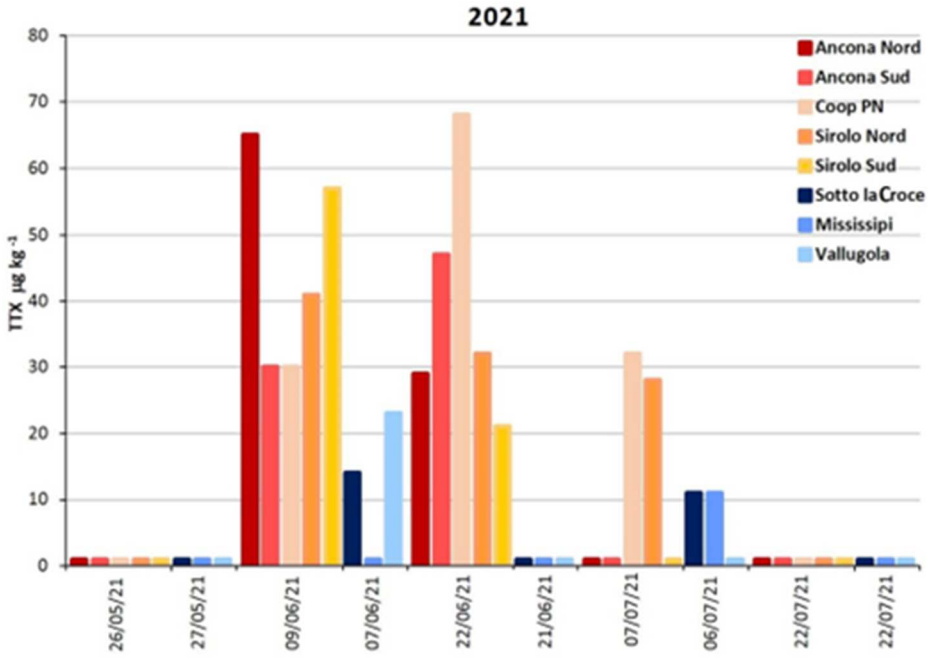

Figure 2.3: TTX levels (µg kg^{-1}) in mussel samples from coastal area of the Marche Region during 2021.

The TTX levels found in mussels in the frame of official control and their temporal trend suggest that the contamination is a recurrent phenomenon occurring between June and August, confirming findings relative to the three previous years of investigation (2018, 2019, 2020). Moreover the TTX contamination showed an increasing trend year after year going from the trace levels reported in 2018 (about 10 µg kg^{-1}) in Pesaro natural beds to amounts exceeding the EFSA guidance level in 2019, 2020 and 2021 (maximum recorded contamination in 2019 was 76 µg kg^{-1} at Sirolo Nord site, in 2020 50 µg kg^{-1} at Ancona Nord site). [Results published in the two papers Bacchiocchi et. al 2021, Bacchiocchi et al. 2023" produced in the frame of this chapter, but not included in this PhD project].

Previously, in Italy, TTXs have been measured at low levels (0.8 – 6.4 µg kg^{-1}) in shellfish collected in spring and summer from 2015 to 2017 in the Syracuse Bay (Sicily) [28] and exceptionally high contamination

levels were reported in the Marano Lagoon (North Adriatic Sea- Friuli Venezia Giulia) in 2017 and 2018 (541 µg kg^{-1} in 2017 and 216 µg kg^{-1} in 2018) [29]. Contamination incidence was greater in mussels of the Ancona area (Conero Riviera) rather than in those of the Pesaro's, suggesting the Conero Riviera as a possible hotspot for TTX accumulation in shellfish. The TTX levels found in mussels were always moderate, with a percentage of the samples containing a measurable concentration of toxin ranging around 22–23% and only few (<5%) with levels above the EFSA threshold. Thus, TTX in commercialized wild mussels from the Marche Region does not represent an imminent concern for consumers, even if the TTX levels seem to increase.

2.3.3 TTX distribution in mussel tissues

Mussel samples harvested from the Ancona area on 9 and 22 June 2021 contaminated by TTX were dissected to study toxin's compartmentalization in different tissues. Considering that a mussel specimen, as experimentally verified, is, on average, composed by weight by 15% DG, 15% G, 30% M and 40% RT, the distribution of total TTX in the tissues (compartmentalization) was evaluated. A homogeneous distribution of TTX among tissues would result in a toxin distribution (calculated as the concentration of the toxin in the specific tissue divided by the total toxin in mussel expressed in %) in the tissues compartment, equal to the mussel composition. Finding of this study showed two different distribution profiles for samples of 9 and 22 June (Figure 2.4). In both cases, albeit to a different extent, TTX showed a preferential accumulation in DG (52% for samples of 9 June and 41% for those of 22 June), but while in the samples of 9 June the remaining TTX was present consistent also in G and M (11 and 23% respectively), in those of 22 June the toxin was almost exclusively in the RT (52%). Then if in the early stage of contamination is evident a preferential TTX accumulation in DG followed by G and M, after about two weeks, despite DG remains the preferential

accumulation tissue, levels in G and M were significantly lower, probably as a consequence of a redistribution in the whole organism and/or different metabolization rates.

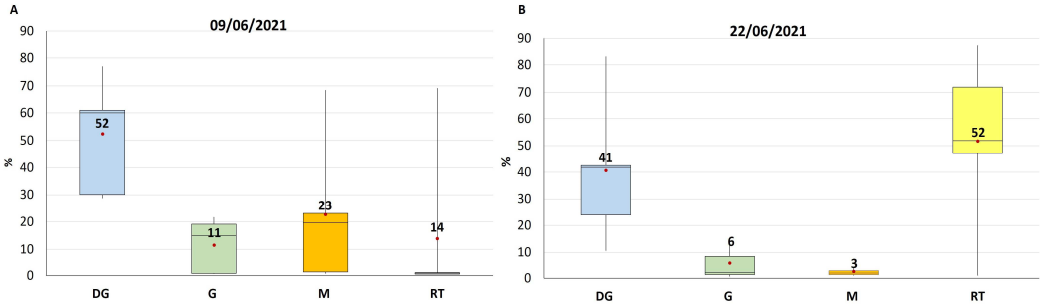

Figure 2.4: Box and whisker plot of TTX distribution in different mussel tissues expressed as percentage %, measured in samples collected on 9 June 2021 (A) and on 22 June 2021 (B). DG = Digestive Gland, G = Gills, M = Mantle, RT = Remaining Tissues.

2.3.4 TTX in biota from *Molo Portonovo*

Mussels from the sampling point MP exhibited a detectable amount of TTX from the first sampling day (4 June 2021), reaching a maximum of 296 µg kg^{-1} on 17 June followed by a detoxification period lasted more than two months (Figure 2.5). These mussels showed a maximum toxin content among the highest ever found in Europe in bivalves, and a longer lasting contamination period. The TTX accumulation rate by mussels was slow during the first week (+5% of the maximum contamination) and extremely fast in the second one (+88%).

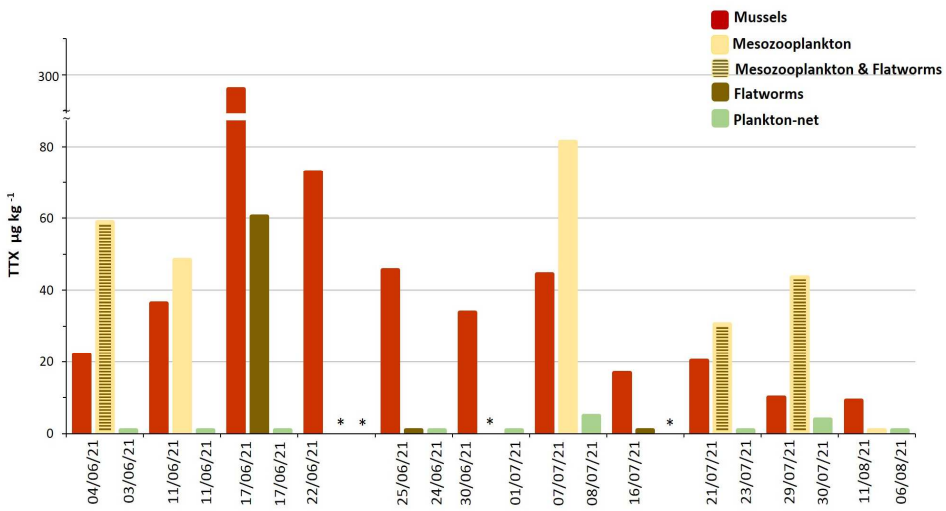

Figure 2.5: TTX contamination in various matrices from *Molo Portonovo* (MP) sampling point during 2021 (* sites not sampled).

After the maximum level was reached, the TTX depletion showed a fast trend during the first week (-75%), followed by a much slower toxin elimination rate (-22%) in the following five weeks (Figure 2.5). The TTX accumulation/depletion rates were extremely rapid, with a one-week scale for 75–80% of the maximum TTX concentration accumulation/detoxification. Similar trends have already been reported by previous studies on bivalves from the United Kingdom [96] and France [106].

The analysis of flatworms and mesozooplankton collected at MP mussel bed showed in some cases detectable amounts of TTX. Among flatworm samples only collected on 17 June, the period of maximum contamination in mussels, showed measurable levels of TTX (60 µg kg^{-1}). In some cases, the flatworms and mesozooplankton samples were not collected separately. When mesozooplankton was analyzed alone or with flatworms, the TTX was always measurable at levels higher than those found in mussels, except in the sampling of 11 August 2021. The analysis of a phytoplankton pellet collected with a net (phytoplankton-net) through the water column showed barely detectable TTX levels (4–5 µg kg^{-1}) in the samples collected on 8 and 30 July

2021 (Figure 2.5). The detectable levels of TTX in mesozooplankton and phytoplankton samples and the study of toxin distribution in mussels (changing over exposure time) described in the section 2.3.3 supported the hypothesis of an exogenous origin of TTX. Probably the TTX is produced externally, reaches the mussels through the diet, accumulates initially in those tissues involved in the filtration (G, M) or digestion (DG) processes and, only after, it redistributes in the rest of tissues.

Moreover, the relevant zooplankton contamination levels, taking into account the little amount of material analyzed, suggests that these organisms likely play an important role in the toxin trophic transfer acting as reservoir and vector to mussels.

Only in one case a sample of flatworms showed detectable levels of TTX when mussels reached the maximum contamination. Flatworms isolated in the MP natural bed were identified as *Stylochus mediterraneus*, a proven mussel *Mytilus galloprovincialis* predator [107]; then, it can be hypothesized they accumulate TTX by eating contaminated mussels.

As regards the phytoplankton, considering that the majority of dinoflagellates are mixotrophic (characteristics that allow them to feed on potentially TTX-producing bacteria), their possible role as vectors in the TTX contamination of mussels might be hypothesized. *Prorocentrum cordatum* was sometimes associated with TTX accumulation in mussels [79, 84, 88]. Moreover studying the phytoplankton annual trend in the Portonovo station (Ancona), *Prorocentrum cordatum* abundance in water reached its maximum just before the period in which mussels were found to be contaminated by TTX [Results published in the paper “Bacchiocchi et al. 2023” produced in the frame of this chapter, but not included in this PhD project].

The specific sampling point MP (not included in official control) object of this study is characterized by shallow waters (20–40 cm), and, during the period of maximum TTX accumulation in mussels, the water temperature ranged

between 20 and 25°C and salinity from 34.3 to 36. These observations suggests that environmental factors such as strong solar radiation and relatively high water temperature may favor TTX accumulation in mussels, as already hypothesized in previous studies [86, 96]. The Portonovo Bay is an area with relevant touristic activities during the summer, where wild mussels are easily accessible and heavily exploited by tourist fishers. The MP mussel natural bed, in particular, is very close to the beach and located in a swallow water area; therefore, the considerable amount of TTX detected in June (about seven-fold the EFSA safe threshold) may represent a cause for concern.

2.3.5 *Vibrio alginolyticus* in biotic and abiotic samples

During 2021, 34 mussel samples from the natural beds of the Conero Riviera were analyzed for *Vibrio* spp. In 32 samples (94%), at least one bacterial strain with *V. alginolyticus* characteristic colonies was isolated. All isolates were then confirmed as *V. alginolyticus* by PCR. No other characteristic colonies belonging to *Vibrio* species were isolated. All the *V. alginolyticus* strains were analyzed for the NRPS and PKS genes and strains with at least one target gene were isolated from 15 mussel samples (44%). In 13 (38%) of these only the NRPS gene was identified, in 2 (6%) only PKS, while in none of the samples both genes were detected. Findings confirms what has already detected in 2019, namely that in all samples analysed *V. alginolyticus* strains were isolated and identified by PCR and in 40% of them NRPS and/or PKS genes were detected [Results published in the paper “Bacchiocchi et al., 2021” produced in the frame of this chapter, but not included in this PhD project].

As regards the *V. alginolyticus* count in mussels from the Conero Riviera natural beds, a significant increase, over three orders of magnitude (from 10^1 to 10^4 UFC g^{-1}), was observed between the first sampling (on 10 May 2021) and that of 9 June 2021. Subsequently, until the last sampling on 11 August 2021, the contamination levels remained high, albeit fluctuating among the sampling points (Figure 2.6).

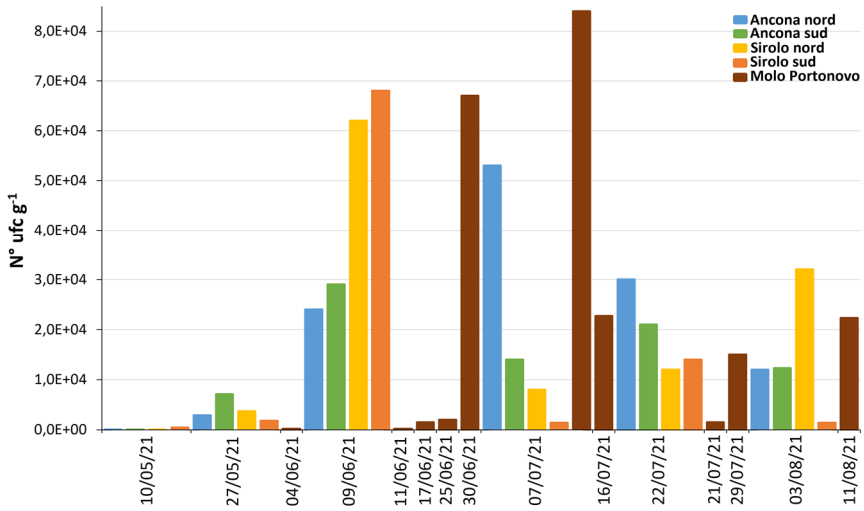

Figure 2.6: *V. alginolyticus* counts on mussel from natural beds and MP of the Conero Riviera during 2021.

The *Vibrio* analyses carried out in water, sediment and phytoplankton-net collected at the MP sampling site showed a similar trend with the maxima recorded during the month of July, as showed in Figure 2.7. *V. alginolyticus* was found in almost all the mussel samples from the MP natural bed, moreover was also isolated from the other biotic and abiotic matrices collected in the same habitat. This result was certainly expected, as it is known that *Vibrio* are the most abundant bacteria in marine environments [108] and that *V. alginolyticus* is the predominant species along the Adriatic coast, followed by *V. parahaemolyticus*, *V. cholerae* and *V. vulnificus* [109].

Furthermore the occurrence of *Vibrio* spp. is positively correlated with temperature, especially in temperate regions [110].

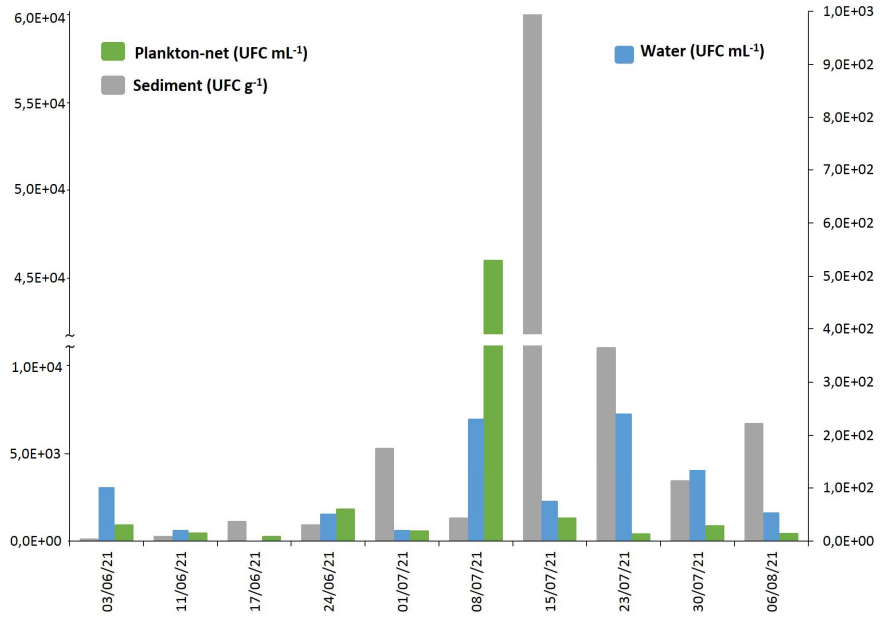

Figure 2.7: *V. alginolyticus* count on various matrices from MP natural bed during 2021.

Also the presence of NRPS and/or PKS genes in the 44% of the analyzed samples may be linked to the warm season.

In order to investigate a possible correlation between *V. alginolyticus*, a TTX potential producer and measurable toxin levels in the mussels, the microbiological and biomolecular results were compared with the chemical ones. Firstly, the accumulation of TTX, the contamination by *V. alginolyticus* in mussels and in the entire natural beds' ecosystem followed fairly similar trends, reaching the maximum levels between June and July. This is surely not sufficient to demonstrate a correlation between the two phenomena, but it highlights that they are certainly favored by the same environmental factors (temperature, water depth and solar radiation).

Thus, the origin of the toxin can reasonably be traced back to microorganisms (bacteria), with ecophysiological characteristics similar to those of *V. alginolyticus*. Furthermore, out of the 27 samples submitted to both chemical and microbiological analyses, 9 (33%) were found to be simultaneously contaminated by *V. alginolyticus* and by TTX, which is 60% of the samples [111] contaminated by *V. alginolyticus* carrying the NRPS/PKS genes and 75% of the samples contaminated by TTX [112]. This is not itself conclusive of a correlation between the two phenomena, but it certainly underlines the need for further investigation.

Chapter 3

PLTXs: study of their presence in wild mussels from the Conero Riviera and of trophic transfer in seabreams *Sparus aurata*

The contents described in this chapter have been reported in the following papers:

- Accoroni, S.; Ubaldi, M.; Bacchiocchi, S. Neri, F.; **Siracusa, M**.; Buonomo, M. G.; Campanelli, A.; Totti, C. Palytoxin-Analogues Accumulation in Natural Mussel Banks during an *Ostreopsis* cf. *ovata* Bloom *Journal of Marine Science and Engineering* **2022**, 10, 1402.

- Giuliani M.E., S.; Bacchiocchi, S.; Accoroni, S.; **Siracusa, M**.; Campacci, D.; Notarstefano, V.; Mezzelani, M.; Piersanti, A.; Totti, C.; Benedetti, M.; Regoli, F.; Gorbi, S. Trophic transfer and subcellular effects of ovatoxins in the gilthead seabream *Sparus aurata*: a focus on lipid metabolism alterations, submitted to *Chemosphere – accepted.*

3.1 Introduction

PLTX is the largest and most potent non-peptide toxin identified to date, with a large and complex molecular structure. It is characterized by a long polyhydroxylated and partially unsaturated aliphatic backbone, with more than 100 carbons with 64 chiral centers [23]. Several congeners called PLTX-like compounds or more recently PLTX-analogues were identified, such as OVTXs. Ovatoxin-a (OVTX-a) was the first analogue studied, and the only for which the molecular structure was elucidated until now.

For the other compounds belonging to OVTX group, only the elemental composition is known. These differ from the parent PLTX for the number of carbon and/or oxygen atoms. In addition, a comparative analysis of the mass fragmentation patterns of PLTX and OVTX-a suggested they share the same A moiety [113]. In Figure 3.1 are reported the chemical structure of PLTX, the molecular formulae of the principal OVTX analogues and the elemental composition of the A and B relevant moieties in mass fragmentation profile.

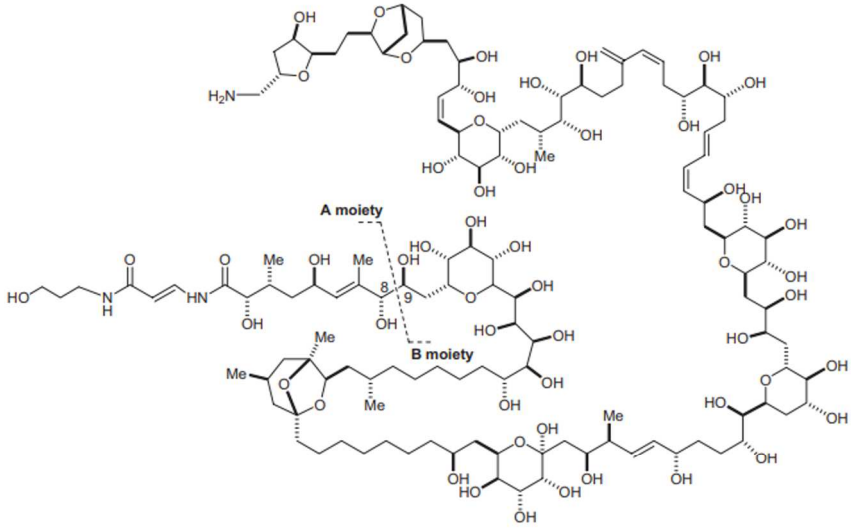

Toxin	M	A moiety	B moiety
Palytoxin	$C_{129}H_{223}N_3O_{54}$	$C_{16}H_{28}N_2O_6$	$C_{113}H_{195}NO_{48}$
Ovatoxin-a	$C_{129}H_{223}N_3O_{52}$	$C_{16}H_{28}N_2O_6$	$C_{113}H_{195}NO_{46}$
Ovatoxin-b	$C_{131}H_{227}N_3O_{53}$	$C_{18}H_{32}N_2O_7$	$C_{113}H_{195}NO_{46}$
Ovatoxin-c	$C_{131}H_{227}N_3O_{54}$	$C_{18}H_{32}N_2O_7$	$C_{113}H_{195}NO_{47}$
Ovatoxin-d	$C_{129}H_{223}N_3O_{53}$	$C_{16}H_{28}N_2O_6$	$C_{113}H_{195}NO_{47}$
Ovatoxin-e	$C_{129}H_{223}N_3O_{53}$	$C_{16}H_{28}N_2O_7$	$C_{113}H_{195}NO_{46}$

Figure 3.1: Chemical structure of PLTX. Molecular formulae (M) of OVTXs and elemental composition of their relevant A and B moieties, as deduced by HR LC–MS and MS^2 experiments (from Ciminiello et al. [41, 113] and Accoroni et al. [31]).

OVTXs are mainly produced by benthic dinoflagellates of *Ostreopsis* genus [24, 114-115]. In particular, *Ostreopsis* cf. *ovata* is a benthic dinoflagellate, epiphytic on red and brown seaweeds and on rocks, sand, mussel shells and benthic invertebrates [30]. This species appearing during yearly seasonal blooms in the Mediterranean Sea, synthesized several OVTXs, OVTX-a, Ovatoxin-b (OVTX-b), Ovatoxin-c (OVTX-c), Ovatoxin-d (OVTX-d), Ovatoxin-e (OVTX-e), Ovatoxin-f (OVTX-f), Ovatoxin-g (OVTX-g), Ovatoxin-h (OVTX-h) and a low amount of isobaric PLTX (isoPLTX) [114].

From 2006 intense seasonal *O.* cf. *ovata* blooms appeared in the North-Central Adriatic Sea, with OVTX-a as the major component of the algal toxin profile [30-31, 112].

PLTXs were detected also in many organisms, e.g. crustaceans, molluscs (bivalves, gastropods, cephalopods), echinoderms and fishes [116-118]. Recently PLTXs were found also in wild mussels from the Conero Riviera, with a toxin profile similar to that of alga [32].

In the temperate areas, such as the Mediterranean Sea, there are no reports of intoxications due to the ingestion of OVTX contaminated seafood [21, 119]. Since the toxicity of OVTXs through diet is unknown, no regulatory limits in seafood are available but only a guidance level is set by EFSA [21].

However, at these latitudes, *O.* cf. *ovata* blooms cause problems related to human health, mostly due to the inhalation of seawater droplets containing aerosolized toxins and/or fragments of microalgal cells, or cutaneous contact with cells [22]. In Italy, specific guidelines regarding the risk management associated with *Ostreopsis ovata* blooms, established a monitoring of coastal waters in bathing period and an intensification of sampling in bivalve sites, if the algal abundances in water column exceeds 10^4 cell L^{-1} [120].

Documented effects on marine fauna due to OVTX bioaccumulation include exoskeleton alterations, developmental effects, and mass mortalities of benthic invertebrates in the worst cases [31, 116, 121-124].

Studies on immunological, histological, lysosomal and neurotoxic alterations were observed both in field mussel samples naturally exposed to *O.* cf*. ovata* blooms occurring in late summer 2009 along the Conero Riviera, that in mussels exposed in laboratory conditions [47-49].

Although accumulation of OVTXs has been mostly reported and experimentally confirmed in herbivores or omnivores organisms feeding directly on *Ostreopsis* spp. or their substrates (e.g. macroalgae), these toxins have also been detected in few carnivorous species (fishes, crustaceans, gastropods, cephalopods), possibly fed on contaminated prays, like molluscs, crustaceans, worms and tunicates [116-118, 125].

However, there is still not clear evidence of the transfer of PLTXs from lower to higher levels of the food chain, in fact the potential trophic-transfer and biomagnification of the OVTXs has not been widely investigated yet.

The aim of this chapter was to investigate by LC-MS/MS the presence of PLTXs in the wild mussels of the Conero Riviera, and eventual relationships with *Ostreopsis* cf. *ovata* blooms. Moreover OVTX trophic transfer was studied through exposure experiments. Transcriptomic analysis based on RNA sequencing, FTIRI measurements and histological analysis were carried to evaluate eventual alterations induced by the OVTX-enriched diet.

3.2 Materials and Methods

3.2.1 Sampling

Mussel (*Mytilus galloprovincialis*) samples were collected from 2 stations Passetto (43°37'09" N, 13°31'54" E) and Portonovo (43°33'41" N 13°36'06" E) along the Conero Riviera from August to October 2021 with approximately weekly frequency, during the *O.* cf. *ovata* bloom. In these stations natural banks of mussels are present, due to environmental features of the habitat with rocky and cliffy coast and shallow water (<5 m). In Figure 3.2 the map of the study area is reported.

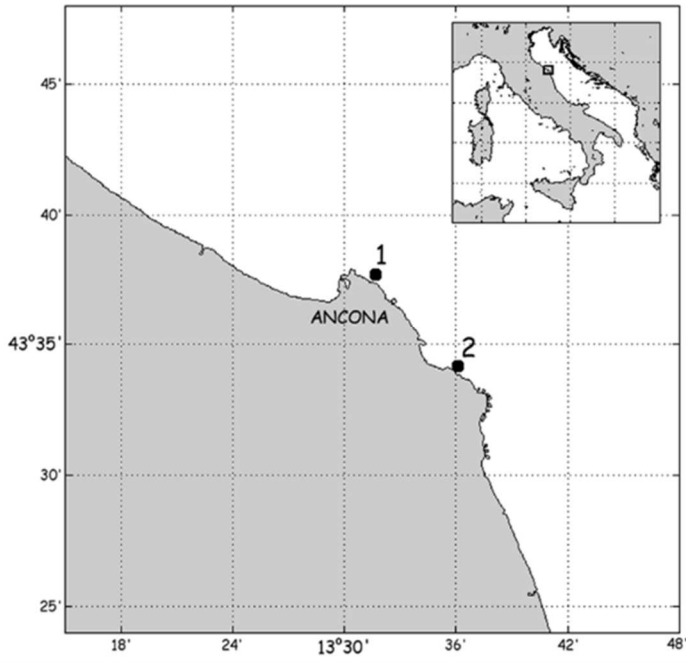

Figure 3.2: Sampling stations of natural banks along the Conero Riviera (North-Central Adriatic Sea) in 2021, 1: Passetto and 2: Portonovo.

Overall 14 mussel samples of commercial size (5–7 cm in length) were collected manually via scuba diving.

3.2.2 Exposure experiment

Microalgal culture

Monoclonal cultures of *O.* cf. *ovata* and *Skeletonema marinoi* were obtained by the marine botany group of DISVA.

Mussel exposure

Mussels *M. galloprovincialis* (480 specimens) were obtained from local farms (Marche coast, Italy, North-Central Adriatic Sea) and acclimated for 7 days to laboratory conditions in 4 recirculating tanks (40 L, 3 individual/L) in artificial seawater (salinity 35, 20 ± 1 °C). After the acclimation period, a pool of 3 organisms' whole tissues, for each tank, were chemically tested for the absence of PLTXs bioaccumulation. Then 200 organisms were dissected and the whole tissue immediately frozen (t0 mussels). For the exposure experiment, 120 specimens (2 tanks, 20 L, 3 individual/L) were daily fed on *O.* cf. *ovata* (10^4 cells L^{-1}) and 120 specimens (2 tanks, 20 L, 3 individual/L) on *S. marinoi* (10^6 cells L^{-1}), for 21 days, to obtain contaminated and control food, respectively, for the subsequent fish exposure. Aliquots of whole tissues (3 mussels) from control and exposed groups were sampled at day 5, 10, 14 and 21 and checked to monitor the PLTXs bioaccumulation level (LC-MS/MS), over the time. Mussel exposure was conducted at facilities of Istituto Zooprofilattico Sperimentale dell'Umbria e delle Marche "Togo Rosati".

Fish exposure

Ten juvenile specimens of *S. aurata* (length=20 ± 1 cm) were obtained from a local farm (Manfredonia, Italy) and acclimated to laboratory conditions (artificial seawater, salinity 34, 22 ± 1 °C) in 10 recirculating 200 L tanks (1 individual per tank) for 10 days, during which they were daily fed on t0 mussels (2 mussels/fish/day). After the acclimation period, 5 tanks were assigned to the control group and 5 to the exposed group (5 fish/group).

Exposed fish were fed with mussels previously contaminated with *O.* cf. *ovata*, while control fish with mussels fed on *S. marinoi*. Two mussels of known weight were provided per fish daily and their ingestion by each fish was verified visually: the number of items ingested by each fish was recorded and non-ingested mussels were removed from the tank. At day 6 of exposure, most of the animals (4 of 5) exposed to contaminated mussels started to reject the food and the experiment was interrupted the following day (day 7). At the end of the experiment, fish were anesthetized on ice and dissected; livers, gills, muscles and gastrointestinal tracts were excised, frozen in liquid nitrogen and stored at – 80 °C.

Experimental procedures on vertebrate animals were approved by the Animal Care and Health Committee (OPBA, Organismo Preposto al Benessere Animale) of Polytechnic University of Marche, and by the General Direction of Animal Health and Veterinary Drugs of the Italian Ministry of Health (Authorization No. 680/2018-PR), and the study was performed according to the EU Directive 2010/63/EU for animal experiments, at DISVA-facilities.

3.2.3 Chemical analysis

Chemicals and Standards

All the reagents were of analytical grade: acetonitrile (LC-MS grade), methanol (HPLC grade) and acetic acid (LC-MS grade). Ultrapure water (18.2 MΩ cm) was produced by a MilliQ water purification system (Millipore Ltd., Bedford, MA, USA).

A non-certified analytical standard of PLTX (CAS RN: 77734-91-9, assay 85.8%) was obtained from Wako Chemicals GmbH (Neuss, Germany) as a colorless film (100 µg). It was dissolved in 5 mL of methanol/water (1:1, v/v), obtaining a stock solution of 20 µg mL^{-1}.

A mussel tissue reference material, certified as negative control (CRM-Zero_Mus), was purchased from the National Research Council Certified Reference Materials Program (Institute for Marine Biosciences, Halifax, NS, Canada) and used to prepare the matrix-matched calibration standards by dilution of the stock.

Field sample treatment

Mussel samples after harvest were transported to the laboratory in refrigerated conditions (4 °C) and opened with 24 h to prevent the processes of metabolizing toxins. The valves were opened, cleaned, and any residual sand and solids were removed with running water. The mollusk flesh was separated from the shell and placed in a large mesh sieve to remove excess water. The pulp was then finely chopped with a Osterizer blender, obtaining a representative sample of 100 g from about 20 specimens used. The homogenate was stored at –20 °C until chemical analysis.

Exposed sample treatment

Exposed mussels after collection were opened, the flesh separated from the shell and the excess water removed. Then the pool of 3 organisms was homogenized by an Ultra Turrax mixer and stored -20 °C until chemical analysis.

Seabream tissues were only homogenized by an Ultra Turrax mixer prior to chemical analysis.

PLTXs extraction from Ostreopsis cf. *ovata*

Chemical analysis of PLTXs in *O.* cf. *ovata* was performed on 1 L of culture (10^6 cells L^{-1}) in the late exponential phase. The entire culture volume (1 L) was centrifuged for 20 min at 2500 x g (4 °C) in 20 centrifuge tubes (50 mL volume). Cell pellets of *O.* cf. *ovata* were combined and extracted with 5 mL

of methanol/water (80:20 v/v), vortex-mixed for 1 min, and sonicated for 10 min. The aliquot was then centrifuged for 10 min at 2500 x g (4 °C), and the supernatant transferred to a 100 mL evaporation flask. Pellet extraction was repeated twice, and the supernatants combined and brought to dryness. The residue was redissolved in 1 mL of methanol/water (80:20 v/v) and filtered through a syringe filter (0.2 µm in nylon) for LC-MS/MS analysis.

PLTXs extraction from mussels and seabream tissues

The extraction was implemented following the protocol already described by Ciminiello et al. [42] with some modifications to improve sensitivity.

Briefly, 10.0g ± 0.5g of mussel homogenate was weighted in a 50 mL PP tube and extracted with 30 mL of methanol/water (80:20 v/v). The sample was homogenized with an Ultra Turrax mixer for 2 min at 9500 rpm and centrifuged for 15 min at 2000 x g (20 °C). The supernatant was transferred in a 100 mL evaporation flask and the solid residue re-extracted twice. The supernatants were collected obtaining a final volume of 90 mL and evaporated to dryness. The residue was dissolved in 5 mL of methanol/water (80:20 v/v), filtered through a syringe filter (0.2 µm in nylon) and analyzed by LC-MS/MS.

Muscle, liver, gills and gastro-intestinal tracts of seabreams were extracted following the protocol already described for mussels, weighting 2.5g ± 0.5g of tissue homogenate and adopting the appropriate volumes (ratio 1:4).

LC-MS/MS conditions

LC-MS/MS analysis of PLTXs was performed using a hybrid triple-quadrupole/linear ion trap 3200 QTRAP mass spectrometer (AB Sciex, Darmstadt, Germany) equipped with a Turbo V source and an electrospray ionization (ESI) probe. The mass spectrometer was coupled to an Agilent 1200 HPLC (Palo Alto, CA, USA), including a solvent reservoir, in-line degasser, quaternary pump, refrigerated autosampler, and column oven.

The method was implemented following Ciminiello et al. [42] and Accoroni et al [31] with slight modifications.

The chromatographic conditions adopted are reported in Table 3.1. Mobile phase A was water and B acetonitrile/water (95:5, v/v), both containing acetic acid (30mM).

Table 3.1: LC conditions for PLTXs analysis.

Column	Gemini® NX-C18 3 µm, 2.1 mm x 100 mm		
Flow	0.2 mL min^{-1}		
Injection volume	10 µl		
Column temperature	40°C		
Gradient	Time (min)	Mobile phase A (%)	Mobile phase B (%)
	0	100	0
	20	50	50
	30	0	100
	35	0	100
	40	100	0
	50	100	0

Infusion experiments were performed using certified reference materials available, listed in the section “Chemicals and Standards” to set turbo IonSpray source parameters (Table 3.2). The mass spectrometer was operated in multiple reaction monitoring (MRM) mode and in positive polarity (ESI^+), selecting two transitions for each toxin to allow for quantification and identification (Table 3.2). Relative retention times were also used to identify PLTXs using the PLTX standard.

Table 3.2: MS parameters and MRM transitions for PLTXs analysis

MS/MS PARAMETERS				
Source type	ESI			
Curtain gas (CUR)	20 psi			
Collision gas (CAD)	medium			
IonSpray voltage (IS)	5000 V			
Source temperature (TEM)	600 °C			
Ion source Gas 1 (GS1)	40 psi			
Ion source Gas 2 (GS2)	20 psi			
MRM TRANSITIONS				
Compound	**Prec. ion (m/z)**	**Prod. ion (m/z)**	**Dwell (msec)**	**CE (eV)**
PLTX/isoPLTX	1340.7	327.1	100	40
	1331.7		100	40
OVTX-a	1324.7	327.1	100	40
	1315.7		100	40
OVTX-b	1346.3	371.2	100	40
	1337.3		100	40
OVTX-c	1354.3	371.2	100	40
	1345.3		100	40
OVTX-d	1332.3	327.1	100	40
	1323.3		100	40
OVTX-e	1332.3	343.1	100	40
	1323.3		100	40

Analytical performances evaluation

Method performances were evaluated through in-house validation experiments in mussels for PLTX, being the only reference material available. Instrumental linearity was investigated by the matrix-matched calibration curves on 5 concentration levels 0.080, 0.13, 0.25, 0.50, 1.5 μg mL^{-1}).

All the calibration points were injected in triplicate in different days and the curves ($y = bx + a$) were obtained plotting the toxins chromatographic peak areas (y) against their concentrations (x).

The best-fit curves were obtained using the least squares regression model. Linearity was evaluated from the correlation coefficients and response factor variation. The LOQ was calculated based on a signal/noise (S/N) ratio. The LOD was derived from the LOQ by dividing by 3.3. Subsequently, the estimated LOQ was experimentally confirmed by spiking blank mussel samples with the PLTX standard.

Accuracy in terms of recovery (R%) and precision in terms of intra-day repeatability (intra-day relative standard deviation RSDr%) were calculated performing replicated analyses (N = 6 in 1 day) on blank mussel samples spiked at 40 µg kg^{-1} (a low contamination level) and 250 µg kg^{-1} (EURLMB provisional limit). The drift in the retention times was considered acceptable if below 1%. Matrix-matched calibration curves were used because of the non-negligible matrix effect. Assuming an equimolar response, matrix-matched calibration curves built using PLTX standard were used to quantify PLTXs.

In matrices different from bivalves, such as seabream tissues and *Ostreopsis* cf. *ovata* strain, samples were spiked at mussel LOQ level with the PLTX standard to check the analytical performances of the method.

3.2.4 Biological analyses

Transcriptomic analysis

The expression profiles in the livers of exposed and control fish were assessed by RNA sequencing. Total RNA was purified from *S. aurata* liver samples (~50 mg each) using the Hybrid-R™ purification kit (GeneAll®), according to the manufacturer's instructions. Total RNA concentrations were measured using Qubit RNA Assay Kit (Thermo Fisher). RNA integrity was checked using a 2100 Bioanalyzer (Agilent Technologies) with RNA 6000 NanoChip. Libraries were prepared from total RNA with Illumina Stranded

mRNA Prep kit, according to manufacturer instructions. Libraries quality was verified on 2100 Bioanalyzer with a DNA HS Chip, and libraries concentrations were determined using Qubit DNA HS Assay Kit. Sequencing was performed on Illumina Novaseq 6000 in the 100PE format.

FPA-FTIRI measurements and data analysis

Focal Plane Array (FPA)-Fourier Transform Infrared Spectroscopy Imaging (FTIRI) measurements were carried out in liver samples of control and exposed fish. For each liver sample, cryostat sections (6 µm) were deposited onto CaF_2 optical windows (1-mm thick, 13-mm diameter) and let air-dry for 30 min without any fixation process, for IR measurements. A Hyperion 3000 Vis–IR microscope coupled with a INVENIO interferometer and equipped with a FPA detector (164x164 micron; 4096 pixel/spectra; 2.56 µm spatial resolution) (Bruker Optics GmbH, Ettlingen, Germany) was used. On each section, 4 IR images were acquired in transmission mode (15X condenser/objective; 4000-900 cm-1; 4 cm^{-1} spectral resolution, and 256 scans). Background spectra were obtained on clean regions of the CaF_2 optical windows with the same acquisition parameters. Raw IR images were corrected with Atmospheric Compensation and Vector Normalization routines (OPUS 7.5 software, Bruker Optics GmbH, Ettlingen, Germany). False color images were generated by integrating IR images in specific spectral regions, to evaluate the spatial distribution and the relative amount of lipids (2995-2828 cm^{-1}, vibrational modes of lipid alkyl chains) and glycosylated compounds, mainly glycogen in liver (1065-1010 cm^{-1}, vibrational modes of C-O groups in carbohydrates and glycosylated compounds). All the spectra composing the chemical map were submitted to the integration procedure (integration Mode B, OPUS 7.5 software): 3031-3000 cm^{-1} (stretching vibration of =CH groups of unsaturated lipid alkyl chains, UNS), 2977-2841cm^{-1} (symmetric and asymmetric stretching modes of CH_3 and CH_2

moieties of lipid alkyl chains, LIP), 1760-1727 cm^{-1} (stretching vibration of C=O ester moieties of fatty acids, FA), 1720-1480 cm^{-1} (vibrational modes of peptide linkage, PRT), and 1065-1010 cm^{-1} (stretching mode of C-O moieties in carbohydrates and glycosylated compounds, GLY). The integrated areas were used to calculate the band area ratios: LIP/PRT (total amount of lipids respect to total proteins); FA/PRT (total amount of fatty acids respect to total proteins); FA/LIP (relative amount of fatty acids respect to total lipids); UNS/FA (relative amount of unsaturated fatty acids among all fatty acids), and GLY/PRT (total amount of glycosylated compounds, mainly glycogen, respect to proteins). PRT was used for band area ratios since its area did not change significantly among the control and exposed samples.

Histological analysis

Neutral lipids content was determined in the liver on duplicate cryostat sections (8 µm thick), which were fixed in Beker's fixative and stained by Oil red O (ORO) before mounting in glycerol gelatin. Quantification of staining intensity was performed with Image-Pro® Plus 6.2 Analysis Software and then normalized to the area of liver section. Five measurements were made on each section.

Statistical analyses

The total toxin intake for each *S. aurata* specimen was estimated by multiplying the total amount of mussels ingested (g) by the average toxin concentration detected in mussel tissues (188 µg kg^{-1}); values were then expressed as µg of toxin per kg of fish weight.

For the analysis of transcriptomic data, the reads pre-processing was performed by using fastp v0.20.0 [126], applying specific parameters to remove residual adapter sequences and to keep only high quality data (qualified_quality_phred=20,unqualified_percent_limit=30,average_qual=25,

low_complexity_filter=True, complexity_threshold=30). The percentage of uniquely mapped reads resulted high with the mean value of 85% (mean value for sample: unmapped reads 9%, quality base >q30 94%). Passing filter reads were mapped to the genome reference (*Spaurus aurata*) using STAR v2.7.0 [127] with standard parameters, except for sjdbOverhang option set on read length. Genome and transcripts annotation provided as input were downloaded from v103 of Ensembl repository. Alignments were then elaborated by RSEM v1.3.3 [128], to estimate transcript and gene abundances. Subsequently, the sample-specific gene-level abundances were merged into a single raw expression matrix applying a dedicated RSEM command (rsem-generate-data-matrix). Genes with at least 10 counts in 50% of samples were then selected. Differential expression (pairwise comparisons) was computed by edgeR [129] from raw counts in each comparison. Multiple testing controlling procedure was applied and genes with a p-value ≤ 0.05 and log Fold-Change (FC) > |0.5| were considered differentially expressed. Annotation of differential expressed genes (DEGs) was performed using the bioMart package [130] into R 4.1, querying available Ensembl Gene IDs and retrieving Gene Names and Entrez gene IDs. Uncharacterized sequences were represented with the LOC# identifier. The functional enrichment analysis of DEGs was performed by the DAVID tool (Database for Annotation, Visualization, and Integrated Discovery; Huang et al., 2009) to identify the most enriched Gene Ontology (GO) terms. In the absence of a well-annotated genome for *S. aurata*, the DEGs were matched to Danio rerio genome, and only results with corrected p-value (ease) < 0.05 were considered. Protein-protein interaction (PPI) analyses were performed by bash scripts on public database STRING, which consist of PPI information including most of the annotated genes for eukaryotes. To conclude, graphical diagrams of PPI including interactions involving annotated differential expressed genes were generated using Cytoscape [131].

For FTIR data and ORO staining data, statistical significances between control and exposed group were calculated by Student's t-test and set at $p < 0.05$.

3.3 Results and Discussion

3.3.1 Method performances

The developed LC-MS/MS method showed good analytical performances. Matrix-matched calibration curves exhibited good linearity with correlation coefficients greater than 0.99 and response factor drift < 10%. The LOD of 5 µg kg^{-1} and LOQ of 13 µg kg^{-1} were adopted for bivalves and algal pellets, LOD of 13 µg kg^{-1} and LOQ of 40 µg kg^{-1} for seabream tissues. The sensitive obtained was good, considering the significant matrix effect of the analysis, moreover the method was excellently suited to identify PLTXs contamination at EFSA guidance level of 30 µg kg^{-1} and at EURLMB provisional limit of 250 µg kg^{-1} in shellfish. Good recoveries (R%) of 74% and 87% and acceptable intra-day repeatability (RSDr%) of 9% and 7% were obtained in mussels spiked at 40 µg kg^{-1} and 250 µg kg^{-1} respectively. The drift in the retention times was widely below 1%.

3.3.2 OVTXs in wild mussels from the Conero Riviera

Mussels from natural banks of the Conero Riviera were contaminated by OVTXs, even if at low levels. OVTX-a was the most abundant toxin (71%–74%) among the PLTXs detected in mussels, followed by OVTX-b (26%–29%). The toxin profile of a field contaminated mussel is reported in Figure 3.3.

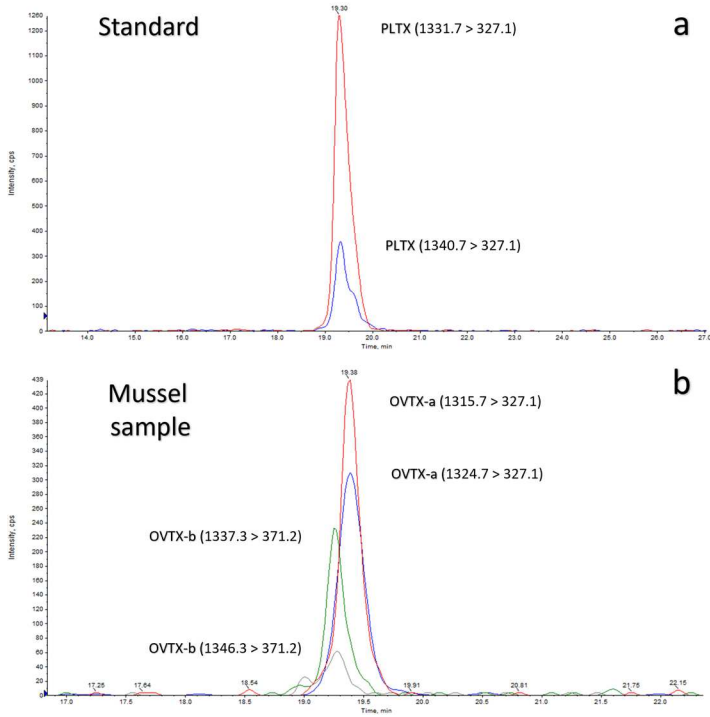

Figure 3.3: LC-MS/MS chromatograms of the (A) PLTX matrix-matched standard, (B) OVTX-a, and OVTX-b in the sample from Portonovo station of 20 September 2021 with MRM transitions.

At Passetto station, OVTXs were first recorded in the mussels sampled on 20 September with a concentration of 16 µg kg^{-1}, that was the highest level detected in this site. At the subsequent sampling date (27 September), OVTX concentrations were drastically lower (<LOD). At Portonovo station, OVTXs were first recorded in mussels on 20 September with the maximum concentration of 36 µg kg^{-1} (Figure 3.4). Then wild mussels bioaccumulated PLTXs at levels generally lower than the EFSA threshold with the exception of Portonovo site, but widely lower than the EURLMB provisional limit.

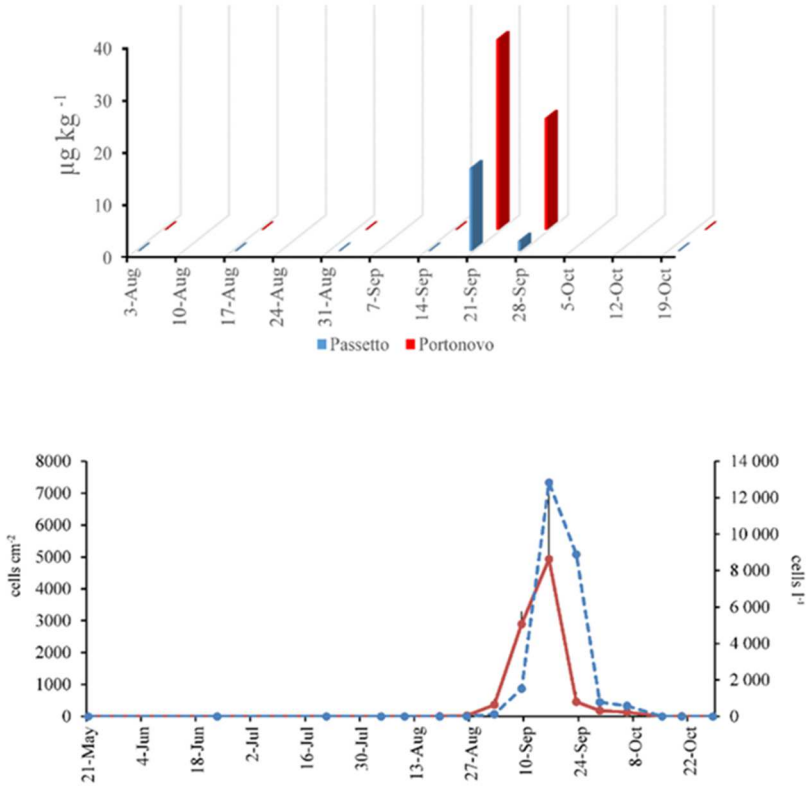

Figure 3.4: OVTX contamination in mussels from natural banks at sampling stations (blue) Passetto and (red) Portonovo in 2021 (in the top). *Ostreopsis* cf. *ovata* abundance on seaweeds (bold line, cells cm^{-2}, left y-axis) and in the water column (dotted line, cells L^{-1}, right y-axis) at the Passetto station in 2021 (in the bottom).

However, shellfish (*M. galloprovincialis*) collected in late summer-early autumn 2016 showed PLTXs maximum contamination of about 350 µg kg^{-1} in the Passetto site [32]. This highlights the necessity of characterizing the hazard posed by oral exposure to these toxins, which still represents a major gap in our knowledge [119]. Moreover, the mussels from natural banks are collected for human consumption by swimmers in summer, being the Conero Riviera a popular area for holidays.

The mussel observed toxin profile fits well with the profile previously detected in field samples of *O.* cf. *ovata* populations in the same study area [132]. The

finding that contaminated mussels showed the same toxin profile as that of the toxic microalga blooming in the area was not so obvious. Because it is well known that biotoxins can be subjected to biotransformation, and/or to a differential accumulation/excretion equilibrium related to the molecular properties of each compound after their ingestion by invertebrates, as described for other marine toxins such as PSP [133] DSP [134], and AZAs [35, 37].

OVTXs were found in the Passetto station 32 days after the appearance of *O.* cf. *ovata* on macroalgae and 18 days after the first record in the water column. The peak of bioaccumulation in mussels was recorded 4 days after the recording of the bloom peak on 16 September. In the following sampling, as for mussels, the abundance of *O* cf. *ovata* decreased significantly, and after 14 consecutive days without records of *O.* cf. *ovata* in seawater, OVTXs were no longer detected in mussels (Figure 3.4). [Results published in the paper “Accoroni et al., 2022” produced in the frame of this chapter, but not included in this PhD project].

The results showed that the bioaccumulation of toxins in wild mussels does not depend only on the abundances of toxic microalgae. Indeed, although higher abundances of *Ostreopsis* have been recorded in Passetto than in Portonovo since 2006 (https://www.arpa.marche.it/balneazione-nuovo/ostreopsis-cf-ovata, accessed on 18 April 2022), mussels bioaccumulated higher OVTX concentrations at the latter site. Several biotic and abiotic factors (intrinsic or non-intrinsic to the vector organisms) play a certain role in this process. In the detail algal growth and toxin production are influenced by different environmental parameters and by physiological status/life cycle stage of the alga [132, 135-136].

Moreover bioaccumulation depends on several boundary conditions, such as the abundance and quality of the whole phytoplankton communities that affect the filtration rates [137], the nature of the contaminating toxins, the

physiology of the shellfish [138] and its history of exposure to toxins [139]. A significant positive Pearson's correlation was found between *O.* cf. *ovata* abundances on macroalgae and OVTXs in mussels ($n = 7$; $r = 0.8336$; $p < 0.05$). A similarly positive correlation was found between *O. cf. ovata* abundances in the water column and OVTXs recorded in mussels ($n = 7$; $r = 0.8574$; $p < 0.05$) [Results published in the paper "Accoroni et al., 2022" produced in the frame of this chapter, but not included in this PhD project]. Although this correlation is observable with abundances of *O.* cf. *ovata* both on benthic substrates and in the water column, it is more evident with the latter. This probably because the fact that this toxic species is benthic rather than planktonic may make it relatively unavailable as a food resource for filter-feeding shellfish except during periods when cells are resuspended in the water column and/or when the biofilm of benthic cells extends onto the mollusc shells.

3.3.3 Chemical characterization of *O.* cf. *ovata* strain and exposed mussels

Chemical characterization of PLTXs produced by *O.* cf. *ovata* strain demonstrated a whole production of 5 pg cell^{-1} of toxins, among which OVTX-a and OVTX–b were predominant, with lower amount of OVTX-c, OVTX-d and OVTX–e; PLTX and isobaric PLTX compounds were undetectable (Figure 3.5).

Then the toxin profile of *O.* cf. *ovata* strain analyzed confirms that this is the most common in the study area and in the Mediterranean Sea [132, 140].

LC-MS/MS analysis of *M. galloprovincialis* daily fed on *O.* cf. *ovata* (10^4 cell L^{-1}) confirmed that the organisms accumulated OVTXs in whole tissues, with major contribution of OVTX-a and OVTX-b and a toxic profile similar to that of *O.* cf. *ovata*, as previously showed in field samples (Figure 3.5).

Then this support the hypothesis that these compounds not undergo biotransformation after ingestion by mussels, as already described in the section 3.3.2.

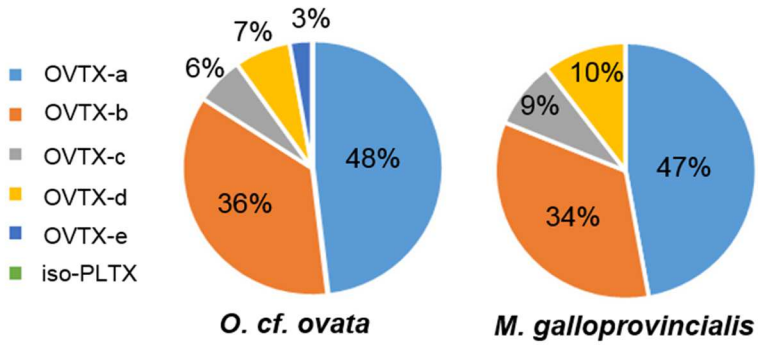

Figure 3.5: Toxic profile of O. cf. *ovata* strain used for the exposure and of *M. galloprovincialis* exposed to the toxic algae; the plots show the percentage of the different analogues detected by LC-MS/MS.

OVTX levels, monitored throughout the exposure, were 31 µg kg^{-1} at day 5 and reached 188 µg kg^{-1} at the end of the exposure (21 days) (Figure 3.6). No toxins accumulation was observed in control mussels fed on the non-toxic microalgae *S. marinoi* (10^6 cells L^{-1}).

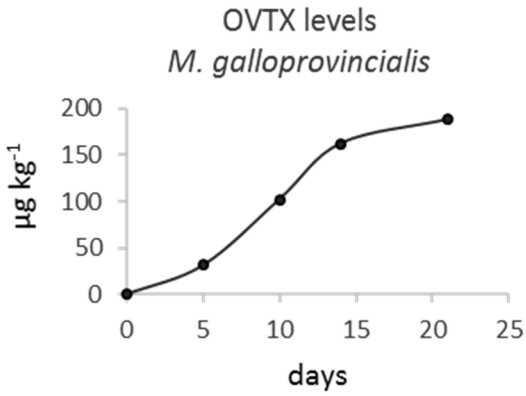

Figure 3.6: Temporal trend of toxin accumulation in *M. galloprovincialis* whole tissues during exposure; values are expressed as µg of toxins per kg of whole tissue.

The maximum contamination level obtained in exposed mussels, using as feeding *O.* cf. *ovata* concentrations comparable to those found during bloom peaks, *i.e* 10^4 cells L^{-1} [141], is similar to the maximum levels detected in wild mussels such as 217 µg kg^{-1} reported by Amzil et al. [142]. Such values are close to the EURLMB provisional value hypothesized for PLTX-group toxins. The OVTX accumulation was not linear with time but rather showed a plateau, possibly because of a reduced filtration rate or an equilibrium between uptake and excretion. The analysis of the toxic profile demonstrated a non-preferential accumulation of specific OVTXs in *M. galloprovincialis* since the main OVTX analogues were found in similar proportions in *O.* cf. *ovata* and mussels' tissues (Figure 3.5).

3.3.4 Toxin levels in *Sparus aurata* fed with OVTX-contaminated mussels

S.aurata fed with OVTX-contaminated mussels suddenly changed their feeding behavior after 6 days of exposure, when they started to reject the food items, which were repeatedly taken and then expelled from the mouth. The estimated OVTX fish intake, calculated considering the total amount of mussels ingested by each fish and the mean OVTX levels in mussels, was between 49 and 78 µg kg^{-1} b.w. However, levels of OVTXs were always below the LOD in liver, muscle, gills and gastro-intestinal tracts of both control and exposed seabreams.

Despite OVTX analogues were previously found in carnivorous fishes [116-118], and the total seabream toxin intake estimated was widely above the LOD of the method, the absence of a detectable trophic transfer of the OVTXs, may depend on the activation of biotransformation and detoxification processes, with the subsequent production of OVTX metabolites which could have been more easily excreted. Even in the absence of toxins accumulation, the biological reactivity of OVTXs was already highlighted after a few days of

OVTX-enriched diet, through the rejection of contaminated mussels by seabreams. Food rejection is an important defence mechanism against harmful compounds [143] which can influence food selection and intake, e.g. by decreasing food palatability and interacting with the fish taste system [143-145].

3.3.5 Transcriptomic responses in livers of fish fed with OVTX-contaminated diet

The analysis of differential expression between exposed and control livers resulted in 268 DEGs ($p < 0.05$), among which 115 were upregulated and 153 downregulated in the exposed group. The hierarchical cluster heatmap of the top 50 DEGs (35 upregulated, 15 downregulated, $log_2FC \geq |1.73|$) revealed a good clustering of control samples; 4 of 5 exposed samples clustered together, while one was separated by the others (#6, Fig. 3.7). Ptprq, me1, cusr, fasn, aclya and acaca were among the most over-expressed genes in the exposed group ($log_2FC > 3$; $FC > 8$); among the most under-expressed genes we found wdr49 ($log_2FC > -3$; $FC < 0.125$) and angptl4 ($log_2FC > -2$; $FC < 0.25$) (Fig. 3.7). Four non-coding RNA (3 upregulated, 1downregulated) were among the most variable transcripts (Fig. 3.7). The analysis of protein-protein interaction (PPI), performed on the whole DEGs set (268 DEGs) and represented through the PPI network, revealed 72 interactions involving 67 proteins (Fig. 3.8). The proteins with the highest number of interactions were tblx1, fads2 (8 interactions), ppargc1a, smarcd3 (6 interactions), ctnnb1, me1 and stat1 (5 interactions).

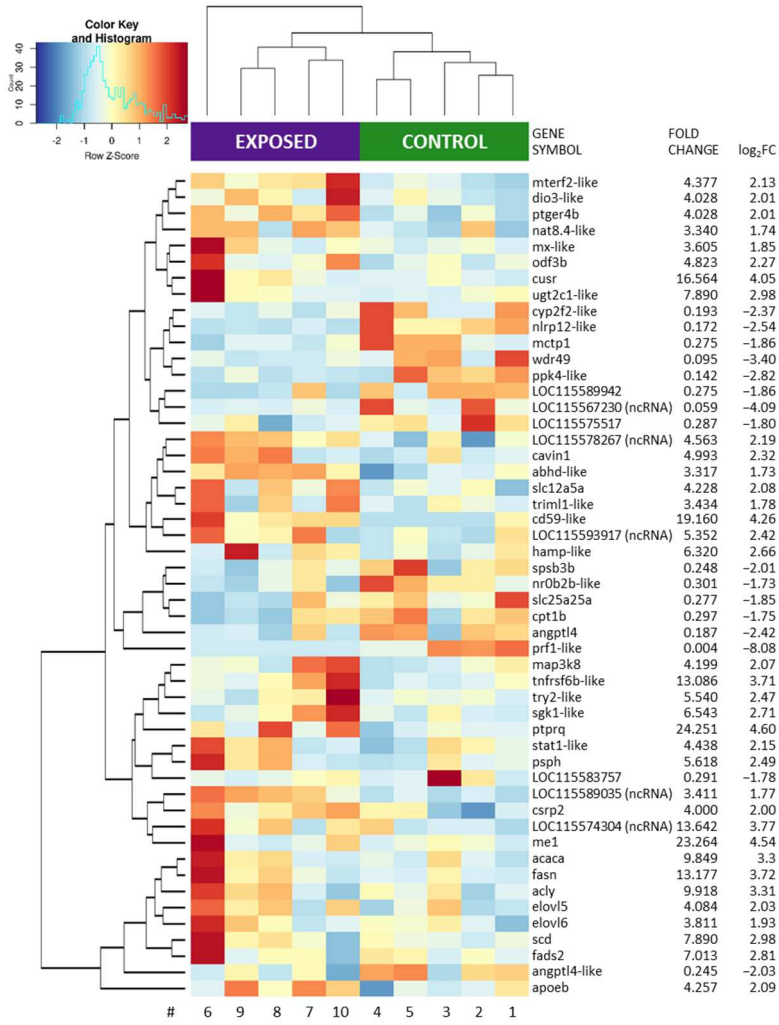

Figure 3.7: Hierarchical cluster heatmap of the top 50 most variable DEGs ($log_2FC \geq |1.73|$) in the hepatic transcriptome of control and exposed *S. aurata*. Colors from blue to red represent increasing expression: orange/red color (Z-score > 1) represents gene abundance higher than the mean, blue color (Z-score < 1) represents gene abundance lower than the mean. # represents specimen numbers (1-5: controls; 6-10: exposed). Gene symbols of annotated genes are defined as in GenBank database (www.ncbi.nlm.nih.gov); sequences with putative annotation are indicated with "-like"; uncharacterized sequences are represented with the LOC# identifier; ncRNA = non-coding RNA. FC = fold change of exposed over control (mean value, n = 5). FC > 1 and positive log_2FC represent upregulated genes; FC < 1 and negative log_2FC represent downregulated genes.

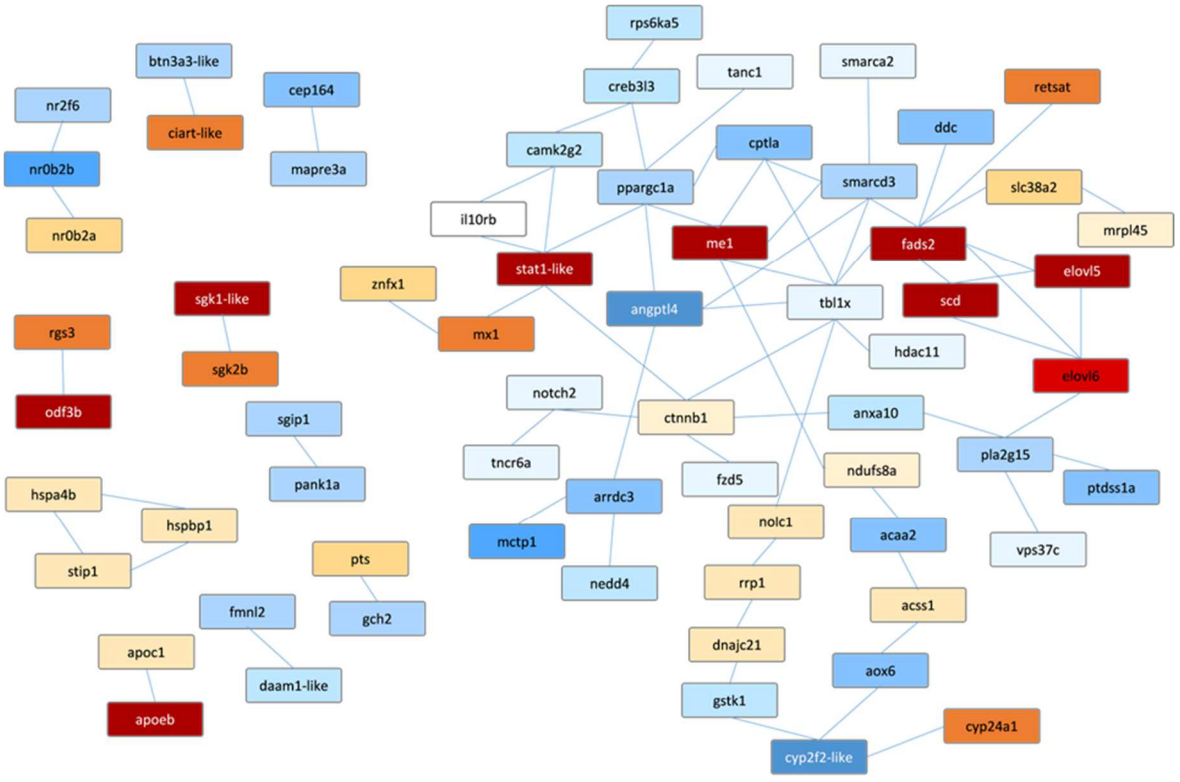

Figure 3.8: Protein-protein interaction network of DEGs. Nodes represent proteins; connecting edges represent protein-protein associations. Blue scale colors: downregulated DEGs. Red scale colors: upregulated DEGs.

Among the biological processes affected in fish fed with *O.* cf. *ovata*-contaminated mussels, a clear alteration was observed in the expression of genes involved in lipid metabolism, in both biosynthetic and catabolic process. In particular, several genes involved in fatty acid biosynthesis were upregulated and those involved in fatty acid degradation were mainly downregulated in the exposed group.

Other processes related to lipid metabolism were enriched, including glycerolipid metabolic process, carboxylic acid transport, plasma lipoprotein clearance, and regulation of ketone metabolism. Other biological processes related to metabolic activities were significantly enriched, namely tricarboxylic acid, sulfur compound and organophosphate (including nucleotide) metabolisms, and the pentose-phosphate shunt. Additional DEGs were involved in regulation of transcription and in protein phosphorylation. "Response to stimuli" processes were also observed, such as response to lipid, oxygen-containing compounds, hormone, iron ion, hypoxia, and biotic stimulus.

In the table 3.3 the enriched biological processes and corresponding DEGs in livers of *S. aurata* exposed to *O.* cf. *ovata*-contaminated diet were reported.

Table 3.3: Enriched Biological Processes and corresponding DEGs; red: upregulated genes; blue: downregulated genes.

Biological Process	Genes (DEGs)
small molecule metabolic process	dnph1, aclya, cap1, elovl5, elovl6, ndufs8a, acaca, aco1, acss1, aldh1l2, apoeb, cmpk, cyp24a1, fads2, fasn, g6pd, gcdha, ldha, me1, mat2ab, pgd, pgam1b, psph, scd pfkfb4a, abcd4, gch2, acaa2, cpt1ab, cpt1b, cyp2y3, ddc, gpd1b, hsd17b7, lipeb, lpin2, ogdha, pank1a, si:zfos-411a11.2, sirt5
organic acid metabolic process	aclya, elovl5, elovl6, acaca, aco1, acss1, aldh1l2, cyp24a1, fads2, fasn, gcdha, ldha, me1, pgd, pgam1b, psph, scd abcd4, gch2, acaa2, cpt1ab, cpt1b, cyp2y3, ddc, lpin2, ogdha, si:zfos-411a11.2
carboxylic acid metabolic process	aclya, elovl5, elovl6, acaca, aco1, acss1, aldh1l2, cyp24a1, fads2, fasn, gcdha, ldha, me1, pgd, pgam1b, psph, scd abcd4, gch2, acaa2, cpt1ab, cpt1b, ddc, lpin2, ogdha
monocarboxylic acid metabolic process	aclya, elovl5, elovl6, acaca, acss1, cyp24a1, fads2, fasn, gcdha, me1, pgd, pgam1b, scd abcd4, acaa2, cpt1ab, cpt1b, lpin2
carboxylic acid metabolic process	aclya, elovl5, elovl6, acaca, aco1, acss1, aldh1l2, cyp24a1, fads2, fasn, gcdha, ldha, me1, pgd, pgam1b, psph, scd abcd4, gch2, acaa2, cpt1ab, cpt1b, ddc, lpin2, ogdha
fatty acid metabolic process	aclya, elovl5, elovl6, acaca, cyp24a1, fads2, fasn, gcdha, scd abcd4, acaa2, cpt1ab, cpt1b, lpin2
single-organism metabolic process	dnph1, aclya, cap1, elovl5, elovl6, ndufs8a, ugp2a, acaca, aco1, acss1, aldh1l2, apoc1, apoeb, cmpk, cyp24a1, fads2, fasn, g6pd, gcdha, gpat3, ldha, me1, mat2ab, map3k5, mxa, pgd, pgam1b, psph, spry4, scd, ulk2 pfkfb4a, abcd4, gch2, abhd6a, acaa2, angptl4, cpt1ab, cpt1b, cyp2y3, dolk, ddc, gpd1b, hsd17b7, lipeb, lpin2, ogdha, pank1a, ptdss1a, pla2g15, si:zfos-411a11.2, sirt5

Biological Process	Genes (DEGs)
acyl-CoA biosynthetic process	aclya, elovl5, elovl6, acaca, acss1, gcdha
lipid metabolic process	aclya, elovl5, elovl6, acaca, apoc1, apoeb, cyp24a1, fads2, fasn, gcdha, gpat3, scd abcd4, abhd6a, acaa2, angptl4, cpt1ab, cpt1b, dolk, hsd17b7, lipeb, lpin2, ptdss1a, pla2g15
cellular lipid metabolic process	aclya, elovl5, elovl6, acaca, apoc1, cyp24a1, fads2, fasn, gcdha, gpat3, scd abcd4, abhd6a, acaa2, cpt1ab, cpt1b, dolk, lipeb, lpin2, ptdss1a, pla2g15
lipid catabolic process	apoc1, apoeb, cyp24a1, gcdha abcd4, abhd6a, acaa2, cpt1ab, cpt1b, lipeb, lpin2
monocarboxylic acid catabolic process	gcdha, pgd abcd4, acaa2, cpt1ab, cpt1b, lpin2
fatty acid oxidation	cyp24a1, gcdha abcd4, acaa2, cpt1ab, cpt1b
fatty acid catabolic process	gcdha abcd4, acaa2, cpt1ab, cpt1b, lpin2
small molecule catabolic process	aldh1l2, apoeb, cyp24a1, gcdha, pgd abcd4, acaa2, cpt1ab, cpt1b, lpin2
fatty acid biosynthetic process	aclya, elovl5, elovl6, acaca, fads2, fasn, scd
cellular lipid catabolic process	gcdha abcd4, abhd6a, acaa2, cpt1ab, cpt1b, lipeb, lpin2
acyl-CoA metabolic process	aclya, elovl5, elovl6, acaca, acss1, gcdha
carboxylic acid biosynthetic process	aclya, elovl5, elovl6, acaca, fads2, fasn, psph, scd gch2

Biological Process	Genes (DEGs)
sulfur compound biosynthetic process	aclya, elovl5, elovl6, acaca, acss1, gcdha, mat2ab
fatty acid beta-oxidation	gcdha abcd4, acaa2, cpt1ab, cpt1b
lymph vessel development	junba acaa2, cpt1ab, notch2, nr2f2, prox1a
monocarboxylic acid biosynthetic process	aclya, elovl5, elovl6, acaca, fads2, fasn, scd
lipid biosynthetic process	aclya, elovl5, elovl6, acaca, fads2, fasn, gpat3, scd dolk, hsd17b7, lpin2, ptdss1a
single-organism catabolic process	dnph1, aldh1l2, apoc1, apoeb, cyp24a1, gcdha, pgd, pgam1b, ulk2 abcd4, abhd6a, acaa2, cpt1ab, cpt1b, lipeb, lpin2
carboxylic acid catabolic process	aldh1l2, gcdha, pgd abcd4, acaa2, cpt1ab, cpt1b, lpin2
small molecule biosynthetic process	aclya, elovl5, elovl6, acaca, fads2, fasn, psph, scd gch2, hsd17b7
single-organism biosynthetic process	aclya, cap1, elovl5, elovl6, ugp2a, acaca, acss1, cmpk, fads2, fasn, gpat3, psph, scd gch2, dolk, hsd17b7, lpin2, pank1a, ptdss1a
acylglycerol metabolic process	apoc1, gpat3 abdh6a, lipeb, lpin2
neutral lipid metabolic process	apoc1, gpat3 abdh6a, lipeb, lpin2
sulfur compound metabolic process	aclya, elovl5, elovl6, acaca, acss1, gcdha, mat2ab gstk1, sult3st1
circadian rhythm	cipcb, ciarta, nr0b2a id3, nr0b2b, nr1d1

Biological Process	Genes (DEGs)
regulation of sequence-specific DNA binding transcription factor activity	nr0b2a jmy, nr0b2b, ppargc1a, prox1a
unsaturated fatty acid biosynthetic process	elovl5, elovl6, fads2, scd
response to lipid	cyp24a1, lgals17, hamp, ptger4b, scd esr1, nfe2l2a
response to fatty acid	ptger4b, scd nfe2l2a
triglyceride metabolic process	apoc1, gpat3 lipeb, lpin2
regulation of lipid catabolic process	apoc1 acaa2, cpt1ab
unsaturated fatty acid biosynthetic process	elovl5, elovl6, fads2, scd
transcription from RNA polymerase II promoter	ctnnb1, nr0b2a smarca2, smarcd3a, creb3l3b, hnf4b, id3, lpin2, nfat5b, nr0b2b, nr1d1, nr2f2, nr2f6a, ppargc1a, si:ch73-61d6.3
cellular response to lipid	lgals17, hamp, ptger4b esr1, nfe2l2a
fatty-acyl-CoA biosynthetic process	elovl5, elovl6, gcdha
monocarboxylic acid transport	fabp4a abcd4, cpt1b, slc16a6b, slc16a13
negative regulation of sequence-specific DNA binding transcription factor activity	nr0b2a nr0b2b, prox1a
organophosphate metabolic process	dnph1, cap1, ndufs8a, cmpk, g6pd, gpat3, pgd, pgam1b pfkfb4a, gch2, dolk, gpd1b, pank1a, ptdss1a, pla2g15
response to oxygen-containing compound	cyp24a1, lgals17, hamp, ptger4b, stat1b, scd esr1, lpin2, nfe2l2a

Biological Process	Genes (DEGs)
circadian rhythm	cipcb, ciarta, nr0b2a id3, nr0b2b, nr1d1
positive regulation of nucleobase-containing compound metabolic process	cap1, ctnnb1 smarca2, smarcd3a, creb3l3b, hnf4b, lpin2, nfe2l2a, nr1d1, ppargc1a, si:ch73-61d6.3, tnrc6a, mafgb
response to hormone	hamp, ptger4b, stat1b esr1, lpin2, nfe2l2a, nr1d1
fatty-acyl-CoA biosynthetic process **positive regulation of RNA metabolic process**	elovl5, elovl6, gcdha ctnnb1 smarca2, smarcd3a, creb3l3b, hnf4b, lpin2, nfe2l2a, nr1d1, ppargc1a, si:ch73-61d6.3, tnrc6a, mafgb
negative regulation of transcription, DNA-templated	cipcb, ciarta, nr0b2a, znfx1 cbx4, id3, nr0b2b, nr1d1, nr2f2, nr2f6a
positive regulation of transcription from RNA polymerase II promoter	ctnnb1 smarca2, smarcd3a, creb3l3b, hnf4b, lpin2, nr1d1, ppargc1a, si:ch73-61d6.3
plasma lipoprotein particle clearance	apoc1, apoeb
regulation of cellular ketone metabolic process	acaa2, cpt1ab, sirt5
carboxylic acid transport	fabp4a, slc38a2 abcd4, cpt1b, slc16a6b, slc16a13
carboxylic acid transport	fabp4a, slc38a2 abcd4, cpt1b, slc16a6b, slc16a13
peptidyl-serine phosphorylation	rps6ka5 mknk2b, sgk2b, si:ch211-195b13.1, ulk2
glycerolipid metabolic process	apoc1, gpat3 abhd6a, lipeb, lpin2, ptdss1a, pla2g15
positive regulation of transcription, DNA-templated	ctnnb1 smarca2, smarcd3a, creb3l3b, hnf4b, lpin2, nfe2l2a, nr1d1, ppargc1a, si:ch73-61d6.3, mafgb

Biological Process	Genes (DEGs)
response to iron ion	aco1 slc11a2
pentose-phosphate shunt, oxidative branch	g6pd, pgd
response to hypoxia	ddit4, ldha camk2g2, ern1
nucleotide metabolic process	dnph1, cap1, ndufs8a, cmpk, g6pd, pgd, pgam1b gpd1b, pank1a
pteridine-containing compound metabolic process	pts, aldh1l2 gch2
peptidyl-serine phosphorylation	rps6ka5 mknk2b, sgk2b, si:ch211-195b13.1, ulk2
response to hypoxia	ddit4, ldha camk2g2, ern1
tricarboxylic acid metabolic process	aclya, aco1 ogdha
tricarboxylic acid metabolic process	aclya, aco1 ogdha
nucleotide metabolic process	dnph1, cap1, ndufs8a, cmpk, g6pd, pgd, pgam1b gpd1b, pank1a
plasma lipoprotein particle clearance	apoc1, apoeb
very long-chain fatty acid metabolic process	elovl5, elovl6 abcd4
response to biotic stimulus	cd59, lgals17, hamp, map3k5, mxa agbl5, angptl4, cpt1b, pank1a
organic anion transport	fabp4a, slc38a2 abcd4, cpt1b, slc16a6b, slc16a13, slco1c1

Some of the most strongly upregulated genes encode enzymes for the *de novo* synthesis of FA (me1, aclya, acaca, fasn), the elongation of long-chain FA (elovl5, elovl6), and the biosynthesis of unsaturated FA (scd, fads2). Among the others, the retsat gene, overexpressed in OVTX-treated fish, positively regulates *de novo* lipogenesis and FA desaturation [146], while the pentose phosphate shunt (g6pd, pgd) is also involved in lipid biosynthesis by generating NADPH. The centrality of FA biosynthetic pathways in exposed seabreams was demonstrated also by the high number of protein interactions for fads2 and me1, which are connected to enzymes (elovl5, elovl6, scd, retsat), transcriptional regulators (ppargc1a, tbl1x, smarcd3), and transporters (cpt1a) involved in lipid metabolism.

On the other hand, several genes with lipid catabolic function were downregulated, further confirming the need for reconstituting the intracellular lipid amount. The main downregulated processes were related to the FA β-oxidation, which was affected at different levels: FA degradation reactions (acaa2), FA transport into mitochondria and peroxisomes (cpt1, abdc4), FA mobilization from phospholipids, mono- and triglycerides (pla2g15, abhd6, lipe), and transcription of β-oxidation genes [ppargc1a, lpin2 [147]. The transcriptional coactivators ppargc1a and lpin2 are key genes for lipid metabolism, and their downregulation reduces the amount of FA oxidation enzymes [148-149]. In particular, ppargc1a is a key “energetic regulator” highly expressed in tissues with elevated energy demand like the liver [148], and its downregulation suggests a reduced use of lipids for energy production, to preserve and restore their storages.

Among other transcriptional regulators modulated in treated seabreams, tbl1x is involved in the hepatic metabolism of lipids, and reduced tbl1x mRNA levels were previously associated to increased levels of triglycerides in mouse liver [150].

Being among the protein with the highest number of protein-protein interactions, we may hypothesise that tbl1x represents an essential protein in the seabream response to lipid depletion.

The upregulation of the apolipoprotein genes in the liver of exposed fish (apoeb, apoc1) suggests that the OVTX-diet stimulated the lipid uptake from circulation. Specifically, apoe is involved in lipoprotein uptake from circulation to hepatocytes [151], and downregulation of angptl4, one of the most under expressed genes in OVTX-exposed fish, would increase the clearance of plasma triglycerides and the cellular uptake of triglycerides-derived FA [152]. Other DEGs and enriched processes confirmed the cellular demand for reconstituting the lipid pool in the hepatocytes of OVTX-treated seabreams. On one side, the downregulation of genes involved in ketone bodies formation (acaa2, cpt1ab, sirt5), which derive from FA breakdown, is in accordance with the reduced β-oxidation profile [153]. On the other side, the increase of cavin1, involved in the formation of neutral lipid droplets, through triglycerides synthesis from FA [154], and the simultaneous downregulation of lipase lipe (responsible for triglycerides degradation) reflects a cellular pathway for restoring the neutral lipid reserves. Even if predominant, the alteration of gene expression in exposed seabream was not limited to lipid metabolism. The upregulation of genes involved in the *de novo* nucleotide biosynthesis (e.g.genes of pentose phosphate shunt and organophosphate metabolism) highlights an intense transcriptional activity. The numerous processes related to “responses to stimuli” are a further indication that, despite the absence of toxin accumulation, the exposure to contaminated food represented a challenge which stimulated several mechanisms of biological response.

3.3.6 Lipid content in liver of fish fed with OVTX-contaminated diet

To further elucidate the effects of the OVTX-diet on metabolic processes including lipid metabolism, the content of lipids and other macromolecules was investigated in fish livers by comparing FTIR images of control and exposed livers. False color images, representing the distribution of lipids (LIP), glycogen (GLY) and proteins (PRT), showed a lower content of LIP and GLY in liver of exposed fish, while PRT amounts were nearly unchanged (Figure 3.9).

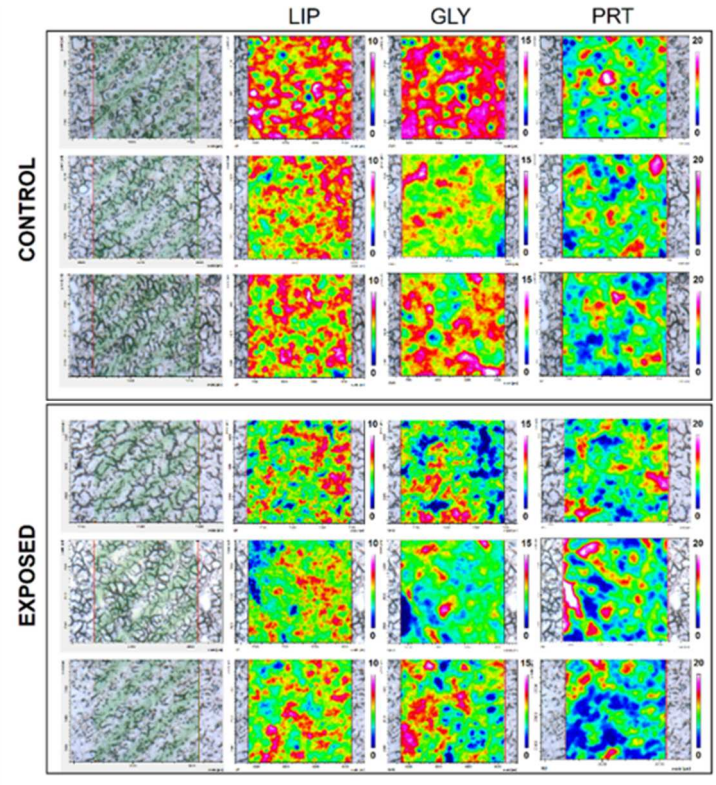

Figure 3.9: Representative microphotograph and IR image displaying the distribution of lipids (LIP), glycogen (GLY) and proteins (PRT) of each liver sample from control and exposed groups. Color scales range from blue (low values) to magenta (high values).

Given the unvaried profile of PRT between exposed and control samples, the band area ratios showed a significantly lower amount of total lipids (LIP/PRT), a lower amount of FA, both respect to proteins (FA/PRT) and to the overall lipids (FA/LIP), and higher levels of unsaturated fatty acids (UNS/FA). The relative amount of glycogen (GLY/PRT) showed a slight but not significant decrease in exposed group (Figure 3.10).

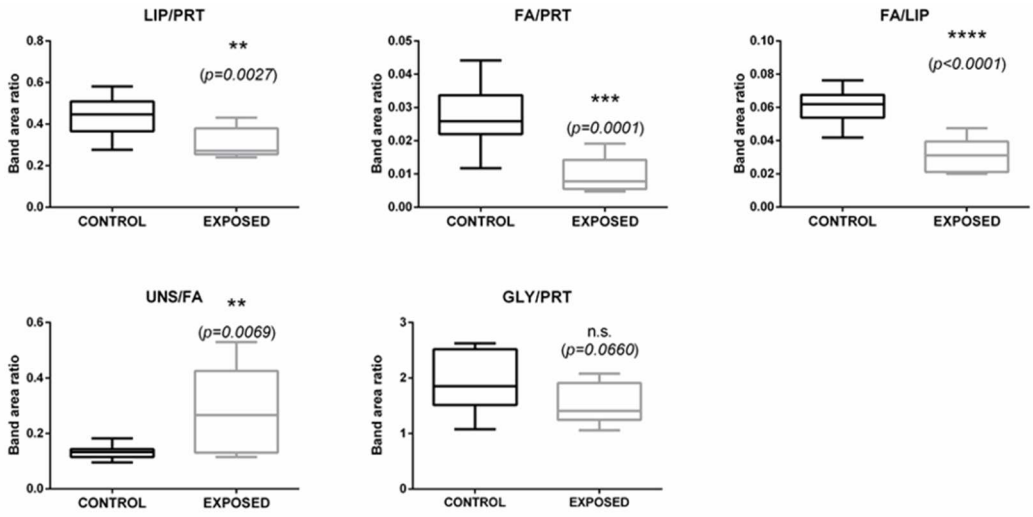

Figure 3.10: Box plots show the values of the LIP/PRT, FA/PRT, FA/LIP, UNS/FA, and GLY/PRT band area ratios calculated in liver samples of control and exposed liver samples: centre line marks the median, edges indicate the 25th and 75th percentile, whiskers indicate the min and max values. Asterisks indicate a statistically significant difference between CONTROL and EXPOSED groups; statistical significance was set at 0.05, and calculated by Student's t-test (n.s. = not significant difference); exact p values are reported.

The decrease of lipid content in the liver of fish fed with contaminated mussels was further confirmed by histochemical analysis (Oil Red O staining), which revealed a significant lower amount of neutral lipid droplets in hepatic sections of exposed organisms (Figure 3.11).

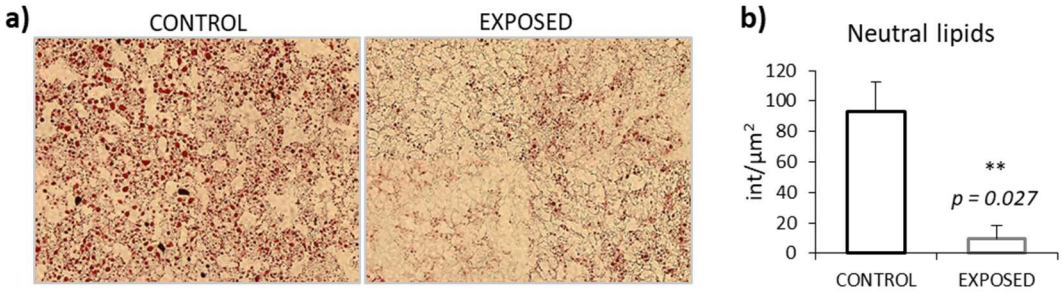

Figure 3.11: Neutral lipid content in the liver of *S. aurata* exposed to OVTX-contaminated mussels. a) Representative pictures of histological sections stained with Oil Red O from control and exposed livers; b) Neutral lipid content in control and exposed livers determined by image analysis and expressed as color intensity per μm^2 of tissue; statistical significance, calculated by Student's t-test, was set at 0.05; the exact p value is reported.

The observed alterations in the feeding behaviour were reflected at molecular and cellular levels by significant changes of lipid metabolism in liver, where metabolization/detoxification activities, may be responsible for observed effects even without an evident toxins accumulation. After 6 days of exposure to contaminated mussels, the amounts of lipids (FA and neutral lipids) in fish liver decreased significantly. Reduced amounts of neutral lipids after *O.* cf. *ovata* exposure were already reported in the digestive tissues of mussels, both in field and in laboratory conditions [47-48].

Since *O.* cf. *ovata* cells are rich in neutral lipid droplets, mainly composed of polyunsaturated lipids [155], the decrease of those substances in mussels and seabream tissues seems a direct effect of the toxins, rather than a

reduced lipid content in the diet. The erosion of lipid content after exposure to marine biotoxins was previously observed for AZA1, which caused a 50% decrease of cholesterol content in human lymphocytes together with the upregulation of genes for lipid biosynthesis [156], similarly to this study. The modulation of genes involved in lipid metabolism in OVTX-treated seabreams may represent a response to the decrease of lipids and a possible mechanism to restore their physiological level.

Conclusions

In this PhD project the presence, the origin, the distribution and the ecotoxicological impact of EMBs in the North-Central Adriatic Sea was widely studied. The use of a multidisciplinary approach allowed to obtain a more complete overview of the topic studied.

CIs and AZAs were present in the mussels of Marche coast but still seem not to represent a risk for human health showing levels very far from EFSA guidance level for CIs (400 µg sum of SPXs kg^{-1}) and legal limit for AZAs (160 µg AZA eq. kg^{-1}). The traces contamination of CIs and AZAs in mussels, made the identification of primary producers difficult, due probably to the low number of toxic microalgal cells in seawater. This underlines the importance to monitor bivalve molluscs being organisms that accumulate toxins, then useful indicators of the presence of these new threats.
Moreover, these findings suggest the need to investigate on these compounds and to their biogenic origin, as well as to consider environmental and climatic changes in progress and their influence on phytoplankton composition and then on eventual contamination phenomenon.

TTX was found in mussels from Marche coast, and in particular from Ancona area, with levels sometimes above the EFSA guidance one. In the specific sampling point *Molo Portonovo*, a high contamination of 296 µg kg^{-1} was recorded on 17 June 2021.
The results described confirmed that the Conero Riviera, rich with wild mussels (*Mytilus galloprovincialis*), is a TTX hot spot in the North-Central

Adriatic Sea, showing environmental features known to lead to TTX accumulation (shallow water). Hence it would be desirable to implement an effective monitoring plan able to promptly report TTX contamination trends in mussels belonging to this area during the warm season and with a high sampling frequency (one week or less). This is important to protect not only human health, being wild mussels widely consumed, but also an important resource for the local fish economy.

The presence of the toxin also outside the mussels, supports the hypothesis that zooplankton and phytoplankton may have a key role in the TTX trophic transfer to mussels. The similar temporal trends of *V. alginolyticus*, often containing the PKS or NRPS genes, and TTX accumulation in mussels and other organisms encourages to pursue the attempt to trace back the source of TTX to this microorganism or microorganisms with similar characteristics. However more investigations to confirm bacteria, as TTX producers, would be useful to better understand the phenomenon.

PLTXs were found at low levels in local mussels from Ancona natural beds, but recurrent *Ostreopsis* cf. *ovata* algal blooms proliferated in the Conero Riviera every year. Even if the Italian guidelines are a useful tool to protect human health in bathing waters affected by *O.* cf. *ovata* blooms and in the managing the risk of human intoxication through the ingestion of contaminated mussels, more specific monitoring plan to better study and forecast the phenomenon would be desirable. In fact, the Conero Riviera is a famous area for holidays, then very popular in summer, critical period for *Ostreopsis* cf. *ovata* algal blooms.

Exposure studies suggest that OVTXs produced by *O.* cf. *ovata* and accumulated in the low trophic level organisms, are not further accumulated at higher levels, supporting the hypothesis of a limited risk associated to biomagnification and human consumption of OVTX-contaminated fish.

But the alterations found in the hepatic metabolism underline that diet OVTX-enriched may be considerably affected the fish liver. Moreover the altered lipid profile could represent an issue for the organoleptic properties and the nutritional value of the fish flesh.

In conclusion, it is important to underline the importance to investigate on EMBs because the scenario is constantly evolving, mainly as consequence of both anthropic and climate changes impacts, with unpredictable repercussions on the phenomenon. Furthermore, in the future other EMBs such as ciguatoxins and brevetoxins, already widely studied in other geographical areas, could appear also in Italian seas thus becoming a new threat to public health and fish economy.

Bibliography

1. Facts on marine biotoxins. Available online: https://www.ecdc.europa.eu/en/all-topics-z/marine-biotoxins/facts-marine-biotoxins (accessed on 21 October 2023).
2. Visciano, P.; Schirone, M.; Berti, M.; Milandri, A.; Tofalo, R.; Suzzi, G. Marine Biotoxins: Occurrence,Toxicity, Regulatory Limits and Reference Methods. *Frontiers in Microbiology* **2016**, 7:1051, doi: 10.3389/fmicb.2016.01051.
3. Poletti, R.; Milandri, A.; Pompei, M. Algal biotoxins of marine origin: new indications from the European Union. *Veterinary Research Communications* **2003**, 27, 173–182, doi: 10.1023/B:VERC.0000014136.98850.b1.
4. EFSA. Scientific Opinion of the Panel on Contaminants in the Food Chain on a request from the European Commission on Marine Biotoxins in Shellfish – Saxitoxin Group. *The EFSA Journal* **2009**, 1019, 1–76.
5. Schwarz, M.; Jandová, K.; Struk, I.; Marešová, D.; Pokorný, J.; Riljak, V. Low dose domoic acid influences spontaneous behavior in adult rats. *Physiological Research* **2014**, 63, 369–376, doi: 10.33549/physiolres.932636.
6. EFSA. Scientific Opinion of the Panel on Contaminants in the Food Chain on a request from the European Commission on Marine Biotoxins in Shellfish – Domoic acid. *The EFSA Journal* **2009**, 1181, 1–61.
7. EFSA. Scientific Opinion of the Panel on Contaminants in the Food Chain on a request from the European Commission on Marine Biotoxins in Shellfish – Okadaic acid and analogues. *The EFSA Journal* **2008**, 589, 1–62.
8. Twiner, M.J.; Rehmann, N.; Hess, P.; Doucette, G.J. Azaspiracid Shellfish Poisoning: A Review on the Chemistry,Ecology, and Toxicology with an Emphasis on Human Health Impacts. *Marine Drugs* **2008**, 6, 39-72; doi: 10.3390/md20080004.
9. Paz, B.; Daranas, A.H.; Norte, M.; Riobó, P.; Franco, J. M.; Fernández J.J. Yessotoxins, a Group of Marine Polyether Toxins: an Overview. *Marine Drugs* **2008**, 6, 73-102, doi: 10.3390/md20080005.
10. EFSA. Scientific Opinion on Marine Biotoxins in Shellfish – Emerging toxins: Brevetoxin Group. *EFSA Journal* **2010**, 8 (7): 1677, 1–29.
11.

12. EFSA. Scientific Opinion on Marine Biotoxins in Shellfish – Emerging toxins: Ciguatoxin Group. *EFSA Journal* **2010**, 8 (6):1627, 1–38.

13. FAO. Marine biotoxins. *FAO FOOD AND NUTRITION PAPER 80* **2004**.

14. Regulation (EC) No 853/2004 of the European Parliament and of the Council of 29 April 2004 laying down specific hygiene rules for on the hygiene of foodstuffs. *Official Journal of the European Union* **2004**, L139/55.

15. Regulation (EU) 2019/627 of 15 March 2019. Laying down Uniform Practical Arrangements for the Performance of Official Controls on Products of Animal Origin Intended for Human Consumption; EU: Brussels, Belgium, **2019**; Volume L131, p. 51.

16. Reverté, L.; Soliño, L.; Carnicer, O.; Diogène, J.; Campàs, M. Alternative Methods for the Detection of Emerging Marine Toxins: Biosensors, Biochemical Assays and Cell-Based Assays. *Marine Drugs* **2014**, 12, 5719-5763, doi:10.3390/md12125719.

17. Karlson, B.; Andersen, P.; Arneborg, L.; Cembella, A.; Eikrem, W.; John, U.; West, J.J.; Klemm, K.; Kobos, J.; Lehtinen, S.; Lundholm, N.; Mazur-Marzec, H.; Naustvoll, L.; Poelman, M.; Provoost, P.; De Rijcke, M.; Suikkanen, S. Harmful algal blooms and their effects in coastal seas of Northern Europe. *Harmful Algae* **2021**, 102, 101989, doi: 10.1016/j.hal.2021.101989.

18. Wells, M. L.; Trainer, V. L.; Smayda, T. J.; Karlson, B.S.O.; Trick, C.G.; Kudela, R.M.; Ishikawa, A.; Bernard, S.; Wulff, A.; Anderson, D.M.; Cochlan, W.P. Harmful algal blooms and climate change: Learning from the past and present to forecast the future. *Harmful Algae* **2015**, 49, 68-93, doi: 10.1016/j.hal.2015.07.009.

19. Comiso, J. Variability and trends of global sea ice cover and sea level: effects on physicochemical parameters. *Climate Change and Marine and Freshwater Toxins* edited by Botana, L.M.; Louzao, M.C.; Vilarino N. Berlin, Boston: De Gruyter **2021**,1-34, doi: 10.1515/9783110625738-001.

20. EFSA.Scientific Opinion on Marine Biotoxins in Shellfish – Cyclic Imines (spirolides, gymnodimines, pinnatoxins and pteriatoxins). *EFSA Journal* **2010**, 8 (6): 1628, 1–39.

21. Knutsen, H.K.; Alexander, J.; Barregård, L.; Bignami, M.; Brüschweiler, B.; Ceccatelli, S.; Cottrill, B.; Dinovi, M.; Edler, L.; Grasl-Kraupp, B.; et al. A Risks for Public Health Related to the Presence of Tetrodotoxin (TTX) and TTX Analogues in Marine Bivalves and Gastropods. *EFSA Journal* **2017**, 15, 47–52, doi: 10.2903/j.efsa.2017.4752.

22. EFSA.Scientific Opinion on marine biotoxins in shellfish—Palytoxin group. *EFSA Journal* **2009**, 7(12), 1393, 1-38.

23. Vila, M.; Abós-Herràndiz, R.; Isern-Fontanet, J.; Àlvarez, J.; Berdalet, E. Establishing the link between *Ostreopsis* cf. *ovata* blooms and human health impacts using ecology and epidemiology. *Scientia Marina* **2016**, 80, 107–115, doi: 10.3989/scimar.04395.08A.

24. Otero, P.; Silva, M. Emerging Marine Biotoxins in European Waters: Potential Risks and Analytical Challenges. *Marine Drugs* **2022**, 20, 199, doi: 10.3390/md20030199.

25. Ciminiello, P.; Dell'Aversano, C.; Fattorusso, E.; Magno, S.; Tartaglione, L.; Cangini, M.; Pompei, M.; Guerrini, F.; Boni, L.; Pistocchi, R. Toxin profile of *Alexandrium ostenfeldii* (Dinophyceae) from the Northern Adriatic Sea revealed by liquid chromatography–mass spectrometry. *Toxicon* **2006**, 47 (5), 597–604, doi: 10.1016/j.toxicon.2006.02.003.

26. Ciminiello, P.; Dell'Aversano, C.; Fattorusso, E.; Forino, M.; Tartaglione, L.; Boschetti, L.; Rubini, S.; Cangini, M.; Pigozzi, S.; Poletti, R. Complex toxin profile of *Mytilus galloprovincialis* from the Adriatic Sea revealed by LC–MS. *Toxicon* **2010**, 55, 280–288, doi: 10.1016/j.toxicon.2009.07.037.

27. Bacchiocchi, S.; Siracusa, M.; Campacci, D.; Ciriaci, M.; Dubbini, A.; Tavoloni, T.; Stramenga, A.; Gorbi, S.; Piersanti, A. Cyclic Imines (CIs) in Mussels from North-Central Adriatic Sea: First Evidence of Gymnodimine A in Italy. *Toxins* **2020**, 12, 370, doi: 10.3390/toxins12060370.

28. Bacchiocchi, S.; Siracusa, M.; Ruzzi, A.; Gorbi, S.; Ercolessi, M.; Cosentino, M.; Ammazzalorso, P.; Orletti, R. Two-Year Study of Lipophilic Marine Toxin Profile in Mussels of the North-Central Adriatic Sea: First Report of Azaspiracids in Mediterranean Seafood. *Toxicon* **2015**, 108, 115–125, doi: 10.1016/j.toxicon.2015.10.002.

29. Dell'Aversano, C.; Tartaglione, L.; Polito, G.; Dean, K.; Giacobbe, M.; Casabianca, S.; Capellacci, S.; Penna, A.; Turner, A.D. First detection of tetrodotoxin and high hevels of paralytic shellfish poisoning toxins in shellfish from Sicily (Italy) by three different analytical methods. *Chemosphere* **2019**, 215, 881–892, doi: 10.1016/j.chemosphere.2018.10.081.

30. Bordin, P.; Dall'Ara, S.; Tartaglione, L.; Antonelli, P.; Calfapietra, A.; Varriale, F.; Guiatti, D.; Milandri, A.; Dell'Aversano, C.; Arcangeli, G.; Barco, L.; First occurrence of tetrodotoxins in bivalve mollusks from Northern Adriatic Sea (Italy). *Food Control* **2021**, 120, 107510, doi: 10.1016/j.foodcont.2020.107510.

31. Totti, C.; Cucchiari, E.; Romagnoli, T.; Penna, A. Bloom of *Ostreopsis ovata* on the Conero riviera (NW Adriatic Sea). *Harmful Algae News* **2007**, 33, 12–13.

32. Accoroni, S.; Romagnoli, T.; Colombo, F.; Pennesi, C.; di Camillo, C.G.; Marini, M.; Battocchi, C.; Ciminiello, P.; Dell'Aversano, C.; Dello Iacovo, E.; Fattorusso, E.; Tartaglione, L.; Penna, A.; Totti, C. *Ostreopsis* cf. *ovata* bloom in the northern Adriatic Sea during summer 2009: Ecology, molecular characterization and toxin profile. *Marine Pollution Bulletin* **2011**, 62, 2512–2519, doi: 10.1016/j.marpolbul.2011.08.003.

33. Siracusa, M.; Bacchiocchi, S.; Piersanti, A. A LC-MS/MS approach to evaluate Palytoxins contamination in wild mussels of the Conero Riviera. In Proceedings of 5th MS Food Day, Bologna, Italy, 11-13 October 2017.

34. Gerssen, A.; Mulder, P.P.J.; Mc Elhinney, M.A.; de Boer, J. Liquid chromatography-tandem mass spectrometry method for the detection of marine lipophilic toxins under alkaline conditions. *Journal of Chromatography A* **2009**, 1216, 1421–1430, doi: 10.1016/j.chroma.2008.12.099.

35. EURLMB. EU-Harmonised Standard Operating Procedure for determination of Lipophilic marine biotoxins in molluscs by LC-MS/MS, 5th Edition. Available online:https://www.aesan.gob.es/en/CRLMB/docs/docs/metodos_analiticos_de_desarrollo/EU-Harmonised-SOP-LIPO-LCMSMS_Version5.pdf (accessed on 21 October 2023).

36. Jauffrais, T.; Marcaillou, C.; Herrenknecht, C.; Truquet, P.; Séchet, V.; Nicolau, E.; Tillmann, U.; Hess, P. Azaspiracid accumulation, detoxification and biotransformation in blue mussels (*Mytilus edulis*) experimentally fed *Azadinium spinosum*. *Toxicon* **2012**, 60, 582–595, doi: 10.1016/j.toxicon.2012.04.351.

37. Blanco, J.; Arevalo, F.; Moroño, A.; Correa, J.; Muñiz, S.; Mariño, C.; Martín, H. Presence of azaspiracids in bivalve molluscs from Northern Spain. *Toxicon* **2017**, 137, 135-143, doi: 10.1016/j.toxicon.2017.07.025.

38. Giuliani, M.E.; Accoroni, S.; Mezzelani, M.; Lugarini, F.; Bacchiocchi, S.; Siracusa, M.; Tavoloni, T.; Piersanti, A.; Totti, C.; Regoli, F.; Rossi, R.; Zingone, A.; Gorbi, S. Biological Effects of the Azaspiracid-Producing Dinoflagellate *Azadinium dexteroporum* in *Mytilus galloprovincialis* from the Mediterranean Sea. *Marine Drugs* **2019**, 17, 595, doi: 10.3390/md17100595.

39. Rossi, R.; Dell'Aversano, C.; Krock, B.; Ciminiello, P.; Percopo, I.; Tillmann, U.; Soprano, V.; Zingone, A. Mediterranean *Azadinium dexteroporum* (Dinophyceae) produces six novel azaspiracids and azaspiracid-35: a structural study by a multi-platform mass spectrometry approach. *Analytical and Bioanalytical Chemistry* **2017**, 409, 1121–1134, doi: 10.1007/s00216-016-0037-4.

40. Turner, A.; Dhanji-Rapkova, M.; Fong, S.; Hungerford, J.; McNabb, P.; Boundy, M.; Harwood, T. Ultrahigh-Performance Hydrophilic Interaction Liquid Chromatography with Tandem Mass Spectrometry Method for the Determination of Paralytic Shellfish Toxins and Tetrodotoxin in Mussels, Oysters, Clams, Cockles, and Scallops: Collaborative Study. *Journal of AOAC International* **2020**, 103, 2, 533-562.

41. EURLMB SOP-Determination of Tetrodotoxin by HILIC-MS/MS, June 2017. Available online: https://www.aesan.gob.es/en/CRLMB/docs/docs/metodos_analiticos_de_desarrollo/HILIC-LCMSMS_SOP_for_TTX_in_mussels.pdf (accessed on 23 October 2023).

42. Ciminiello, P.; Dell'Aversano, C.; Dello Iacovo, E.; Fattorusso, E.; Forino, M.; Grauso, L.; Tartaglione, L.; Guerrini, F.; Pistocchi, R. Complex palytoxin-like profile of *Ostreopsis ovata*. Identification of four new ovatoxins by high-resolution liquid chromatography/mass spectrometry. *Rapid Communications in Mass Spectrometry* **2010**, 24, 2735–2744, doi: 10.1002/rcm.4696.

43. Ciminiello, P.; Dell'Aversano, C.; Dello Iacovo, E.; Fattorusso, E.; Forino, M.; Tartaglione, L.; Rossi, R.; Soprano, V.; Capozzo, D.; Serpe, L. Palytoxin in seafood by liquid chromatography tandem mass spectrometry: Investigation of extraction efficiency and matrix effect. *Analytical and Bioanalytical Chemistry* **2011**, 401, 1043–1050, doi: 10.1007/s00216-011-5135-8.

44. Pinto, A.; Botelho, M.J.; Churro, C.; Asselman, J.; Pereira, P.; Pereira, J.L. A review on aquatic toxins - Do we really know it all regarding the environmental risk posed by phytoplankton neurotoxins? *Journal of Environmental Management* **2023**, 345, 118769, doi: 10.1016/j.jenvman.2023.118769.

45. Silins, I.; Högberg, J. Combined Toxic Exposures and Human Health: Biomarkers of Exposure and Effect. *International Journal of Environmental Research Public Health* **2011**, 8(3), 629-647, doi: 10.3390/ijerph8030629.

46. Jauffrais, T.; Contreras, A.; Herrenknecht, C.; Truquet, P.; Séchet, V.; Tillmann, U.; Hess, P. Effect of *Azadinium spinosum* on the feeding behaviour and azaspiracid accumulation of *Mytilus edulis*. *Aquatic Toxicology* **2012**, 124–125, 179–187, doi: 10.1016/j.aquatox.2012.08.016.

47. Ji, Y.; Qiu, J.; Xie, T.; McCarron, P.; Li, A. Accumulation and transformation of azaspiracids in scallops (*Chlamys farreri*) and mussels (*Mytilus galloprovincialis*) fed with *Azadinium poporum*, and response of antioxidant enzymes. *Toxicon* **2018**, 143, 20–28, doi: 10.1016/j.toxicon.2017.12.040.

48. Gorbi, S.; Bocchetti, R.; Binelli, A.; Bacchiocchi, S.; Orletti, R.; Nanetti, L.; Raffaelli, F.; Vignini, A.; Accoroni, S.; Totti, C.; Regoli, F. Biological effects of palytoxin-like compounds from *Ostreopsis* cf. *ovata*: A multibiomarkers approach with mussels *Mytilus galloprovincialis*. *Chemosphere* **2012**, 89, 623–632, doi: 10.1016/j.chemosphere.2012.05.064.

49. Gorbi, S.; Avio, G.C.; Benedetti, M.; Totti, C.; Accoroni, S.; Pichierri, S.; Bacchiocchi, S.; Orletti, R.; Graziosi, T.; Regoli, F. Effects of harmful dinoflagellate *Ostreopsis* cf. *ovata* exposure on immunological, histological and oxidative responses of mussels *Mytilus galloprovincialis*. *Fish & Shellfish Immunology* **2013**, 35, 941–950, doi: 10.1016/j.fsi.2013.07.003.

50. Carella, F.; Sardo, A.; Mangoni, O.; Di Cioccio, D.; Urciuolo, G.; De Vico, G.; Zingone, A. Quantitative histopathology of the Mediterranean mussel (*Mytilus galloprovincialis* L.) exposed to the harmful dinoflagellate *Ostreopsis* cf. *ovata*. *Journal of Invertebrate Pathology* **2015**, 127, 130–140, doi: 10.1016/j.jip.2015.03.001.

51. Nicolas, J.; Bovee, T.F.H.; Kamelia, L.; Rietjens, I.M.C.M.; Hendriksen, P.J.M. Exploration of new functional endpoints in neuro-2a cells for the detection of the marine biotoxins saxitoxin, palytoxin and tetrodotoxin. *Toxicology in Vitro* **2015**, 30, 341–347, doi: 10.1016/j.tiv.2015.10.001.

52. Giuliani, M.E.; Sparaventi,E.; Lanzoni, I.; Pittura, L.; Regoli, F.; Gorbi, S. Precision-Cut Tissue Slices (PCTS) from the digestive gland of the Mediterranean mussel *Mytilus galloprovincialis*: An *ex vivo* approach for molecular and cellular responses in marine invertebrates. *Toxicology in Vitro* **2019**, 61, 104603, doi: 10.1016/j.tiv.2019.104603.

53. Stivala, C.E.; Benoit, E.; Aráoz, R.; Servent, D.; Novikov, A.; Molgó, J.; Zakarian, A. Synthesis and biology of cyclic imine toxins, an emerging class of potent, globally distributed marine toxins. *Natural Product Reports* **2015**, 32, 411–435, doi: 10.1039/c4np00089g.

54. Zurhelle, C.; Nieva, J.; Tillmann, U.; Harder, T.; Krock, B.; Tebben, J. Identification of Novel Gymnodimines and Spirolides from the Marine Dinoflagellate *Alexandrium ostenfeldii*. *Marine Drugs* **2018**, 16, 446, doi: 10.3390/md16110446.

55. FAO; IOC; WHO. Report of the Joint FAO/IOC/WHO ad hoc Expert Consultation on Biotoxins in Bivalve Molluscs. In Proceedings of the Joint FAO/IOC/WHO ad hoc Expert Consultation on Biotoxins in Bivalve, Oslo, Norway, 26–30 September 2004; pp. 1–31.

56. Cembella, A.D.; Lewis, N.I.; Quilliam, M.A. Spirolide composition of micro-extracted pooled cells isolated from natural plankton assemblages and from cultures of the dinoflagellate *Alexandrium ostenfeldii*. *Natural Toxins* **1999**, 7, 197–206, doi: 10.1002/1522-7189(200009/10)7.

57. Cembella, A.D.; Lewis, N.I.; Quilliam, M.A. The marine dinoflagellate *Alexandrium ostenfeldii* (Dinophyceae) as the causative organism of spirolide shellfish toxins. *Phycologia* **2000**, 39, 67–74, doi: 10.2216/i0031-8884-39-1-67.1.

58. Touzet, N. Morphogenetic diversity and biotoxin composition of *Alexandrium* (Dinophyceae) in Irish coastal waters. *Harmful Algae* **2008**, 7, 782–797, doi: 10.1016/j.hal.2008.04.001.

59. Seki, T.; Satake, M.; Mackenzie, L.; Kaspar, H.F.; Yasumoto, T. Gymnodimine, a new marine toxin of unprecedented structure isolated from New Zealand Oysters and the dinoflagellate, *Gymnodinium Sp. Tetrahedron Letters* **1995**, 36, 7093–7096, doi: 10.1016/0040-4039(95)01434-J.

60. Hess, P.; Abadie, E.; Hervé, F.; Berteaux, T.; Séchet, V.; Aráoz, R.; Molgó, J.; Zakarian, A.; Sibat, M.; Rundberget, T.; Miles, C.O.; Amzil, Z. Pinnatoxin G is responsible for atypical toxicity in mussels (*Mytilus galloprovincialis*) and Clams (*Venerupis decussata*) from Ingril, a French Mediterranean Lagoon. *Toxicon* **2013**, 75, 16–26 doi: 10.1016/j.toxicon.2013.05.001.

61. García-Altares, M.; Casanova, A.; Bane, V.; Diogène, J.; Furey, A.; De la Iglesia, P. Confirmation of Pinnatoxins and Spirolides in Shellfish and Passive Samplers from Catalonia (Spain) by Liquid Chromatography Coupled with Triple Quadrupole and High-Resolution Hybrid Tandem Mass Spectrometry. *Marine Drugs* **2014**, 12, 3706–3732, doi: 10.3390/md12063706.

62. Varriale, F.; Tartaglione, L.; Milandri,A.; Dall'Ara, S.; Calfapietra, S.; Dell'Aversano, C. Looking for cyclic imines and their fatty acid derivatives in Italian, Spanish and Tunisian shellfish. In Proceedings of 1st MS Sea Day, Livorno, Italy, 6-7 June 2019.

63. Selwood, A.I.; Miles, C.O.; Wilkins, A.L.; van Ginkel, R.; Munday, R.; Rise, F.; McNabb, P. Isolation, Structural Determination and Acute Toxicity of Pinnatoxins E., F and G. *Journal of Agricultural and Food Chemistry* **2010**, 58, 6532–6542, doi: 10.1021/jf100267a.

64. Tillmann, U.; Elbrächter, M.; Krock, B.; John, U.; Cembella, A. *Azadinium spinosum* gen. et sp. nov.(Dinophyceae) identified as a primary producer of azaspiracid toxins. *European Journal of Phycology* **2009**, 44, 63–79, doi: 10.1080/09670260802578534.

65. Krock, B.; Tillmann, U.; Voß, D.; Koch, B.P.; Salas, R.; Witt, M.; Potvin, É.; Jeong, H.J. New azaspiracids in Amphidomataceae (Dinophyceae). *Toxicon* **2012**, 60, doi: 830–839. 10.1016/j.toxicon.2012.05.007.

66. Percopo, I.; Siano, R.; Rossi, R.; Soprano, V.; Sarno, D.; Zingone, A. A new potentially toxic Azadinium species (Dinophyceae) from the Mediterranean Sea, *A. dexteroporum* sp. nov. *Journal of Phycology* **2013**, 49, 950–966, doi: 10.1111/jpy.12104.

67. Hess, P.; McCarron, P.; Krock, B.; Kilcoyne, J.; Miles, C.O. Azaspiracids: Chemistry, biosynthesis, metabolism, and detection. In Seafood and Freshwater Toxins: Pharmacology, Physiology, and Detection, 3rd ed.; Botana, L.M., Ed.; CRC Press: Boca Raton, FL, USA, **2014**.

68. Jauffrais T.; Herrenknecht, C.; Séchet, V.; Sibat, M.; Tillmann, U.; Krock, B.; Kilcoyne, J.; Miles, C.O.; McCarron, P.; Amzil, Z.; Hess, P. Quantitative analysis of azaspiracids in *Azadinium spinosum* cultures, *Analytical and Bioanalytical Chemistry* **2012**, 403, 833–846, doi: 10.1007/s00216-012-5849-2.

69. Revelante, N.; Gilmartin, M. The lateral advection of particulate organic matter from the Po delta region during summer stratification, and its implications for the northern Adriatic. *Estuarine, Coastal and Shelf Science* **1992**, 35, 191–212, doi: 10.1016/S0272-7714(05)80113-1.

70. Bernardi Aubry, F.B.; Berton, A.; Bastianini, M.; Socal, G.; Acri, F. Phytoplankton succession in a coastal area of the NW Adriatic, over a 10-year sampling period (1990–1999). *Continental Shelf Research* **2004**, 24, 97–115, doi: 10.1016/j.csr.2003.09.007.

71. Pigozzi, S.; Bianchi, L.; Boschetti, L.; Cangini, M.; Ceredi, A.; Magnani, F.; Milandri, A.; Montanari, S.; Pompei, M.; Riccardi, E.; et al. First evidence of spirolide accumulation in northwestern Adriatic shellfish. In Proceedings of the 12th International Conference on Harmful Algae, Copenhagen, Denmark, 4–8 September 2006; Moestrup, Ø., Ed.; ISSHA and IOC of UNESCO: Copenhagen, Denmark, 2008; pp. 319–322.

72. Uwe, J.; Quilliam, M.; Medlin, L.; Cembella, A. Spirolide production and photoperiod-dependent growth of the marine dinoflagellate *Alexandrium ostenfeldii*. In Proceedings of the 9th International Conference on Harmful Algal Blooms, Hobart, Australia, 7–11 February, 2001; pp. 299–302.

73. Maclean, C.; Cembella, A.; Quilliam, M. Effects of Light, Salinity and Inorganic Nitrogen on Cell Growth and Spirolide Production in the Marine Dinoflagellate *Alexandrium ostenfeldii* (Paulsen) Balech et Tangen. *Botanica Marina* **2003**, 46, 466–476, doi: 10.1515/BOT.2003.048.

74. Otero, P.; Alfonso, A.; Vieytes, M.R.; Cabado, A.G.; Vieites, J.M.; Botana, L.M. Effects of environmental regimens on the toxin profile of *Alexandrium ostenfeldii*. *Environmental Toxicology and Chemistry* **2010**, 29, 301–310, doi:10.1002/etc.41.

75. Salgado, P.; Riobó, P.; Rodríguez, F.; Franco, J.M.; Bravo, I. Differences in the toxin profiles of *Alexandrium ostenfeldii* (Dinophyceae) strains isolated from different geographic origins: Evidence of Paralytic Toxin, Spirolide, and Gymnodimine. *Toxicon* **2015**, 103, 85–98, doi: 10.1016/j.toxicon.2015.06.015.

76. Medhioub, W.; Sechet, V.; Truquet, P.; Bardouil, M.; Amzil, Z.; Lassus, P.; Soudant, P. *Alexandrium ostenfeldii* growth and spirolide production in batch culture and photobioreactor. *Harmful Algae* **2011**, 10, 794–803, doi:10.1016/j.hal.2011.06.012.

77. Medhioub, W.; Lassus, P.; Truquet, P.; Bardouil, M.; Amzil, Z.; Sechet, V.; Sibat, M.; Soudant, P. Spirolide uptake and detoxification by *Crassostrea gigas* exposed to the toxic dinoflagellate *Alexandrium ostenfeldii*. *Aquaculture* **2012**, 358–359, 108–115, doi: 10.1016/j.aquaculture.2012.06.023.

78. Gu, H.; Luo, Z.; Krock, B.; Witt, M.; Tillmann, U. Morphology, phylogeny and azaspiracid profile of *Azadinium poporum* (Dinophyceae) from the China Sea. *Harmful Algae* **2013**, 21-22, 64-75, doi: 10.1016/j.hal.2012.11.009.

79. Yotsu-Yamashita, M.; Sugimoto, A.; Takai, A.; Yasumoto, T. Effects of Specific Modifications of Several Hydroxyls of Tetrodotoxin on Its Affinity to Rat Brain Membrane. *Journal of Pharmacology and Experimental Therapeutics* **1999**, 289, 1688–1696.

80. Bane, V.; Lehane, M.; Dikshit, M.; O'Riordan, A.; Furey, A. Tetrodotoxin: Chemistry, Toxicity, Source, Distribution and Detection. *Toxins* **2014**, 6, 693–755, doi: 10.3390/toxins6020693.

81. Do, H.K.; Kogure, K.; Simidu, U. Identification of Deep-Sea-Sediment Bacteria Which Produce Tetrodotoxin. *Applied and Environmental Microbiology* **1993**, 56, 1162–1163, doi: 0.1128/aem.56.4.1162-1163.19.

82. Lee,M.-J.; Jeong, D.-Y.; Kim,W.-S.; Kim, H.-D.; Kim, C.-H.; Park,W.-W.; Park, Y.-H.; Kim, K.-S.; Kim, H.-M.; Kim, D.-S. A Tetrodotoxin-Producing Vibrio Strain, LM-1, from the Puffer Fish Fugu *Vermicularis radiatus*. *Applied and Environmental Microbiology* **2000**, 66, 1698–1701, doi: 10.1128/AEM.66.4.1698-1701.200.

83. Wu, Z.; Yang, Y.; Xie, L.; Xia, G.; Hu, J.; Wang, S.; Zhang, R. Toxicity and Distribution of Tetrodotoxin-Producing Bacteria in Puffer Fish *Fugu rubripes* Collected from the Bohai Sea of China. *Toxicon* **2005**, 46, 471–476, doi: 10.1016/j.toxicon.2005.06.002.

84. Magarlamov, T.Y.; Melnikova, D.I.; Chernyshev, A.V. Tetrodotoxin-Producing Bacteria: Detection, Distribution and Migration of the Toxin in Aquatic Systems. *Toxins* **2017**, 9, 166, doi: 10.3390/toxins9050166.

85. Pratheepa, V.; Alex, A.; Silva, M.; Vasconcelos, V. Bacterial Diversity and Tetrodotoxin Analysis in the Viscera of the Gastropods from Portuguese Coast. *Toxicon* **2016**, 119, 186–193, doi: 10.1016/j.toxicon.2016.06.003.

86. Turner, A.D.; Powell, A.; Schofield, A.; Lees, D.N.; Baker-Austin, C. Detection of the Pufferfish Toxin. Tetrodotoxin in European Bivalves, England, 2013 to 2014. *Eurosurveillance* **2015**, 20, 21009, doi: 10.2807/1560-7917.es2015.20.2.21009.

87. Leão, J.M.; Lozano-Leon, A.; Giráldez, J.; Vilariño, Ó.; Gago-Martínez, A. Preliminary Results on the Evaluation of the Occurrence of Tetrodotoxin Associated to Marine *Vibrio* Spp. in Bivalves from the Galician Rias (North-west of Spain). *Marine Drugs* **2018**, 16, 81, doi: 10.3390/md16030081.

88. Kodama, M.; Sato, S.; Sakamoto, S.; Ogata, T. Occurrence of Tetrodotoxin in Alexandrium tamarense, a Causative Dinoflagellate of Paralytic Shellfish Poisoning. *Toxicon* **1996**, 34, 1101–1105, doi: 10.1016/0041-0101(96)00117-1.

89. Vlamis, A.; Katikou, P.; Rodriguez, I.; Rey, V.; Alfonso, A.; Papazachariou, A.; Zacharaki, T.; Botana, A.M.; Botana, L.M. First Detection of Tetrodotoxin in Greek Shellfish by UPLC-MS/MS Potentially Linked to the Presence of the Dinoflagellate *Prorocentrum minimum*. *Toxins* **2015**, 7, 1779–1807, doi: 0.3390/toxins7051779.

90. Rodríguez, I.; Alfonso, A.; Alonso, E.; Rubiolo, J.A.; Roel, M.; Vlamis, A.; Katikou, P.; Jackson, S.A.; Menon, M.L.; Dobson, A.; Botana, L.M. The association of bacterial C 9 -based TTX-like compounds with *Prorocentrum minimum* opens new uncertainties about shellfish seafood safety. *Scientific Reports* **2017**, 7, 1–12, doi: 10.1038/srep40880.

91. Kotaki, Y.; Shimizu, Y. 1-Hydroxy-5,11-Dideoxytetrodotoxin, the First N-Hydroxy and Ring-Deoxy derivative of Tetrodotoxin Found in the Newt Taricha granulosa. *Journal of the American Chemical Society* **1993**, 115, 827–830, doi: 10.1021/ja00056a001.

92. Chau, R.; Kalaitzis, J.A.; Neilan, B.A. On the Origins and Biosynthesis of Tetrodotoxin. *Aquatic Toxicology* **2011**, 104, 61–72, doi: 1016/j.aquatox.2011.04.001.

93. Wang, X.J.; Yu, R.C.; Luo, X.; Zhou, M.J.; Lin, X.T. Toxin-screening and identification of bacteria isolated from highly toxic marine gastropod *Nassarius semiplicatus*. *Toxicon* **2008**, 52, 55–61, doi: 10.1016/j.toxicon.2008.04.170.

94. Biessy, L.; Pearman, J.K.; Smith, K.F.; Hawes, I.; Wood, S.A. Seasonal and Spatial Variations in Bacterial Communities From Tetrodotoxin-Bearing and Non-Tetrodotoxin-Bearing Clams. *Frontiers in Microbiology* **2020**, 11, doi: 10.3389/fmicb.2020.01860.

95. Rodriguez, P.; Alfonso, A.; Vale, C.; Alfonso, C.; Vale, P.; Tellez, A.; Botana, L.M. First Toxicity Report of Tetrodotoxin and 5,6,11-trideoxyTTX in the Trumpet Shell Charonia lampas lampas in Europe. *Analytical Chemistry* **2008**, 80, 5622–5629, doi: 10.1021/ac800769e.

96. Gerssen, A.; Bovee, T.; Klijnstra, M.D.; Poelman, M.; Portier, L.; Hoogenboom, R. First Report on the Occurrence of Tetrodotoxins in Bivalve Mollusks in The Netherlands. *Toxins* **2018**, 10, 450, doi: 0.3390/toxins10110450.

97. Turner, A.; Dhanji-Rapkova, M.; Coates, L.; Bickerstaff, L.; Milligan, S.; Oneill, A.; Faulkner, D.; Mceneny, H.; Baker-Austin, C.; Lees, D.; Algoet, M. Detection of Tetrodotoxin Shellfish Poisoning (TSP) Toxins and Causative Factors in Bivalve Molluscs from the UK. *Marine Drugs* **2017**, 15, 277, doi: 10.3390/md15090277.

98. ISO 6887-3. Microbiology of the Food Chain-Preparation of Test Samples, Initial Suspension and Decimal Dilutions for Microbiological Examinations-Part 3: Specific Rules for the Preparation of Fish and Fishery Products. Available online: https://www.iso.org/standard/77420.html (accessed on 21 October 2023).

99. ISO 21872-1:2017. Microbiology of the Food Chain—Horizontal Method for Determination of Vibrio spp.—Part 1: Detection of Potentially Enteropathogenic *Vibrio parahaemolyticus*, *Vibrio cholerae* and *Vibrio vulnificus*. Available online: https://www.iso.org/standard/74112.html (accessed on 21 October 2023).

100. Hartnell, R.E.; Stockley, L.; Keay, W.; Rosec, J.-P.; Hervio-Heath, D.; Van den Berg, H.; Leoni, F.; Ottaviani, D.; Henigman, U.; Denayer, S.; . Serbruyns, B.; Georgsson, F.; Krumova-Valcheva, G.; Gyurova, E.; Blanco, C.; Copin, S.; Strauch, E.; Wieczorek, K.; Lopatek, M.; Britova, A.; Hardouin, G.; Lombard, B.; in't Veld, P.; Leclercq, A.; Baker-Austin, C. A Pan-European ring trial to validate an International Standard for detection of *Vibrio cholerae*, *Vibrio parahaemolyticus* and *Vibrio vulnificus* in seafoods. *International Journal of Food Microbiology* **2019**, 288, 58–65, doi: 10.1016/j.ijfoodmicro.2018.02.008.

101. Chen, M.-X.; Li, H.-Y.; Li, G.; Zheng, T.-L. Distribution of *Vibrio Alginolyticus*-like species in Shenzhen coastal waters, China. *Brazilian Journal of Microbiology* **2011**, 42, 884–896, doi: 10.1590/S1517-83822011000300007.

102. Froelich, B.A.; Ayrapetyan, M.; Fowler, P.; Oliver, J.D.; Noble, R.T. Development of a Matrix Tool for the Prediction of *Vibrio* Species in Oysters Harvested from North Carolina. *Applied and Environmental Microbiology* **2015**, 81, 1111–1119, doi: 10.1128/AEM.03206-14.

103. Turner, S.; Pryer, K.M.; Miao, V.P.; Palmer, J.D. Investigating Deep Phylogenetic Relationships among Cyanobacteria and Plastids by Small Subunit RRNA Sequence Analysis. The Journal of Eukaryotic *Microbiology* **1999**, 46, 327–338, doi: 10.1111/j.1550-7408.1999.tb04612.x.

104. Luo, P.; Hu, C. Vibrio alginolyticus gyrB sequence analysis and gyrB-Targeted PCR identification in environmental isolates. *Diseases of Aquatic Organisms* **2008**, 82, 209–216, doi: 10.3354/dao01984.

105. Tambadou, F.; Lanneluc, I.; Sablé, S.; Klein, G.L.; Doghri, I.; Sopéna, V.; Didelot, S.; Barthélémy, C.; Thiéry, V.; Chevrot, R. Novel nonribosomal peptide synthetase (NRPS) genes sequenced from intertidal mudflat bacteria. *FEMS Microbiology Lett*ers **2014**, 357, 123–130, doi: 10.1111/1574-6968.12532.

106. Moffitt, M.C.; Neilan, B.A. On the presence of peptide synthetase and polyketide synthase genes in the cyanobacterial genus Nodularia. *FEMS Microbiology Lett*ers **2001**, 196, 207–214, doi: 10.1111/j.1574-6968.2001.tb10566.x.

107. Réveillon, D.; Savar, V.; Schaefer, E.; Chevé, J.; Halm-Lemeille, M.-P.; Hervio-Heath, D.; Travers, M.-A.; Abadie, E.; Rolland, J.-L.; Hess, P. Tetrodotoxins in French Bivalve Mollusks-Analytical Methodology, Environmental Dynamics and Screening of Bacterial Strain Collections. *Toxins* **2021**, 13, 740, doi: 10.3390/toxins13110740.

108. Galleni, L.; Tongiorgi, P.; Ferrero, E.; Salghetti, U. *Stylochus mediterraneus* (Turbellaria: Polycladida), predator on the mussel *Mytilus Galloprovincialis. Marine Biology* **1980**, 55, 317–326, doi: 10.1007/BF00393784.

109. Thompson, F.L.; Iida, T.; Swings, J. Biodiversity of vibrios. *Microbiology and Molecular Biology Reviews* **2004**, 68, 403–431, doi: 10.1128/MMBR.68.3.403-431.2004.

110. Barbieri, E.; Falzano, L.; Fiorentini, C.; Pianetti, A.; Baffone,W.; Fabbri, A.; Matarrese, P.; Casiere, A.; Katouli, M.; Kühn, I.; Möllby, R.; Bruscolini, F.; Donelli, G. Occurrence, diversity, and pathogenicity of halophilic *Vibrio* spp. and non-O1 *Vibrio cholerae* from estuarine waters along the Italian Adriatic coast. *Applied and Environmental Microbiology* **1999**, 65, 2748–2753, doi: 10.1128/aem.65.6.2748-2753.1999.

111. Urakawa, H.; Rivera, I. *The Biology of Vibrios. Aquatic Environment*; ASM Press: Washington, DC, USA, **2006**; pp. 175–189.

112. Silva, M.; Azevedo, J.; Rodriguez, P.; Alfonso, A.; Botana, L.M.; Vasconcelos, V. New Gastropod Vectors and Tetrodotoxin Potential Expansion in Temperate Waters of the Atlantic Ocean. *Marine Drugs* **2012**, 10, 712–726, doi: 10.3390/md10040712.

113. McNabb, P.S.; Taylor, D.I.; Ogilvie, S.C.; Wilkinson, L.; Anderson, A.; Hamon, D.; Wood, S.A.; Peake, B.M. First detection of tetrodotoxin in the bivalve Paphies australis by liquid chromatography coupled to triple quadrupole mass spectrometry with and without precolumn reaction. *Journal of AOAC International* **2014**, 97, 325–333, doi: 10.5740/jaoacint.sgemcnabb.

114. Ciminiello, P.; Dell'Aversano, C.; Fattorusso, E.; Forino, M.; Tartaglione, L.; Grillo, C.; Melchiorre, N. Putative Palytoxin and Its New Analogue, Ovatoxin-a, in *Ostreopsis ovata* Collected Along the Ligurian Coasts During the 2006 Toxic Outbreak. *Journal of the American Society for Mass Spectrometry* **2008**, 19: 111-120, doi: 10.1016/j.jasms.2007.11.001.

115. Brissard, C.; Hervé, F.; Sibat, M.; Séchet, V.; Hess, P.; Amzil, Z.; Herrenknecht, C. Characterization of ovatoxin-h, a new ovatoxin analog, and evaluation of chromatographic columns for ovatoxin analysis and purification. *Journal of Chromatography A* **2015**, 1388, 87–101, doi: 10.1016/j.chroma.2015.02.015.

116. Accoroni, S.; Romagnoli, T.; Penna, A.; Capellacci, S.; Ciminiello, P.; Dell'Aversano, C.; Tartaglione, L.; Abboud-Abi Saab, M.; Giussani, V.; Asnaghi, V.; Chiantore, M.; Totti, C. Ostreopsis fattorussoi sp. nov. (Dinophyceae), a new benthic toxic Ostreopsis species from the eastern Mediterranean Sea. *Journal of Phycology* **2016**, 52, 1064–1084, doi: 10.1111/jpy.12464.

117. Aligizaki, K.; Katikou, P.; Milandri, A.; Diogène, J. Occurrence of palytoxin-group toxins in seafood and future strategies to complement the present state of the art. *Toxicon* **2011**, 57(3): 390-9, doi: 10.1016/j.toxicon.2010.11.014.

118. Biré, R.; Trotereau, S.; Lemée, R.; Delpont, C.; Chabot, B.; Aumond, Y.; Krys, S. Occurrence of palytoxins in marine organisms from different trophic levels of the French Mediterranean coast harvested in 2009. *Harmful Algae* **2013**, 28,10–22, doi: 10.1016/j.hal.2013.04.007.

119. Biré, R.; Trotereau, S.; Lemée, R.; Oregioni, D.; Delpont, C.; Krys, S.; Guérin, T. Hunt for Palytoxins in a Wide Variety of Marine Organisms Harvested in 2010 on the French Mediterranean Coast. *Marine Drugs* **2015**, 13(8): 5425-46, doi: 10.3390/md13085425.

120. Tubaro, A.; Durando, P.; Del Favero, G.; Ansaldi, F.; Icardi, G.; Deeds, J.R.; Sosa, S. Case definitions for human poisonings postulated to palytoxins exposure. *Toxicon* **2011**, 57, 478–495, doi: 10.1016/j.toxicon.2011.01.005.

121. Funari, E.; Manganelli, M.; Testai, E. *Ostreospis* cf. *ovata* blooms in coastal water: Italian guidelines to assess and manage the risk associated to bathing waters and recreational activities. *Harmful Algae* **2015**, 50, 45–56, doi: 10.1016/j.hal.2015.10.008.

122. Ramos, V.; Vasconcelos, V. Palytoxin and analogs: biological and ecological effects. *Marine Drugs* **2010**, 8(7): 2021-37. doi: 10.3390/md8072021.

123. Sardo, A.; Rossi, R.; Soprano, V.; Ciminiello, P.; Fattorusso, E.; Cirino, P.; Zingone A. The dual impact of *Ostreopsis* cf. *ovata* on *Mytilus galloprovincialis* and *Paracentrotus lividus*: Toxin accumulation and pathological aspects. *Mediterranean Marine Science* **2021**, 22(1), 59–72, doi: 10.12681/mms.24160.

124. Shears, N.T.; Ross, P.M. Blooms of benthic dinoflagellates of the genus *Ostreopsis*; an increasing and ecologically important phenomenon on temperate reefs in New Zealand and worldwide. *Harmful Algae* **2009**, 8, 916–925, doi: 10.1016/j.hal.2009.05.003.

125. Shears, N.T.; Ross, P.M. Toxic cascades: multiple anthropogenic stressors have complex and unanticipated interactive effects on temperate reefs. *Ecology Letters* **2010**, 13, 1149–1159, doi: 10.1111/j.1461-0248.2010.01512.

126. Gleibs, S.; Mebs D. Distribution and sequestration of palytoxin in coral reef animals. *Toxicon* **1999**, 37(11):1521-7. doi: 10.1016/s0041-0101(99)00093-8.

127. Chen, S.; Zhou, Y.; Chen,Y.; Gu J. fastp: an ultra-fast all-in-one FASTQ preprocessor. *Bioinformatics* **2018**, 34(17): i884-i890. doi: 10.1093/bioinformatics/bty560.

128. Dobin, A.; Davis, C.A.; Schlesinger, F.; Drenkow, J.; Zaleski, C.; Jha, S.; Batut, P.; Chaisson, M.; Gingeras, T.R. STAR: ultrafast universal RNA-seq aligner. *Bioinformatics* **2013**, 29(1):15-21, doi: 10.1093/bioinformatics/bts635.

129. Li, B.; Dewey, C.N. RSEM: accurate transcript quantification from RNA-Seq data with or without a reference genome. *BMC Bioinformatics* **2011**, 12:323. doi: 10.1186/1471-2105-12-323.

130. McCarthy, D.J.; Chen, Y.; Smyth, G.K. Differential expression analysis of multifactor RNA-Seq experiments with respect to biological variation. *Nucleic Acids Research* **2012**, 40(10):4288-97,doi: 10.1093/nar/gks042.

131. Durinck, S.; Spellman, P.T.; Birney, E.; Huber, W. Mapping identifiers for the integration of genomic datasets with the R/Bioconductor package biomaRt. *Nature Protocols* **2009**, 4(8):1184-91, doi: 10.1038/nprot.2009.97.

132. Shannon, P.; Markiel, A.; Ozier, O.; Baliga, N.S.; Wang, J.T., Ramage, D.; Amin, N.; Schwikowski, B.; Ideker, T. Cytoscape: a software environment for integrated models of biomolecular interaction networks. *Genome Research* **2003**, 13(11): 2498-504. doi: 10.1101/gr.1239303.

133. Accoroni, S.; Tartaglione, L.; Dello Iacovo, E.; Pichierri, S.; Marini, M.; Campanelli, A.; Dell'Aversano, C.; Totti, C. Influence of environmental factors on the toxin production of *Ostreopsis* cf. *ovata* during bloom events. Mar. Pollut. Bull. **2017**, 123, 261–268, doi: 10.1016/j.marpolbul.2017.08.049.

134. Reis Costa, P.; Braga, A.; Turner, A. Accumulation and Elimination Dynamics of the Hydroxybenzoate Saxitoxin Analogues in Mussels *Mytilus galloprovincialis* Exposed to The Toxic Marine Dinoflagellate *Gymnodinium catenatum. Toxins* **2018**, 10, 428, doi: 10.3390/toxins10110428.

135. Blanco, J. Accumulation of *Dinophysis* Toxins in Bivalve Molluscs. *Toxins* **2018**, 10, 453, doi: 10.3390/toxins10110453.

136. Lin, C.; Accoroni, S.; Glibert, P. *Karlodinium veneficum* feeding responses and effects on larvae of the eastern oyster *Crassostrea virginica* under variable nitrogen:phosphorus stoichiometry. *Aquatic Microbial Ecology* **2017**, 79, 101–114, doi: 10.3390/toxins10110453.

137. Gémin, M.-P.; Réveillon, D.; Hervé, F.; Pavaux, A.-S.; Tharaud, M.; Séchet, V.; Bertrand, S.; Lemée, R.; Amzil, Z. Toxin content of *Ostreopsis* cf. *ovata* depends on bloom phases, depth and macroalgal substrate in the NW Mediterranean Sea. *Harmful Algae* **2020**, 92, 101727, doi: 10.3390/toxins10110453.

138. Andersen, P. Monitoring Toxic Algae in Relation to the Danish Mussel Fisheries 1991–1997; Technical Report for The Danish Veterinary and Food Administration: Frederiksberg, Denmark, 1998; pp. 1–19.

139. Reguera, B.; Riobó, P.; Rodríguez, F.; Díaz, P.A.; Pizarro, G.; Paz, B.; Franco, J.M.; Blanco, J. *Dinophysis* toxins: Causative Organisms, Distribution and Fate in Shellfish. *Marine Drugs* **2014**, 12, 394–461, doi : 10.3390/toxins10110453.

140. Landsberg, J.H. The Effects of Harmful Algal Blooms on Aquatic Organisms. *Reviews in Fisheries Science* **2002**, 10, 113–390, doi: 10.3390/toxins10110453.

141. Tartaglione, L.; Dello Iacovo, E.; Mazzeo, A.; Casabianca, S.; Ciminiello, P.; Penna, A.; Dell'Aversano, C. Variability in Toxin Profiles of the Mediterranean *Ostreopsis* cf. *ovata* and in Structural Features of the Produced Ovatoxins. *Environmental Science & Technology* **2017**, 51, 13920–13928, doi: 10.1021/acs.est.7b03827.

142. Vassalli, M.; Penna, A.; Sbrana, F.; Casabianca, S.; Gjeci, N.; Capellacci, S., Asnaghi, V.; Ottaviani, E.; Giussani, V.; Pugliese, L.; Jauzein, C.; Lemée, R.; Hachani, M.A.: Souad, T.S.; Açaf, L.; Abboud-Abi, S.M.; Fricke, A.; Mangialajo, L.; Bertolotto, R.; Totti, C.; Accoroni, S.; Berdalet, E.; Vila, M.; Chiantore, M. Intercalibration of counting methods for *Ostreopsis* spp. blooms in the Mediterranean Sea. *Ecological Indicators* **2018**, 85,1092-1100, doi: 10.1016/j.ecolind.2017.07.063.

143. Amzil, Z.; Siba,t M.; Chomerat, N.; Grossel, H.; Marco-Miralles, F.; Lemee, R.; Nezan, E.; Sechet, V. Ovatoxin-a and Palytoxin Accumulation in Seafood in Relation to *Ostreopsis* cf. *ovata* Blooms on the French Mediterranean Coast. *Marine Drugs* **2012**, 10, 477-496, doi: 10.3390/md10020477.

144. Kasumyan, A.O. The taste system in fishes and the effects of environmental variables. *Journal of Fish Biology* **2019**, 95(1):155-178, doi: 10.1111/jfb.13940.

145. Azizishirazi, A.; Dew, W.A.; Forsyth, H.L.; Pyle, G.G. Olfactory recovery of wild yellow perch from metal contaminated lakes. *Ecotoxicology and Environmental Safety* **2013**, 88: 42-7, doi: 10.1016/j.ecoenv.2012.10.015.

146. Lürling, M.; Scheffer M. Info-disruption: pollution and the transfer of chemical information between organisms. *Trends in Ecology & Evolution* **2007**, 22(7): 374-9, doi: 10.1016/j.tree.2007.04.002.

147. Heidenreich, S.; Witte, N.; Weber, P.; Goehring, I.; Tolkachov, A.; von Loeffelholz, C.; Döcke, S.; Bauer, M.; Stockmann, M.; Pfeiffer, A.F.H.; Birkenfeld, A.L.; Pietzke, M.; Kempa, S.; Muenzner, M.; Schupp, M. Retinol saturase coordinates liver metabolism by regulating ChREBP activity. *Nature Communications* **2017**, 8(1): 384, doi: 10.1038/s41467-017-00430-w.

148. Grabner, G.F.; Xie, H.; Schweiger, M.; Zechner, R. Lipolysis: cellular mechanisms for lipid mobilization from fat stores. *Nature Metabolism* **2021**, 3(11): 1445-1465, doi: 10.1038/s42255-021-00493-6.

149. Knutti, D.; Kralli A. PGC-1, a versatile coactivator. *Trends in Endocrinology & Metabolism* **2001**, 12(8): 360-5, doi: 10.1016/s1043-2760(01)00457-x.

150. Chen, Y.; Rui, B.B.; Tang, L.Y.; Hu, C.M. Lipin family proteins--key regulators in lipid metabolism. *Annals of Nutrition and Metabolism* **2015**, 66(1): 10-8, doi: 10.1159/000368661.

151. Kulozik, P.; Jones, A.; Mattijssen, F.; Rose, A.J.; Reimann, A.; Strzoda, D.; Kleinsorg, S.; Raupp, C.; Kleinschmidt, J.; Müller-Decker, K.; Wahli, W.; Sticht, C.; Gretz, N.; von Loeffelholz, C.; Stockmann, M.; Pfeiffer, A.; Stöhr, S.; Dallinga-Thie, G.M.; Nawroth, P.P.; Diaz, M.B.; Herzig, S. Hepatic deficiency in transcriptional cofactor TBL1 promotes liver steatosis and hypertriglyceridemia. *Cell Metabolism* **2011**, 13(4): 389-400, doi: 10.1016/j.cmet.2011.02.011.

152. Subramanian, S.; Gottschalk, W.K.; Kim, S.Y.; Roses, A.D.; Chiba-Falek, O. The effects of PPARγ on the regulation of the TOMM40-APOE-C1 genes cluster. *Biochimica et Biophysica Acta: Molecular Basis of Disease* **2017**, 1863(3): 810-816, doi: 10.1016/j.bbadis.2017.01.004.

153. Kersten, S. Role and mechanism of the action of angiopoietin-like protein ANGPTL4 in plasma lipid metabolism. *Journal of Lipid Research* **2021**, 62: 100150. doi: 10.1016/j.jlr.2021.100150.

154. Grabacka, M.; Pierzchalska, M.; Dean, M.; Reiss K. Regulation of Ketone Body Metabolism and the Role of PPARα. *International Journal of Molecular Sciences* **2016**, 17(12): 2093, doi: 10.3390/ijms17122093.

155. Yokomori, H.; Ando, W.; Oda, M. Cavin-1 is linked to lipid droplet formation in human hepatic stellate cells. *Medical Molecular Morphology* **2020**, 53(1): 56-59. doi: 10.1007/s00795-019-00219-4.

156. Honsell, G.; Bonifacio, A.; De Bortoli, M.; Penna, A.; Battocchi, C.; Ciminiello, P.; Dell'aversano, C.; Fattorusso, E.; Sosa, S.; Yasumoto, T.; Tubaro, A. New insights on cytological and metabolic features of *Ostreopsis* cf. *ovata* Fukuyo (Dinophyceae): a multidisciplinary approach. *PLoS One*. 2013, 8(2):e57291, doi: 10.1371/journal.pone.0057291.

157. Twiner, M.J., Ryan, J.C.; Morey, J.S.; Smith, K.J.; Hammad, S.M.; Van Dolah F.M., Hess, P.; McMahon, T.; Satake, M.; Yasumoto, T.; Doucette, G.J. Transcriptional profiling and inhibition of cholesterol biosynthesis in human T lymphocyte cells by the marine toxin azaspiracid. *Genomics* **2008**, 91(3): 289-300. doi: 10.1016/j.ygeno.2007.10.015.

Abbreviations

A. ostenfeldii: Alexandrium ostenfeldii

A. peruvianum: Alexandrium peruvianum

AN: Ancona

ASP: Amnesic Shellfish Poisoning

ASPW: alkaline saline peptone water

AZA1: Azaspiracid 1

AZA2: Azaspiracid 2

AZA3: Azaspiracid 3

3-epi-AZA7: 3-epi Azaspiracid 7

AZA17: Azaspiracid 17

AZA19: Azaspiracid 19

AZA54: Azaspiracid 54

AZA55: Azaspiracid 55

AZAs: Azaspiracids

AZP: Azaspiracid Poisoning

BS: breeding sties

BTXs: Brevetoxins

CAD: collision gas

CE: Collision Energy

CEP: Cell Entrance Potential

CFP: Ciguatera Fish Poisoning

CIs: Cyclic Imines

CRM: certified reference material

$CTRL^{+}$: positive control

$CTRL^{-}$: negative control

CTXs: Ciguatoxins

CUR: curtain gas

CXP: Cell Exit Potential

DA: Domoic acid

DEGs: differential expressed genes

13-desMe SPX C: 13-desmethyl spirolide C

DG: digestive gland

13,19-didesMe SPX C: 13,19-didesmethyl spirolide C

DISVA: Dipartimento di Scienze della Vita e dell'Ambiente

DP: Declustering Potential

DSP: Diarrhetic Shellfish Poisoning

DTXs: Dinophysistoxins

EFSA: European Food Safety Authority

ELISA: competitive enzyme-linked immunosorbent assay

EMB: Emerging Marine Biotoxins

EP: Entrance Potential

ESI: electrospray ionization

EU: European Union

EURLMB: EU Reference Laboratory for Monitoring of Marine Biotoxins

FA: fatty acids

FA/LIP relative amount of fatty acids respect to total lipids

FA/PRT: total amount of fatty acids respect to total proteins

FM: Fermo

FN: Fano

FTIRI: Focal Plane Array (FPA)-Fourier Transform Infrared Spectroscopy Imaging

G: gills

GLY: glycosylated compounds, mainly glycogen

GLY/PRT: total amount of glycosylated compounds, mainly glycogen, respect to proteins

GO: Gene Ontology

GS1: Ion source Gas 1

GS2: Ion source Gas 2

GYM A: Gymnodimine A

GYMs: Gymnodimines

HAB: Harmful algal blooms

HILIC-MS/MS: Hydrophilic Interaction Chromatography coupled to tandem Mass Spectrometry

IS: IonSpray voltage

LC-MS: Liquid Chromatography coupled to Mass Spectrometry

LC-MS/MS: Liquid Chromatography coupled to tandem Mass Spectrometry

LIP: total lipids

LIP/PRT: total amount of lipids respect to total proteins

LOD: limit of detection

LOQ: limit of quantification

M: mantle

M. galloprovincialis: Mytilus galloprovincialis

MBs: Marine Biotoxins

MC: Macerata

Min: minutes

MP: Molo Portonovo

MPL/MPLs: Maximum permitted limit/limits

MRM: multiple reaction monitoring

NPS: Neurotoxic Shellfish Poisoning

NRPS : non-ribosomal peptide synthetase

O. cf. *ovata*: *Ostreopsis* cf. *ovata*

OA: Okadaic acid

OPBA: Organismo Preposto al Benessere Animale

ORO: Oil red O

OVTX-a, -b, -c, -d, -e, -f, -g, -h: Ovatoxin -a, -b, -c, -d, -e, -f, -g, -h

OVTXs: Ovatoxins

PCR: Polymerase Chain Reaction

PCTS: precision-cut tissue slices

PKS: polyketide synthase

PLTX: Palytoxins

PN: Portonovo

PnTX G: Pinnatoxin G

PnTXs: Pinnatoxins

PPI: Protein-protein interaction

Prec. ion: precursor ion

Prod. ion: Product ion

PRT: total proteins

PS: Pesaro

PSP: Paralytic Shellfish Poisoning

PtTXs: Pteriatoxins

R%: recovery

RSDr%: intra-day relative standard deviation

RSD_R%: inter-day relative standard deviation

RT: remaining tissues

SB: San Benedetto del Tronto

SG: Senigallia

Skeletonema marinoi: S. marinoi

S/N: signal/noise

Sparus aurata: S. aurata

SPX A: Spirolide A

SPX B: Spirolide B

SPX E: Spirolide E

SPX F: Spirolide F

SPXs: Spirolides

STX-group toxins: Saxitoxin and its analogues

TCBS: Thiosulfate citrate bile sucrose agar

TEM: Source temperature

TEQ: Toxicity Equivalency

TSA: Tryptic soy agar

TTX: Tetrodotoxin

TTXs: Tetrodotoxins

UNS/FA: relative amount of unsaturated fatty acids among all fatty acids

V. alginolyticus: *Vibrio alginolyticus*

V. cholerae: Vibrio cholerae

V. parahaemolyticus: Vibrio parahaemolyticus

V. vulnificus: Vibrio vulnificus

YTXs: Yessotoxins

List of publications/conferences/courses/schools

PUBLICATIONS ON INTERNATIONAL JOURNALS

J1. Giulietti, S.; Romagnoli, T.; **Siracusa, M.**; Bacchiocchi, S.; Totti, C.; Accoroni, S. Integrative taxonomy of the *Pseudo-nitzschia* (Bacillariophyceae) populations in the NW Adriatic Sea, with a focus on a novel cryptic species in the *P. delicatissima* species complex. *Phycologia* **2021**, 60:3, 247-264, DOI: 10.1080/00318884.2021.1899733.

J2. Bacchiocchi, S.; Campacci, D.; **Siracusa, M.**; Dubbini, A.; Leoni, F.; Tavoloni, T.; Accoroni, S.; Gorbi, S.; Giuliani, M.E.; Stramenga, A.; Piersanti, A. Tetrodotoxins (TTXs) and *Vibrio alginolyticus* in Mussels from Central Adriatic Sea (Italy): Are They Closely Related? *Marine Drugs* **2021**, 19, 304, DOI: 10.3390/md19060304.

J3. Giulietti, S.; Totti, C.; Romagnoli, T.; **Siracusa, M**.; Bacchiocchi, S.; Accoroni, S. *Nitzschia gobbii* sp. nov. (Bacillariophyceae): a common but overlooked planktonic diatom species from the northwestern Adriatic Sea. *Phycologia* **2021**, 60:6, 558-571, DOI: 10.1080/00318884.2021.1952513.

J4. **Siracusa, M.**; Bacchiocchi, S.; Dubbini, A.; Campacci, D.; Tavoloni, T.; Stramenga, A.; Ciriaci, M.; Dall'Ara, S.; Piersanti, A. A High Throughput Screening HPLC-FLD Method for Paralytic Shellfish Toxins (PSTs) Enabling Effective Official Control. *Molecules* **2022**, 27, 4702, DOI: 10.3390/molecules27154702.

J5. Accoroni, S.; Ubaldi, M.; Bacchiocchi, S.; Neri, F.; **Siracusa, M.**; Buonomo, M.G.; Campanelli, A.; Totti, C. Palytoxin-Analogues Accumulation in Natural Mussel Banks during an *Ostreopsis* cf. *ovata Bloom. Journal of Marine Science and Engineering* **2022**, 10, 1402, DOI: 10.3390/jmse10101402.

J6. Bacchiocchi, S.; Campacci, D**.; Siracusa, M**.; Dubbini, A.; Accoroni, S.; Romagnoli, T.; Campanelli, A.; Griffoni, F.; Tavoloni, T.; Gorbi, S.; Totti, C.; Piersanti, A. A Hotspot of TTX Contamination in the
Adriatic Sea: Study on the Origin and Causative Factors. *Marine Drugs* **2023**, 21, 8, DOI: 10.3390/md21010008.

J7. Giuliani, M.E.; S.; Bacchiocchi, S.; Accoroni, S.; **Siracusa, M.**; Campacci, D.; Notarstefano, V.; Mezzelani, M.; Piersanti, A.; Totti, C.; Benedetti, M.; Regoli, F.; Gorbi, S. Trophic transfer and subcellular effects of ovatoxins in the gilthead seabream *Sparus aurata*: a focus on lipid metabolism alterations, submitted *to Chemosphere* - under revision.

CONFERENCES ATTENDED AND CONTRIBUTIONS PRESENTED

- IX CONGRESSO NAZIONALE SIRAM " Molluschicoltura, salute e ambiente", Trieste 11-12 November 2022, **Siracusa, M**.; Bacchiocchi, S.; Campacci, D.; Accoroni, S.; Totti, C.; Barchiesi, F.; Piersanti, A. *Un hot spot di Tetrodotossina nel Mar Adriatico: studio dell'origine e dei meccanismi di contaminazione nei mitili.* - **poster**.

- X CONGRESSO NAZIONALE SIRAM "Molluschicoltura fra tradizione e innovazione ", Cagliari 13-14 October 2023, **Siracusa, M**.; Bacchiocchi S., Giuliani, M.E.; Calandri, E.; Ferroni, L.; Ciriaci, M.; Tavoloni, T.; Gorbi, S.; Maresca, C.; Barchiesi, F.; Piersanti, A. *Trend temporali e geografici di acido Okadaico e Yessotossine nei mitili della costa marchigiana: il ruolo delle piogge come possibile strumento di previsione* – **oral communication**.

COURSES/SEMINARS/SCHOOLS

- INTEGRATION OF THE ECOLOGICAL AND OCEANOGRAPHIC OBSERVATIONS WITHIN THE CONSERVATION STRATEGIES FOR NATURA 2000 SITES - NEEDS AND CHALLENGES TO BUILD THE ADRIATIC ECOLOGICAL OBSERVING SYSTEM "ECOAdS"- online 3 December 2020.

- I PRINCIPI DELLE 3R NEGLI STUDI BIOMEDICI- online 9 May 2022.

- SCUOLA DI ANALISI MULTIVARIATA- online 25-29 September 2023.

INTERDISCIPLINARY CREDITS

- ✓ Design of Research: European projects -UNIVPM
- ✓ Technology Transfer and Innovation- UNIVPM
- ✓ Analisi di regressione mediante Microsoft Excel -DISVA
- ✓ Theory and application of complex networks -DISVA

DISCIPLINARY CREDITS – DISVA

Specific lessons

- ✓ Assessing oxidative stress in biological systems
- ✓ Environmental sustainability: the life cycle assessment, LCA
- ✓ Global change and anthropogenic impacts on marine ecosystems
- ✓ Alimentazione e Salute: studio della qualità nutrizionale degli alimenti
- ✓ Elements of Marine Policy
- ✓ Microbial-mediated processes in aquatic ecosystems: from basic to applied research toward solving environmental problems

Individual internship

- ✓ Biological effects of chemicals in sentinel species: from molecular to cellular and organism level

Aknowledgements

Thanks to the working team of Laboratorio di Ecotossicologia e Chimica Ambientale- Università Politecnica delle Marche and of Laboratorio Contaminanti Organici, Metalli Pesanti e Biotossine Algali - Istituto Zooprofilattico Sperimentale dell'Umbria e delle Marche Togo Rosati".